Since January 2020 Elsevier has created a COVID-19 resource centre with free information in English and Mandarin on the novel coronavirus COVID-19. The COVID-19 resource centre is hosted on Elsevier Connect, the company's public news and information website.

Trends in Analytical Chemistry 157 (2022) 116814

Contents lists available at ScienceDirect

Trends in Analytical Chemistry

journal homepage: www.elsevier.com/locate/trac

Merging microfluidics with luminescence immunoassays for urgent point-of-care diagnostics of COVID-19

Huijuan Yuan [1], Peng Chen [1], Chao Wan, Yiwei Li**, Bi-Feng Liu*

The Key Laboratory for Biomedical Photonics of MOE at Wuhan National Laboratory for Optoelectronics-Hubei Bioinformatics & Molecular Imaging Key Laboratory, Systems Biology Theme, Department of Biomedical Engineering, College of Life Science and Technology, Huazhong University of Science and Technology, Wuhan, 430074, China

ARTICLE INFO

Article history:
Received 21 June 2022
Received in revised form
29 October 2022
Accepted 30 October 2022
Available online 7 November 2022

Keywords:
Luminescence immunoassays
COVID-19
Microfluidic chips
POCTs

ABSTRACT

The Coronavirus disease 2019 (COVID-19) outbreak has urged the establishment of a global-wide rapid diagnostic system. Current widely-used tests for COVID-19 include nucleic acid assays, immunoassays, and radiological imaging. Immunoassays play an irreplaceable role in rapidly diagnosing COVID-19 and monitoring the patients for the assessment of their severity, risks of the immune storm, and prediction of treatment outcomes. Despite of the enormous needs for immunoassays, the widespread use of traditional immunoassay platforms is still limited by high cost and low automation, which are currently not suitable for point-of-care tests (POCTs). Microfluidic chips with the features of low consumption, high throughput, and integration, provide the potential to enable immunoassays for POCTs, especially in remote areas. Meanwhile, luminescence detection can be merged with immunoassays on microfluidic platforms for their good performance in quantification, sensitivity, and specificity. This review introduces both homogenous and heterogenous luminescence immunoassays with various microfluidic platforms. We also summarize the strengths and weaknesses of the categorized methods, highlighting their recent typical progress. Additionally, different microfluidic platforms are described for comparison. The latest advances in combining luminescence immunoassays with microfluidic platforms for POCTs of COVID-19 are further explained with antigens, antibodies, and related cytokines. Finally, challenges and future perspectives were discussed.

1. Introduction

The COVID-19 is an infectious disease caused by the severe acute respiratory syndrome coronavirus 2 (SARS-CoV-2), which causes a global epidemic. At the moment we organizing this review, there have been more than 520 million confirmed cases and 6 million deaths [1]. Besides, viruses carrying RNA as germ plasm are prone to mutate, producing greater infectivity and harm [2]. There have already been over 1000 mutant strains of the SARS-CoV-2 virus around the world, among which Delta and Omicron strains are highly contagious variants raising global concerns [3]. The Omicron variant has been rapidly spreading world-widely, as it is more contagious than any earlier coronavirus strains. Particularly, Omicron even gained potent capabilities for immune evasion [4].

Early detection and isolation are necessary steps to prevent the further spreading of the epidemic [5–7], which requires rapid, sensitive, and accurate detections and quantifications [8]. Now available methods for COVID-19 diagnosis mainly include nucleic acid assays, immunoassays, and radiological imaging [9–11]. Radiological imaging shows visible results of whether there are lung lesions, but is not able to diagnose the type of virus [12–14]. It also requires large imaging equipment and specialized medical staff [15]. Nucleic acid assays, the gold standard for COVID-19 diagnosis, have played an irreplaceable role in epidemic prevention and control [9,16], which can detect patients in the window period and achieve early diagnosis accurately [17]. However, time-consuming amplification, requirements for professional equipment and operation limit their rapid detection [18]. Alternatively, immunoassays, especially test strips, have been used for COVID-19 diagnosis, reducing false negatives partly and providing household convenience [19–22]. For comparison, nucleic acid assays require long-term processes of nucleic acid extraction, sample pretreatment,

* Corresponding author.
** Corresponding author.
E-mail addresses: yiweili@hust.edu.cn (Y. Li), bfliu@mail.hust.edu.cn (B.-F. Liu).
[1] These authors contributed equally to this work.

https://doi.org/10.1016/j.trac.2022.116814
0165-9936/

and temperature cycling, while immunoassays enable exceptionally rapid antigen detection without the requirements of pretreatments [23]. More importantly, immunoassays are able to accurately evaluate the infectivity of COVID-19, since there is a strong positive correlation between the antigen level and the infectivity [24]. Thus, immunoassays can provide clinicians with enough diagnostic information to determine the current stages of viral infection in patients. Immunoassays, particularly antibody tests, indicate ongoing or past infections, promoting a better understanding of the transmission dynamic [25,26]. The speed and versatility of immunoassays make them invaluable tests for pandemic monitoring, and commercialization efforts to produce them on a massive scale are beginning to ramp up [27]. Additionally, cytokine storm, known as aggressive inflammatory responses characterized by the elevated release of cytokines, has been described as features associated with life-threatening complications in COVID-19 patients [28,29]. Critical evaluations of cytokine levels and research on the underlying mechanism greatly rely on immunoassays. Therefore, it is urgent to establish proven and effective platforms for immunoassays, since the currently available platforms are designed for traditional immunoassays, which are still limited by the high cost and low automation. Thus, how to enable point-of-care (POC) immunoassays for miniaturization of experimental instruments, simplification of operation methods, and instantaneous reporting of results was urgently required [30–32]. Particularly, the microfluidic chips provide more possibilities for POCTs [18,33–35].

Towards this end, microfluidic chips could be a powerful tool to enable POC immunoassays [36–38]. In 1990, Manz et al. firstly proposed the concept of micro total analysis systems, also latterly termed microfluidic chips or lab-on-a-chip [39]. Microfluidic technology offers great potential to revolutionize the way of sampling, sample separation, mixing, chemical reaction, and detection [40,41]. It is of high throughput, low reagent/sample consumption, and less pollution, which is conducive to miniaturization and automation [42–44].

For POC immunoassays, microfluidic platforms for POCTs consist of two basic parts: analyte recognition and signal detection. There are couples of ways for signal detection in the measurements, which include luminescence [45–47], surface-enhanced Raman scattering (SERS) [48–50], surface plasmon resonance (SPR) [51–53], colorimetry [54–60], distance reading [61,62], giant magnetoresistance effect (GMR) [63,64], and electrochemistry [65–68], and etc. Among them, luminescence detection is one of the most widely-used with several advantages [69–71]. Compared with naked-eye detection, luminescence provides more quantitative and sensitive data [72–74]. Compared with SPR, GMR, etc., luminescence is less costly and more readily available [75,76]. Furthermore, relatively simple peripherals of luminescence detection facilitate integration and automation.

Despite microfluidic chips for POCTs having been recently reviewed [40,77–82], as far as we know, very few articles have been written from the perspective of luminescence immunoassays. Besides, our review outlooks the future of the post-pandemic era in the coming years, strengthening the importance of monitoring the severity of COVID-19 in patients and treatment of sequelae. We first present immunological signatures of COVID-19 infection, emphasizing the necessity of immunoassays. Then we introduce microfluidic chips based on luminescence immunoassays, including heterogeneous and homogeneous immunoassays (Fig. 1). Given the importance of sensitivity, digital immunoassays based on luminescence are also discussed in this paper. We also describe the characteristics of the integrated microfluidic platforms. More specifically, the microfluidic devices for POC immunoassays of COVID-19 are highlighted, including antigen, antibody, cytokine storm, and combination tests. Finally, the challenges and future perspectives in the development of POCTs were discussed in depth.

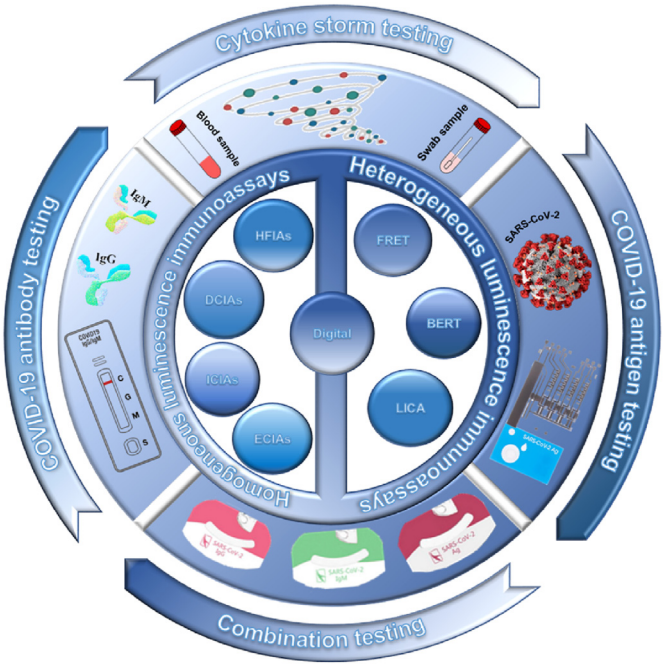

Fig. 1. Schematic illustration of luminescence immunoassays on microfluidic chips. (Reprinted with permission from Refs. [88,333,365]).

2. immunological signatures of the life cycles of COVID-19 in patients

It has been more than two years since the outbreak of COVID-19, but no effective antiviral drugs or treatments have been found. Early detection, diagnosis, reporting, isolation, and treatment are the most effective prevention and control means [5,83,84]. Compared with the first outbreak in Wuhan, we now have a more mature health care system and a better plan to cope with it. Omicron, the main circulating strain nowadays, is highly contagious and does little harm [85]. The vast majority of those infected are asymptomatic or mild. Diagnosis and treatment protocol for novel coronavirus pneumonia (Trial Version 9) does not require hospitalization for mild cases. However, we have to admit that the epidemic is still going on, and its effects will continue to be felt. As we can see in the post-pandemic era, the epidemic is far from over, and there are still local outbreaks. We need to establish a perfect coping mechanism to reduce the impact.

SARS-Cov-2 is a new coronavirus that binds to host cells' surface via spike proteins and is endocytosed into cells via clathrin-mediated membrane fusion [86–88]. Viruses that are not destroyed by non-specific immunity would be presented to T cells, stimulating the specific immune response. Then specific antibodies, including immunoglobulin G (IgG), immunoglobulin M (IgM), and so on, are produced to remove viruses in the form of immunocomplexes. Generally, IgM can be detected about a week after infection, while IgG comes after IgM at about two weeks [89,90]. When IgG gradually disappeared, IgM content reached its peak [91]. IgM is long-lasting and plays a major role in removing viruses and maintaining long-term immunity [92]. So antibodies in the blood are indirect evidence of COVID-19 infection and reveal the process.

When the immune system is overactivated, excess cytokines are

released, causing positive feedback, and leading to systemic inflammatory responses, eventually forming cytokine storms [28,93]. Studies have shown that cytokine storm is an important point in the transition from mild to severe and critical COVID-19, and is also a cause of death in severe and critical COVID-19 [29,94,95]. And it is well established that cytokine storm is highly correlated with the severity of COVID-19 symptoms and mortality [96–98]. Hence, real-time monitoring of cytokine levels greatly reduces the risk of COVID-19 patients. Another point is that sequelae exist in cured patients, especially in critically ill patients [99–102]. SARS-CoV-2 attacks the human nervous system, causing a proven loss of smell and taste [103–105]. In other words, sequelae from infected patients could become a global phenomenon. Hence, prognostic assessment or long-term monitoring is critical.

Although no antibodies are observed in the window period or even early infection, immunoassays still work to distinguish the remaining different stages of the infection [37,106,107]. Additionally, as mentioned above, antibodies can be monitored to ascertain the severity of the disease and recovery progress. Immunoassays are irreplaceable in assessments of severity, risks of cytokine storm, and outcomes of treatments.

3. Luminescence immunoassays on microfluidic chips

Based on whether labels are required to be isolated, immunoassays are divided into two major types: heterogeneous and homogeneous immunoassays [108]. The signal can be outputted directly without washing in homogeneous immunoassays [109]. In heterogeneous immunoassays, analytes are bound to solid substrates specifically for following cleaning and further readout.

Luminescence is a non-thermal emission of light from substances, including fluorescence, chemiluminescence and so on [110]. It is a process that occurs when photons of electromagnetic radiation are absorbed by molecules, raising them to some excited state, and then, on returning to a lower energy state, the molecules emit radiation or rather luminesce [111]. Luminescence has been engaged with immunoassays for POCTs in many fields.

3.1. Heterogeneous luminescence immunoassays on microfluidic chips

In heterogeneous luminescence immunoassays, identifiers, such as capture antibodies (cAbs) or antigens, are incubated on solid phases [112]. Then, analytes and labels are identified and fixed while the remaining free molecules are washed out. Hence, fixed luminescent labels can be used for quantitative analysis. Currently, heterogeneous luminescence immunoassays are widely-used methods of immunoassays that separate fixed labels to be measured from analysis systems before detection, such as well-known enzyme-linked immunoadsorption (ELISA) and chemiluminescence immunoassays [113–115].

3.1.1. Heterogeneous fluorescence immunoassays on microfluidic chips

Usually, heterogeneous fluorescence immunoassays (FIAs) use fluorescently labeled antigens or antibodies to localize, characterize, and quantify analytes by recognizing corresponding antigens or antibodies [79]. Fluorescent molecules as labels for detection show well practicability. The commonly used fluorescent labels are luciferin and rhodamine dyes. Take luciferin as an example, Zhao et al. developed an automated microfluidic system for rapid and quantitative analysis of chloramphenicol (CAP) via competitive immunoassays (Fig. 2A) [116]. Some self-driven microfluidic chips without additional actuators were also described [47,117]. Immunochromatographic assay (ICA) is a typical example with simplicity, and rapidity but uncontrollable flow rates [118–120]. To improve it, Hemmig et al. fabricated a capillary-driven microfluidic chip integrating a self-coalescence and a bead lane module to detect cardiac marker troponin I via one step sandwich FIAs (Fig. 2B) [121].

Besides traditional fluorescent molecules, some nanomaterials have also been widely employed for heterogeneous FIAs due to their excellent fluorescence properties, such as aggregation-induced emission (AIE) luminogens (AIEgens) [122–124], quantum dots (QDs) [125–127], upconversion nanoparticles (UCNPs) [128–130], and time-resolved fluorescent materials [73,131,132]. Unlike conventional fluorescent molecules, the luminescence intensity of AIEgens increases with the concentrations of labels without aggregation-caused quenching. AIEgen-based nanoparticles have been designed to obtain highly efficient luminescence for immunoassays [133–135]. Wu et al. reported a sensitive fluorescence ELISA platform based on AIEgens nanobeads for carcinoembryonic antigen (CEA) quantification [135]. In another work, Tang's group designed a dual-modality readout immunoassay platform based on AIEgens for EV71 virions detection (Fig. 2C) [136]. Two-channel detection has higher fault tolerance for more accurate analysis. Fluorescent microspheres, loading multiple fluorescent molecules, also serve as signal labels for extensive use. For COVID-19 tests combined with ICA, polystyrene nanoparticles loaded with 3.18×10^6 dyes ($AIE_{810}NP$) as luminous labels detected IgM or IgG in sequential clinical samples earlier than commercial gold nanoparticles (AuNPs) based test strips (Fig. 2D). [137].

QDs are nanoscale, low-dimensional semiconductor materials that have attracted attention with their desirable optical properties, such as broad excitation spectrum, narrow symmetric emission spectrum, precise tunability of emission peak, long fluorescence lifetime, photochemical stability, and negligible photobleaching [138–140]. QDs-ICA employs QDs as readout signals to increase sensitivity, which benefits from both ICA and QDs [46,127,141,142]. As shown in Fig. 3A, Huang et al. used compact and hierarchical magneto–fluorescent assemblies as both target-enrichment substrates and luminescent sensing labels for ICA [143]. Similarly, Zhou et al. developed a quantum dot nanobead-based ICA to detect SARS-CoV-2 total antibodies within 15 min [144]. The platform performed well in the dynamic monitoring of serum antibody levels in the whole course of SARS-CoV-2 infection with the sample added.

In addition, some enzyme-induced fluorescence substrates are also employed for fluorescent quantitation [145,146]. In particular, Reis's group developed a series of lab-on-a-stick platforms, which combined the simplicity of dipstick tests with the high performance of 10-bore fluoropolymer microcapillary microfluidic devices for heterogeneous FIAs [147–150]. To improve portability, they fabricated a new, simple, and affordable microfluidic platform with the assistance of a smartphone camera for *Escherichia coli* detection without sample preparation or concentration [151]. Quantitation was achieved by a highly sensitive fluorescence substrate, AttoPhos, cleaved by alkaline phosphatase (ALP) to produce bright green fluorescence when an analyte is enzymatically detected. To reduce manual steps, they also designed a power-free microfluidic device, called gravity-driven microfluidic siphons, for multiplex protein analysis (Fig. 3B) [152].

Compared with aforesaid down conversion fluorescent materials converting short-wavelength light into long-wavelength light, UCNPs capable of converting near-infrared excitation into ultraviolet or visible emissions exhibit significant advantages, such as narrow emission peaks, low toxicity, photobleaching resistance, and stability [154–156]. Notably, the luminescence of UCNPs requires near-infrared excitation without autofluorescence, largely improving the sensitivity [157]. Zhao et al. proposed an electro-driven ICA by electroosmotic flow (EOF) and UCNPs for rapid

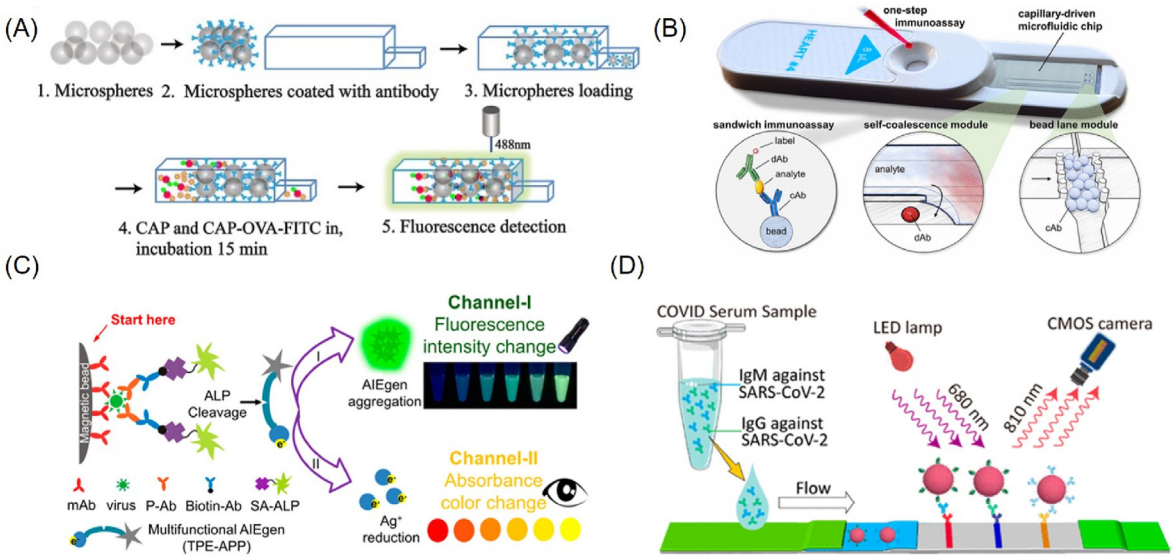

Fig. 2. (A) Schematic illustration of the competitive immunoassays on microfluidic chips for CRP detection. (Reprinted with permission from Ref. [116]). (B) Diagram of a test strip transformed into a capillary-driven microfluidic chip. (Reprinted with permission from Ref. [121]). (C) Schematic diagram of AIEgens for dual-modality readout immunoassays. (Reprinted with permission from Ref. [136]). (D) Schematic diagram of the AIE_{810}NP-based test strip for IgM, IgG against SARS-CoV-2 detection. (Reprinted with permission from Ref. [137]).

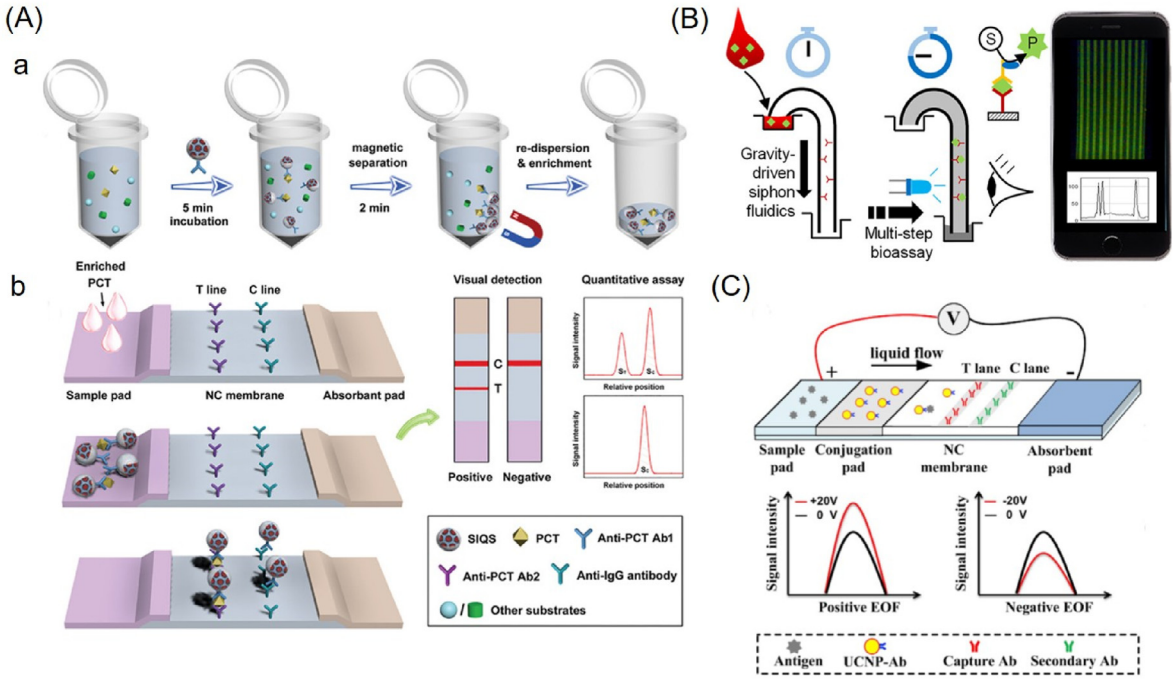

Fig. 3. (A) Schematic diagram of magneto–fluorescent assemblies for ICA. (a) Principle of PCT separation and enrichment. (b) Schematic illustration of the whole workflow of ICA and corresponding results. (Reprinted with permission from Ref. [143]). (B) Schematic diagram of gravity-driven microfluidic siphons for immunoassays with a mobile phone. (Reprinted with permission from Ref. [152]). (C) Schematic diagram of electro-driven ICA integrated with UCNPs. (a) Principle of the electro-driven ICA. (Reprinted with permission from Ref. [153]).

detection [153]. As demonstrated in Fig. 3C, signal intensities increased by 64.0% and time was reduced from 15 min to 5 min when EOF was in the same direction as the capillary force-driven flow. Besides, the emission wavelength of UCNPs can be adjusted by changing the type and doping ratio of rare-earth ions for multiplex detection [158–160]. Kazakova et al. described a novel multiplex microarray immunoassay to measure virus-specific IgG and IgM antibodies simultaneously [169]. In this platform, Erbium-UCNPs and thulium-UCNPs enabled 12 different spots for samples from different periods. This platform has potential for vaccine immunity studies with high throughput.

3.1.2. Heterogeneous chemiluminescence immunoassays on microfluidic chips

Chemiluminescence immunoassays (CLIAs) determine the content of analytes based on the intensity of the radiated light

produced by chemical reactions, integrating chemiluminescence with immunoassays. Heterogeneous CLIAs are novel immunological analytical methods for detecting trace amounts of protein with low backgrounds. No additional light sources are required in heterogeneous CLIAs, avoiding the interference of scattering light and luminescent impurities. Heterogeneous CLIAs have made great strides and have been extensively used in life sciences [161], clinical diagnosis [162,163], environmental monitoring [164,165], food safety [52,166], pharmaceutical analysis [167,168] and other fields, benefitting from their high sensitivity, wide linear range, no scattered light interference, no radioactive contaminants, and good reproducibility [169].

3.1.2.1. Direct chemiluminescence immunoassays on microfluidic chips. Direct chemiluminescence immunoassays (DCLIAs) require the direct labeling of antigens or antibodies with chemiluminescent agents [170,171]. Immunocomplexes are formed by utilizing the excellent specificity of antigen-antibody interactions. With the introduction of oxidant and pondus hydrogenii correction solution, chemiluminescence agents decompose and emit light for quantification [172]. Nowadays, isoluminol, acridine ester, and their derivatives are commonly used.

Lee's group designed aptamer-antibody on-chip sandwich immunoassays integrated with acridine ester for automated analysis [173–175]. Magnetic beads (MBs) modified with aptamers can not only capture but also separate analytes (Fig. 4A). Pump-driven pneumatic valves can be used for flow closure as well as drainage. Min. et al. reported an automated microfluidic chemiluminescence immunoassay platform for the quantitative detection of ferritin [176]. Besides acridine ester, 6-[N-(4-aminobutyl)-Nethylamino]-2,3-dihydro-1,4-phthalazinedione (ABEI) is also applied for DCLIAs. However, these chemiluminescence substrates exhibit flash-type light emission, which requires rapid signal acquisition. In addition, it is hard to distinguish simultaneous flashes, hindering further application for multiplex testing. To improve throughput without mutual interference, Cui's group devised a three-dimensional microfluidic paper-based device to simultaneously detect early acute myocardial infarction (AMI) biomarkers by Co^{2+}/ABEI functionalized magnetic carbon composites [177]. Three time-resolved chemiluminescence signals were generated in one chemiluminescence detection run by time-delayed transport of H_2O_2 to different detection zones (Fig. 4B). Another possible approach is turning flash into glow-type through controlled release. For instance, Wu et al. structured a doxorubicin-ABEI chimeric magnetic DNA hydrogel (MDH) as a novel protease-free and long-lasting chemiluminescence system (Fig. 4C) [178]. The MDH effectively delayed the diffusion rate of reactants because of the dense network structure and then transformed flash-type ABEI/H_2O_2/Co^{2+} reaction into a glow-type chemiluminescence system, making the chemiluminescence reaction gradually occur.

3.1.2.2. Indirect chemiluminescence immunoassays on microfluidic chips. Indirect chemiluminescence immunoassays (ICLIAs) are usually based on enzyme proteins labeling antigens or antibodies, which catalyze chemiluminescence agents to produce chemiluminescence signals for measurements [114,179]. Currently, the commonly used enzymes are horseradish peroxidase (HRP) and ALP. Liu's group designed an active droplet-array microfluidic system based on CLIAs to analyze procalcitonin (PCT) automatically (Fig. 5A) [174]. This platform employed ALP as chemiluminescence labels. In comparison, HRP was more commonly applied for ICLIAs. They also designed active droplet-array microfluidics with HRP labels for ICLIAs [180]. Dynamic solid-phase immunoassays with a pseudo-homogeneous format, where MBs coated with cAbs are dispersed in solution, enable fast and sensitive detection due to violent molecular diffusion [181]. Another option is traditional ELISA with cAbs pre-coated on the surface of microfluidic chips [182,183]. For example, Wang's group fabricated a microfluidic microarray immunoassay platform called BioIC, for the determination of 20-target allergens simultaneously (Fig. 5B) [184,185]. Furthermore, Jiang's group developed a microfluidic platform integrated with on-chip valves and CLIAs for the quantitative detection of multiple biomarkers (Fig. 5C) [186,187]. Then they introduced electrospun microfibers for improvements with larger specific surface areas compared with tin foil for dynamic multiplexed immunoassays [188]. Instead of actuators, self-driven is another choice. Dai et al. designed a flux-adaptable and self-contained microfluidic platform for automated CLIAs (Fig. 6A). [189]. In addition to quantitative analysis sample pretreatment, sample pretreatment is still required in microfluidic systems. Indeed, an ultra-sensitive detection device for proteins extracted from within single cells was developed and validated [190].

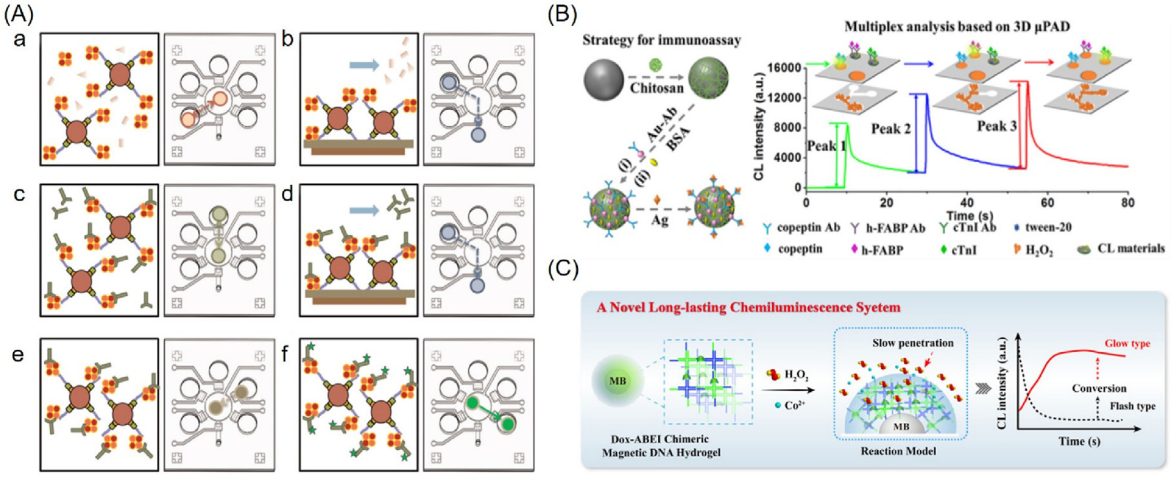

Fig. 4. DCLIAs on microfluidic chips. (A) Schematic illustration of the aptamer-antibody DCLIAs on the integrated microfluidic system. (a) Transfer of the MBs to the transportation unit for reaction. (b) Washing with phosphate buffer. (c) Transfer of acridinium ester-labeled antibodies to the transportation unit for reaction. (d) Washing with phosphate buffer once again. (e) Transfer of H_2O_2 to the transportation unit. (f) Transfer of the complexes to the NaOH chamber for chemiluminescence immunoassays. (Reprinted with permission from Ref. [174]). (B) Schematic illustration of three heart disease biomarkers by magnetic carbon composites and the three-dimensional microfluidic paper-based device. (Reprinted with permission from Ref. [177]). (C) Schematic diagram of novel long-lasting chemiluminescence system. (Reprinted with permission from Ref. [178]).

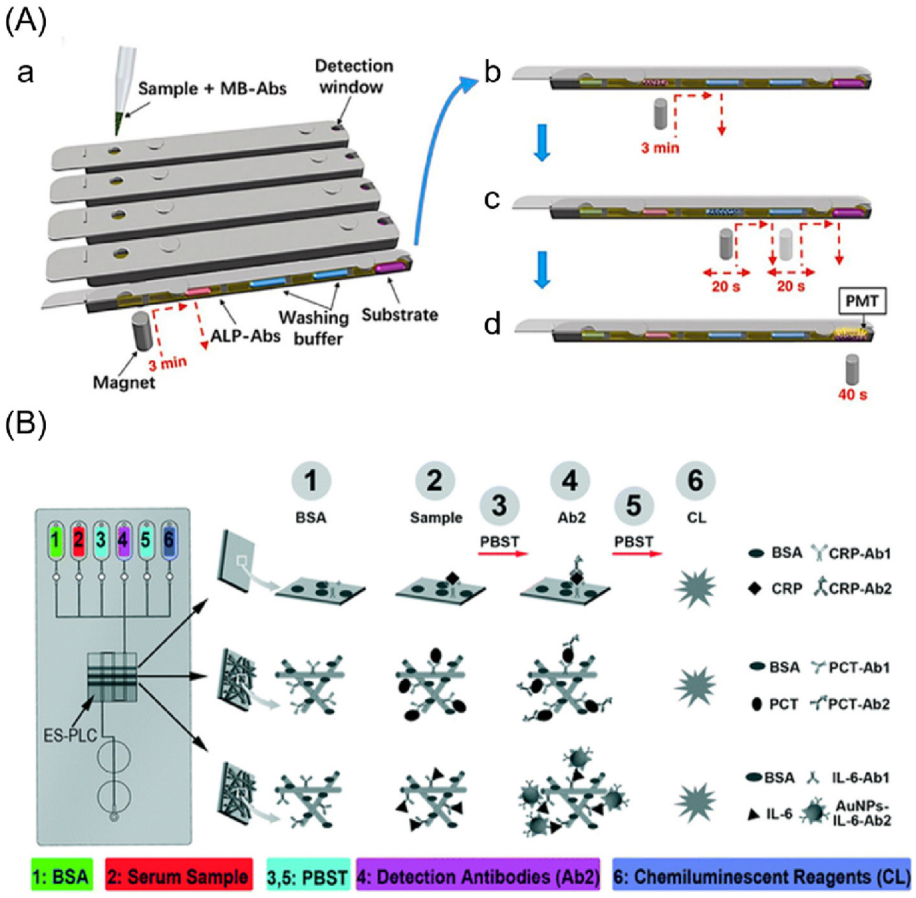

Fig. 5. (A) Workflow of active droplet-array microfluidics-based ICLIAs. (Reprinted with permission from Ref. [194]). (B) Schematic illustration of the on-chip valve-assisted microfluidic chip for multiple biomarkers with dynamic detection ranges. (Reprinted with permission from Ref. [188]).

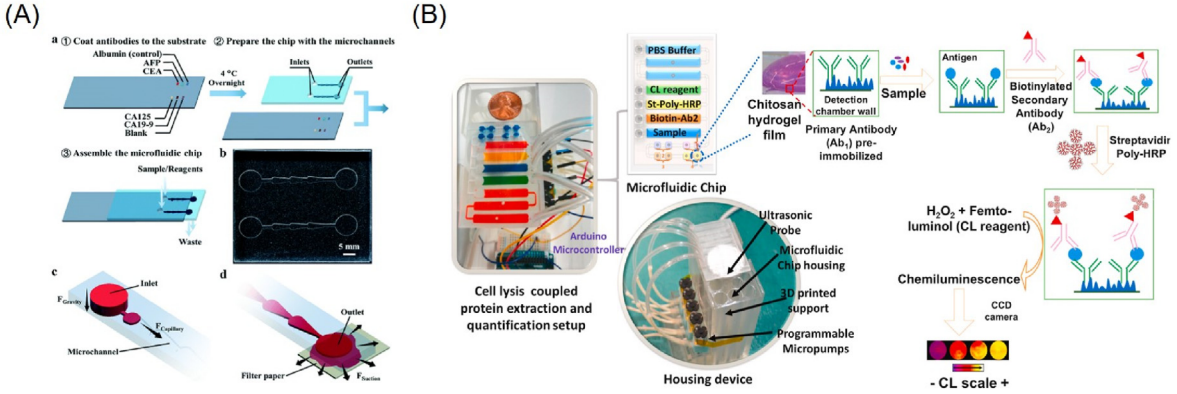

Fig. 6. (A) Schematic illustration of the flux-adaptable and pump-free microfluidic system. (Reprinted with permission from Ref. [189]). (B) Schematic illustration of the 3D-printed microfluidic chip with online cell lysis for biomarkers detection at single-cell levels. (Reprinted with permission from Ref. [190]).

Antibodies were immobilized on chitosan hydrogel film with an open-network 3D structure, which increased surface coverage and availability (Fig. 6B). It seems that dimensional structure is better for increasing sensitivity because of the high specific surface area [121,191–193].

3.1.2.3. Electrochemiluminescence immunoassays on microfluidic chips. Electrochemiluminescence is an energy-relaxation process by the optical emission of an excited molecule produced by an applied potential at an electrode surface [195–197]. Similar to chemiluminescence mentioned above, electrochemiluminescence has a low background as no light sources have been involved [195,198,199]. Since the electrochemiluminescence immunoassays (ECLIAs) are electrically induced, they are more controllable than chemiluminescence reactions involving uncontrollable reagents. Besides, due to the final balance between redox indicators, namely $[Ru(bpy)_3]^{3+}$ and $[Ru(bpy)_3]^{2+}$, the most widely used electrochemiluminescence labels, output signals with circle amplification are of high sensitivity and stability.

Chen et al. developed a paper-based electrochemiluminescence

method for hepatitis B surface antigen detection combined with screen-printed electrodes (Fig. 7A) [200]. They omitted to apply hydrophobic materials and complex reaction channels to avoid low transportation efficiency, not fully controllable flow direction and inaccurate positioning. However, such a simple design makes it hard to integrate. Valves play an important role in microfluidic chips for precisely controlling fluid movements [184–187]. Sun et al. described a novel rotational paper-based analytical device with integrated rotational valves for ECLIAs [201]. The "On/Off" states of valves were controlled by rotating the auxiliary disc and the washing disc (Fig. 7B). Nonetheless, low emission efficiency and the high cost of electrochemiluminescence are big problems [202]. Hence, new improvements are needed for the further application of ECLIAs. Since the electrochemiluminescence phenomenon of QDs was first observed during the study of silicon semiconductors in 2002 [203], many nanomaterial-based electrochemiluminescence emitters with different sizes, shapes, and compositions have been used for bioanalysis. Li et al. used modified hollow titanium dioxide hollow spheres (THS) and SnS_2 QDs to build novel ECLIAs for the ultrasensitive detection of CAP [204]. Additionally, Guo et al. synthesized several ruthenium and iridium complexes for multiplex immunoassays with different electrochemiluminescence emission wavelengths from 491 to 636 nm [205]. These new materials show great potential for electrochemiluminescence, whereas how to improve their properties, even for commercial use, is a big challenge.

3.2. Homogeneous luminescence immunoassays on microfluidic chips

In homogeneous immunoassays, quantitative analysis is achieved without extra steps, such as separation and washing [206,207]. With reagents added and mixed, signals could be read out after reactions. Luminescence resonance energy transfer (LRET) is one of the most common methods for homogeneous immunoassays [208]. It is a non-radiative energy transfer between a donor and an acceptor that occurs at a close enough distance (generally less than 10 nm) [209]. There are many kinds of LRET, mainly including fluorescence resonance energy transfer, bioluminescence resonance energy transfer, and chemiluminescence resonance energy transfer [208]. LRET has been applied widely for biomedical applications, such as clinical diagnosis, environmental monitoring,

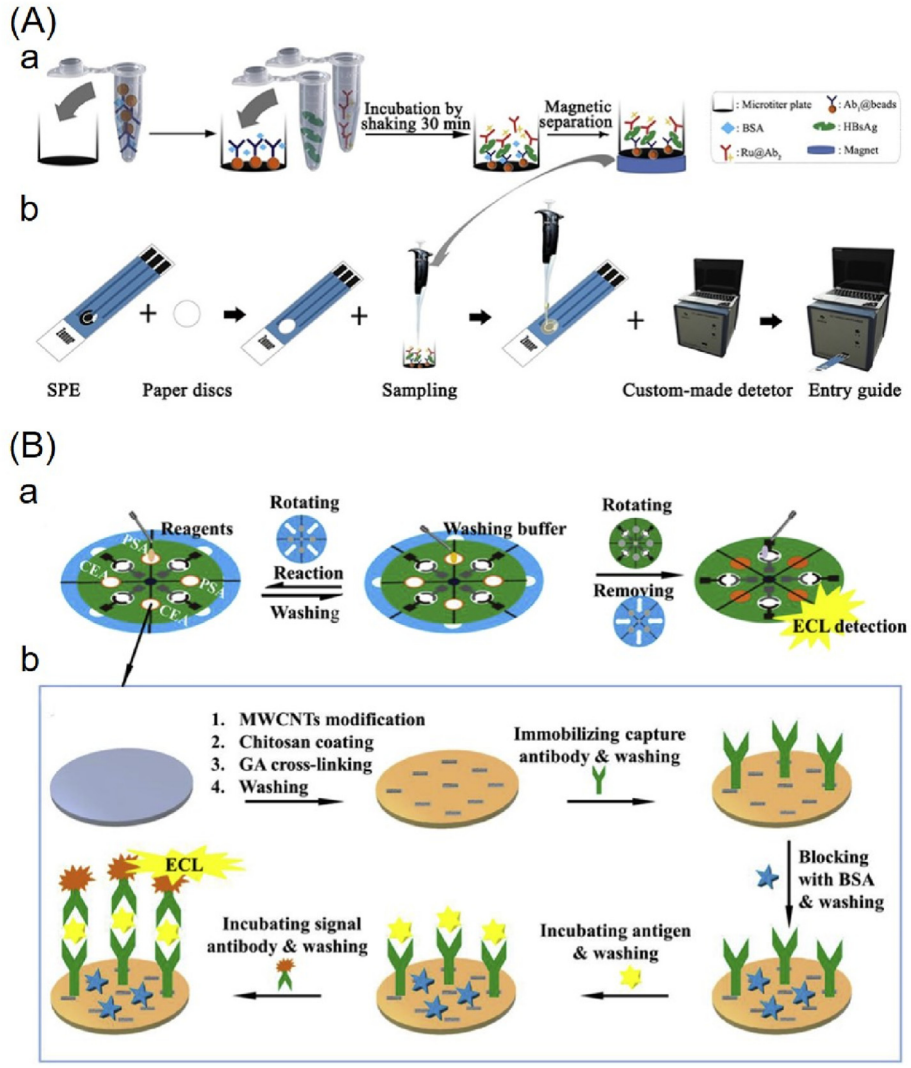

Fig. 7. ECLIAs on microfluidic chips. (A) Schematic illustration of the paper-based ECL biosensing platform. (a) Procedure of immunoassay in tubes. (b) Fabrication of paper-based screen-printed electrodes and matched detection device. (Reprinted with permission from Ref. [200]). (B) Schematic illustration of the rotational paper-based analytical device. (a) Step by step immunoassays controlled by the rotational valves. (b) The whole workflow of ECLIAs on the device (Reprinted with permission from Ref. [201]).

and food safety [210–212]. For bioassays, the donors and acceptors get close to each other by antibody-antigen interactions with LRET. The LRET process directly reveals the presence or absence of analytes with only one step. Sandwich immunoassays integrated with these techniques are homogeneous without washing. Compared with the above-mentioned heterogeneous immunoassays, these methods are much simpler. Besides, antibody incubation is not required, making it more suitable for integration and automation. Meanwhile, ratiometric sensors with a ratio value of the fluorescence intensity between receptors and donors have strong anti-interference abilities and more accurate analysis results.

3.2.1. Fluorescence resonance energy transfer immunoassays on microfluidic chips

FRET is a nonradiative process whereby an excited state donor (usually a fluorophore) transfers energy to a proximal ground-state acceptor through long-range dipole-dipole interactions [213]. FRET usually occurs over distances comparable to the dimensions of most biological macromolecules, that is, about 1–10 nm [214]. Notably, the emission spectrum of the donors ought to overlap with the absorption spectrum of the acceptors.

Samson et al. reported responsive FRET signals generated on paper for detecting cyclic AMP (cAMP)-specific phosphodiesterase 4B (PDE4B) inhibitory using inkjet-printing technology with four cartridges [215]. The principle was the competition between the europium (Eu) chelate-labeled cAMP tracer and sample cAMP for binding sites on cAMP-specific monoclonal antibodies labeled with the ULight dye on parchment paper. Compared with conventional fluorophores, time-resolved fluorophores generate signals with higher fluorescence intensity signal-to-noise ratio [216–219]. They use trivalent rare earth ions and their chelates as labels, which can achieve time-resolved imaging with a long fluorescence lifetime [218,220–222]. Time-resolved FIAs integrate time-resolved fluorescence with immunoassays, which exhibit high sensitivity and linearity [131,132,223]. For instance, Rusanen et al. designed a time-resolved FRET immunoassay platform for the detection of both N and S proteins of SARS-CoV-2 simultaneously [224]. A strong association between the sample infectivity and positive antigen test results was observed with high throughput. Nevertheless, sensitivity was lower than those of enzyme-based assays. It might be caused by interference of the sample matrix.

3.2.2. Bioluminescence resonance energy transfer immunoassays on microfluidic chips

Bioluminescent resonance energy transfer (BRET) was developed on the basis of FRET, which was first presented and used for the study of cyanobacterial biological clock proteins by Xu et al., in 1999 [225]. They used a bioluminescent luciferase rather than fluorophore as the donor. Bioluminescence appeared with luciferin substrate added, which served as an energy source for the receptors. Clearly, BRET immunoassays without external light sources are required to feature less background interference than FRET immunoassays.

Merkx's group designed a series of BRET platforms based on smartphones for protein quantification. They presented a new sensor platform called LUMABS, which were single-protein sensors consisting of the blue-light emitting luciferase NanoLuc connected via a semiflexible linker to the green fluorescent acceptor protein mNeonGreen [226]. The presence of analytes disrupted the interaction between the donors and acceptors, resulting in a large decrease in BRET efficiency. Then a fully integrated "sample-in-signal-out" microfluidic paper-based analytical device relying on LUMABS for analyte recognition and colorimetric signal generation was developed [227]. With only 20 μL sample added, the signals could be read out by a digital camera within 20 min, and results were available after simple processing. With improvements of chip design, they presented a thread-based analytical device for POCTs (Fig. 8A) [228]. LUMABS and furimazine were positioned on two intertwisted threads in close proximity to each other. Therefore, it achieved higher throughput with simpler paper chips.

3.2.3. Light initiated chemiluminescence immunoassays on microfluidic chips

Ullman et al. reported luminescent oxygen channeling immunoassays in 1994 for the first time [229]. Molecular oxygen is excited by a photosensitizer and an antenna dye, which diffuses to the second particle and initiates a chemiluminescent reaction. Thus, combined with immunoassays, energy transfer occurs between the two particles in the presence of analytes. On the

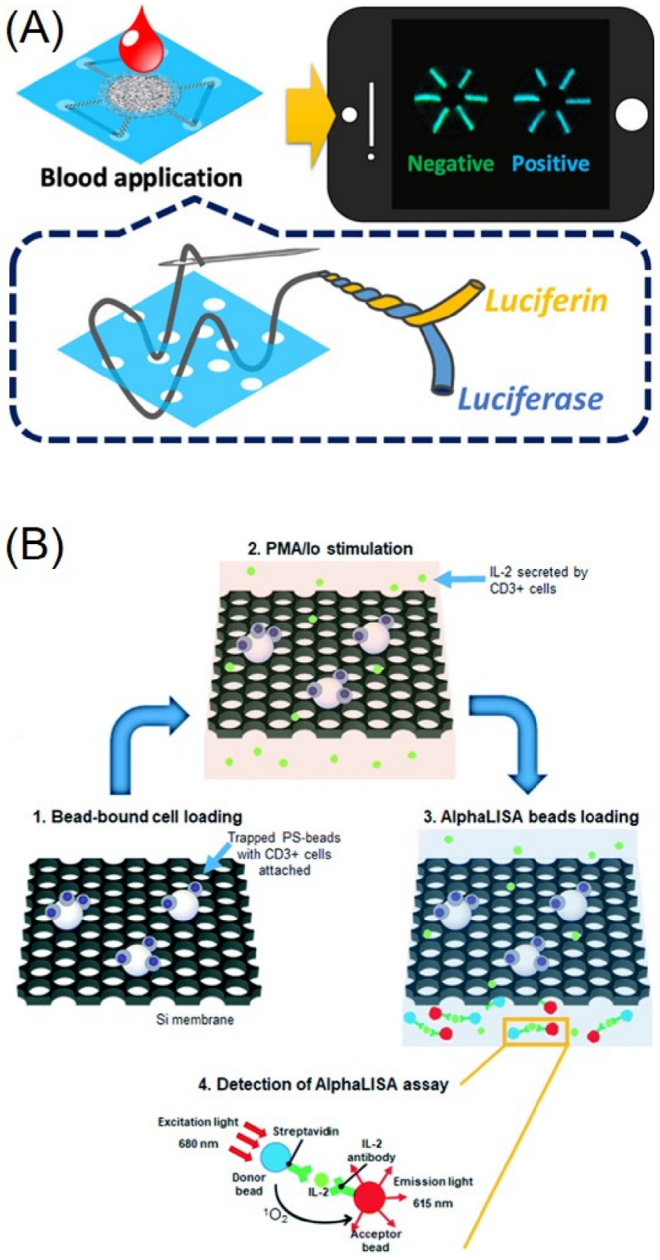

Fig. 8. LRET immunoassays on microfluidic chips. (A) Schematic illustration of BRET immunoassays on the microfluidic thread-based analytical devices with a mobile phone. (Reprinted with permission from Ref. [228]). (B) The on-chip immunophenotyping immunoassays by AlphaLISA. (Reprinted with permission from Ref. [234]).

contrary, no energy transfer and chemiluminescence appear as molecular oxygen decays. There are some commercial reagents for light-initiated chemiluminescence assay (LICA), such as AlphaScreen [230,231] and AlphaLISA [232,233]. LICA is a chemiluminescent immunoassay but quite different from heterogeneous chemiluminescence immunoassays. Multi-step incubation and washing are required for signal output without exciting light in heterogeneous CLIAs, while light and appropriate distance are requested in LICA.

Stephens et al. presented a batch-fabricated, robust, and mass-producible immunophenotyping microfluidic chip by silicon micromachining processes for specific leukocyte subset isolation immunophenotyping, and personalized immunomodulatory drug screening (Fig. 8D) [234]. The CD^{3+} Jurkat T-cells were isolated by beads, and cytokines were secreted into the immunoassay chamber. Then AlphaLISA with some modification on the chip was conducted for LICA.

3.3. Digital immunoassays on microfluidic chips

Some biomarkers have very low concentrations, lower than 10^{-12} M, which exceed the detection limit of conventional immunoassays [235,236]. In consideration of sensitivity, we then introduced digital immunoassays for quantitative analysis of low-abundance protein biomarkers. Digital immunoassays with millions of assays in parallel within femtoliter volume droplets were developed to overcome this concern. The essence of digital immunoassays is counting proteins to achieve absolute quantification with higher sensitivity and lower detection limit compared to conventional immunoassays [236–240]. Based on the way of forming droplets, digital immunoassays can be generally grouped into two categories based on the types of microfluidic chips: microstructured microfluidic chip [240–242] and droplet microfluidic chip [243–245]. Usually, digital immunoassays on microstructured microfluidic chips separate liquids by microchannels or microwells, while digital immunoassays on droplet microfluidic chips are performed by generating droplets with shear force change.

3.3.1. Digital immunoassays on microstructured microfluidic chips

The digital immunoassays on microstructured microfluidic chips seal nL-level liquid in microarrays for step-by-step immunoassays. The whole reaction process is similar to traditional microfluidic immunoassays, but in much more and smaller reaction chambers. MBs are widely used for immobilizing antibodies in digital immunoassays on microfluidic chips [246,247]. In particular, Kurabayashi's group proposed a pre-equilibrium digital ELISA microarray, which united a spatial-spectral microfluidic encoding scheme and an image data analysis algorithm based on machine learning for single-molecule protein digital counting (Fig. 9A) [241,248]. However, the cost, external magnetic field, high losses, and complex modification process hinder the further applications of MBs. Qian et al. performed bead-free digital immunoassays with polydopamine microspot arrays [249]. Then cAbs were incubated on the polydopamine arrays directly. The method has high sensitivity with a detection limit of 26 fg mL^{-1}. But compared to the bead-based digital assays, the current platform showed limited capture efficiency. In addition, chips with bead-based digital assays are potential for reuse, while chips modified with cAbs directly are one-off.

3.3.2. Digital immunoassays on droplet microfluidic chips

Digital immunoassays on droplet microfluidic chips are performed by generating discrete droplets containing reaction reagents. Droplet formation includes active and passive ways. The active approach applies an external force to microfluidics, including opto-electrowetting [250–252], magnetism [253–255], thermo-capillary forces [256,257], surface acoustic waves [258–260], dielectrophoresis (DEP) [261–263], electrowetting-on-dielectric (EWOD) [264–266], etc. However, these methods are suitable for manipulating droplets but not for massive droplet generation to meet digital immunoassays. The passive method generates droplets by adjusting the flow rate and channel structure, mainly including T-channel [267,268], flow focusing [145,269], and coaxial flow focusing [270,271]. Conventional droplet assays can generate a mass of monodisperse droplets but with low throughput. As an improvement, Yelleswarapu et al. designed a microdroplet Mega-scale Detector integrated with a parallelized microfluidic droplet generator for faster and multiple detections (Fig. 9B) [240]. Besides, combined with a mobile imaging technique based on cloud computing, this platform achieved throughputs as high as one million droplets per second. Usually, digital immunoassays improve sensitivity by counting single analytes dispersed in tens of thousands to millions of tiny units. However, it greatly decreases the sampling of rare events, leading to excessive Poisson noise. With this in mind, Wlat's group developed droplet digital ELISA to detect proteins in the low attomolar range [272]. The higher sensitivity was achieved by improving the sampling efficiency and counting more target molecules.

As illustrated in Table 1, homogeneous and heterogeneous luminescence immunoassays were compared, and their advantages and disadvantages were discussed. Heterogeneous luminescence immunoassays require solid phases for washing steps, greatly prolonging reaction time and increasing operation complexity, which place a high demand on the design of microfluidic chips and the automation of peripherals. But stepwise reactions reduce nonspecific adsorption to some extent, then sensitivity and specificity are improved. Homogeneous luminescence immunoassays with one step are easier to integrate. Nevertheless, impurities in the tests seriously affect the stability precision and repetition of the results. The hook effect also occurs in an improper proportion of antigens and antibodies, which leads to false-negative errors. Different immunoassays on microfluidic chips achieve effective protein detection but with non-negligible factors (Table 2). Heterogeneous FIAs suffer from a relatively high background in heterogeneous luminescence immunoassays, and new fluorescent molecules with improved optical properties are still a long way from commercial applications. Heterogeneous CLIAs with high sensitivity and wide detection range demand require a high level of imaging systems, and the stability of the reagent hinders further application. In contrast, heterogeneous CLIAs with high performance tend to replace heterogeneous FIAs gradually. Homogeneous immunoassays on microfluidic chips with one step require strict reagent and reaction conditions. LRET immunoassays with simple steps are easily disturbed by environmental sample impurities. But we have to realize that these homogeneous immunoassays with unique advantages are likely to become more widely used in the future. Digital immunoassays are of extremely high sensitivity but have a low degree of automation. Hence, more efforts will be focused on how to optimize these methods, integrate them into the POCTs, and further meet clinical needs.

4. Integrated microfluidic chip platforms

Microfluidic chip manufacturing technologies include soft lithography, injection molding, laser engraving, screen printing, and etc. As mentioned above, microfluidic chips integrated with different modules have been employed on sundry occasions, especially in POCTs. For example, Lansionbio Biotechnology Co., Ltd designed a series of active microfluidic platforms with controllable

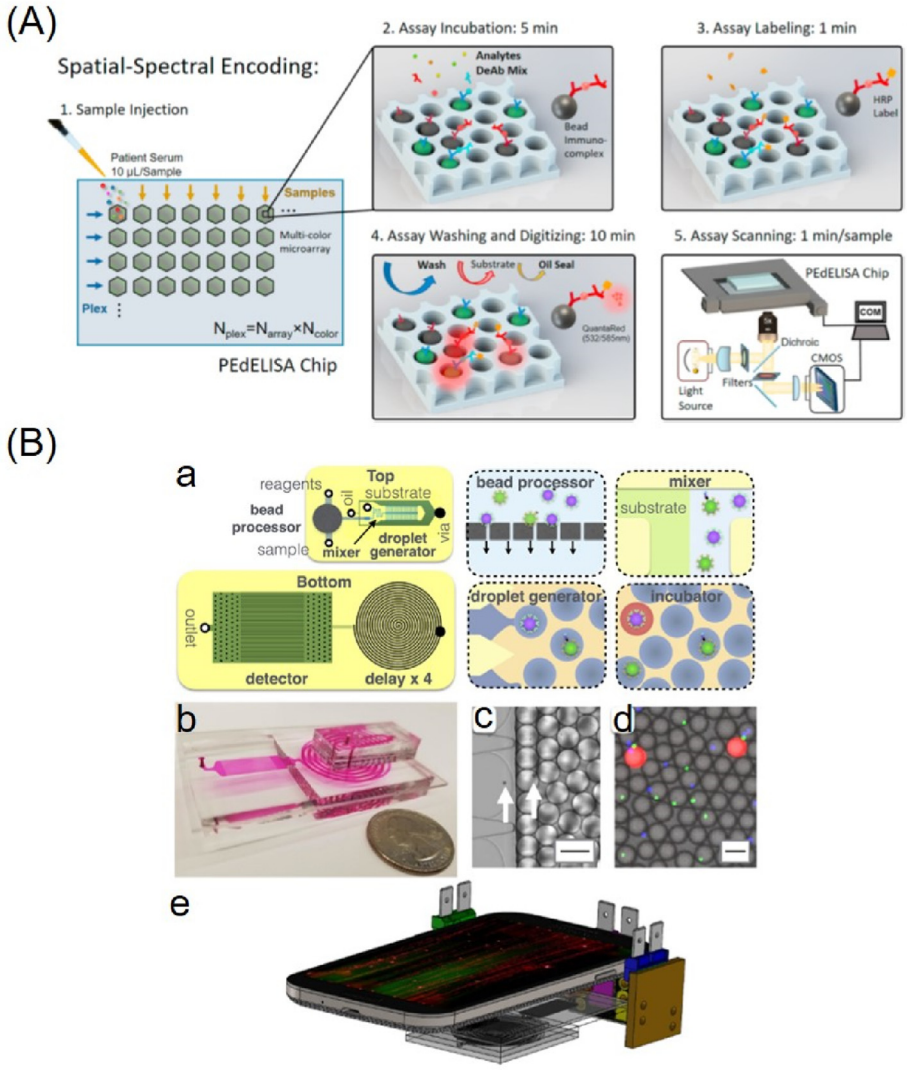

Fig. 9. Digital immunoassays on microfluidic chips. (A) Schematic illustration of multiplexed digital immunoassays on the microstructured microfluidic chip. (Reprinted with permission from Ref. [248]). (B) Design of the microdroplet Megascale Detector system. (a) The top view and bottom view of the chip. (b) Photograph of the chip. (c) Micrograph of the droplet generator encapsulate microbeads into droplets. (d) Fluorescence micrograph of the droplets. (e) Diagram of the system, including the microdroplet Megascale Detector chip and a mobile phone, and three light sources. (Reprinted with permission from Ref. [240]).

Table 1
Comparisons of d homogeneous and heterogeneous luminescence immunoassays.

Methods	Advantages	Disadvantages
Heterogeneous luminescence immunoassays	Low background, high specificity	Complex processing, multi-step washing
Homogeneous luminescence immunoassays	Simple processing without washing	Hook effect, weak anti-interference, high cost, high requirements for reagents

reaction time, flow direction and rate [273]. BluSense Diagnostics company developed centrifugal microfluidic discs-ViroTrack and portable medical testing platforms-BluBox for immunoassays with a drop of blood [274]. Herein, we summarize the types of various integrated microfluidic platforms which would contribute significantly to developing POCTs for the prevention and control of COVID-19. We also compare their characteristics, such as fabrication, principle, and design.

4.1. Lab on a cartridge chip (LOCC)

LOCC is the first micro total analysis system that integrates actuators or self-drive units for flow control. There are no specific requirements for distributing microfluidic channels and chambers, so LOCC with a small size has higher space utilization. It also has low demand for materials. LOCC with active actuators, such as pumps, is relatively less integrated, while LOCC with self-drive units is less stable but more convenient. Hence, it is quite necessary to establish a stable and convenient LOCC system for applications.

Capillary pumps consisting of small parallel microchannels provided main, reliable and adjustable power for self-driven. Gao et al. designed a pump-free LOCC platform based on a comb-like structure channel for driving fluids through the entire channel [275]. Similarly, Wang et al. fabricated a LOCC system integrated with nanorod arrays for flow-through immunoassays [276]. In

Table 2
Comparisons of different luminescence immunoassays.

Methods		Advantages		Disadvantages	
Heterogeneous fluorescence immunoassays	Fluorescent molecules	Low cost	High commercialization	High background	Aggregation caused quenching, photobleaching
	AIEgens		Aggregation induced emission		Synthetic complexity
	QDs		Broad excitation spectrum, tunable Spectroscopy		High toxicity, low water solubility
	Enzyme catalysis		Signal amplification		Enzyme activity effects
	UCNPs		Tunable spectroscopy, photobleaching resistance		Low upconversion efficiency
Heterogeneous chemiluminescence immunoassays	DCLIAs	High sensitivity, low background, wide linear dynamic ranges	High luminous intensity and efficiency	High requirements for imaging systems, enzyme activity effects	Low stability, short-lived luminescence
	ICLIAs		Long-lived luminescence, signal stabilization		High cost, weak anti-interference ability
	ECLIAs		High controllability		
LRET immunoassays	FRET BRET	Simple operation, no-wash	Low background	High cost, environmental sensitivity, hook effect	High background Low luminous intensity
	LICA		Multi-stage signal amplification		
Digitalimmunoassays	Microstructure	Low detection limit, absolute quantification	Rapid droplet generation	Complex platforms, low level of automation and integration	High requirements for fabricating microfluidic chips
	Droplet		Reusability		Requirements multiphase flow

another work, Machado et al. presented an autonomous and cascaded capillary chip aligned with a mobile application for parallel mycotoxin detection [277]. The speed can be adjusted by the size of corresponding capillary pumps. Besides microstructures serving as power for self-driven, gravity and suction are also applied for fluid control [152,278,279]. As shown in Fig. 10 A, Xiang et al. present a recyclable gravity-driven LOCC system for competitive immunoassays [278]. In the alternative, finger-driven microfluidic chips have attracted wide attention, eliminating the need for any skilled personnel with simple design and operation [35,280–282]. In particular, Lammertyn's group presented a new iSIMPLE (infusion Self-powered Imbibing Microfluidic Pump by Liquid Encapsulation) concept, which required liquid encapsulation and a finger-actuated mechanism [283–286]. As an example, they put it into use for therapeutic drug monitoring of adalimumab in patients diagnosed with autoimmune diseases [287]. Alternatively, pumps as external actuators are engaged for fluid control [190,288]. In consideration of unexpected air bubbles, air clogs, and irregular fluidic filling, Bhuiyan et al. designed an artificial intelligence-controlled LOCC system for fluid automation and bubble removal operated by a smartphone [278,289]. The AI image recognition app was implemented to ameliorate several inaccurate microfluidic states, thus resulting in lowering the limit of detection (LOD).

4.2. Lab on a disc (LOAD)

LOAD integrates all parts onto a compact disk (CD)-shaped chip, driven by centrifugal actuators, which was first proposed with the concept of LabCD [290,291]. Usually, microchannels are distributed radially, in the same direction as the centrifugal force. The fluids then move along the network of microchannels away from the center and toward the edge by the synthetic action of centrifugal

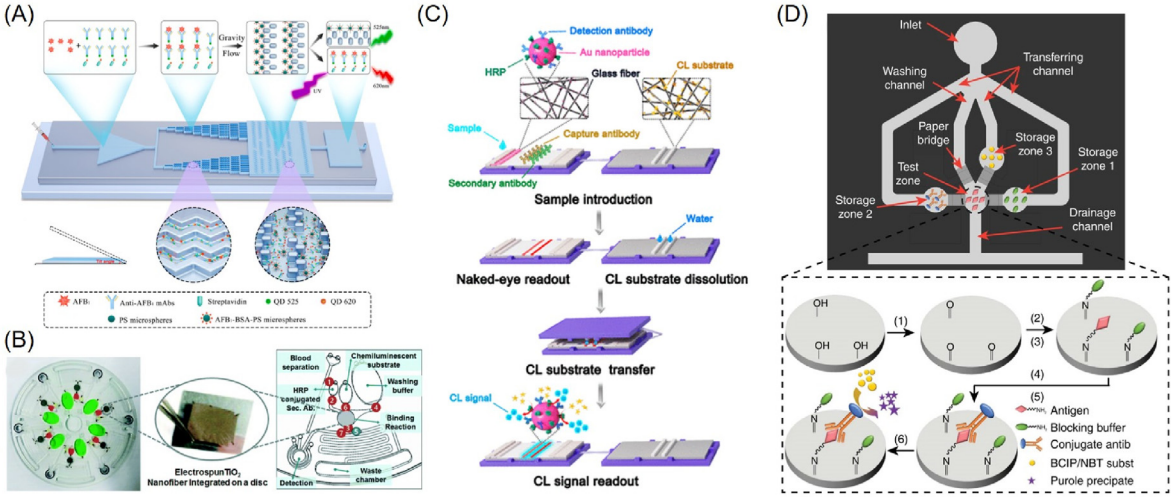

Fig. 10. Integrated microfluidic platforms. (A) Schematic illustration of the gravity-driven chip. (Reprinted with permission from Ref. [278]). (B) Photograph and schematic illustration of the fabricated LOAD. (Reprinted with permission from Ref. [296]). (C) Images of Scheme of the chemiluminescent LFIAs for the detection of targets. (Reprinted with permission from Ref. [312]). (D) Schematic diagrams of the μPADs design and the direct ELISA protocol. (Reprinted with permission from Ref. [318]).

forces, capillary forces, Euler forces and Coriolis forces [292–294]. Besides, mixture and washing are much easier by centrifugation and oscillation. Thus, microfluidics could be controlled by regulating speed of centrifugal actuators rather than pumps. It is easy to see that LOAD with simplex peripherals has a high degree of parallelization and a huge capacity for total integration [295].

Nowadays, plentiful LOAD systems have been developed for applications in immunoassays, nucleic acid assays, and biochemical analysis. Cho's group designed a LOAD system integrated with electrospun TiO_2 nanofiber and phase change valves for protein detection (Fig. 10B) [296]. By opening the valves one by one, reagents were moved from one chamber to another by centrifugal force, then immunoassays on LOAD were accomplished step by step [297]. In addition, TiO_2 nanofibers with high specific surface area and active functional groups capture large amounts of antibodies and improve detection sensitivity. Apart from physical excitation, Delgado et al. present an electrified LOAD (eLOAD) system permitting valve actuation during rotation by wireless control of rotor-based resistive heaters, which was also for additional flow control and sensing capabilities [298,299]. In another work, Xu's group designed an electromagnet-triggered pillar valve on LOAD for mycotoxin detection [300]. They also designed pinch-valves on LOAD based on magnetic actuation [301]. As an alternative, passive valves are easy to fabricate and simple to actuate with surface modification. For example, Xu's group fabricated an Euler force-assisted LOAD system for sequential liquid release [302]. They also put forward a centrifugation-assisted lateral flow immunoassay with enhanced sensitivity [303]. Combinations of passive valves and active valves are performed to play to their strengths and mitigate their weaknesses. Henderson et al. combined event-triggered dissolvable film valves with centrifugal-pneumatic siphon structure to control fluid flow [304]. Xu's group added pillar valves on the centrifugation-assisted lateral flow immunoassay platform mentioned above for better fluid control [305]. Although these have no requirements for additional pumps, they suffer from the unidirectional nature of the centrifugal force. That is the reason for the large size of LOAD as space utilization is relatively low. For more reliable applications, romero-Soto et al. presented another eLOAD system integrated with electrolysis pumps and reversible thermo-pneumatic valves [306]. The new 3D pump design occupied a much smaller space of the disc, which enabled the implementation of more fluidic components to automate complex sequential bioassays.

4.3. Lateral flow immunochromatographic assays (LFIAs)

A test strip for LFIAs consists of an absorbent pad, nitrocellulose membrane marked with test lines and control lines, conjugate pad embedded with detection antibodies, sample pad, adhesive backing, and base cover, which is the most classical POCTs based on immunoassays [307]. Generally, the whole detection procedure is as follows: a small volume of sample is dropped onto the sample pad, migrates on the conjugated pad, then carries conjugated particles to the test pad; Target antigens in the given sample are recognized and bonded with detection antibodies on reporter surface in the conjugated pad, where complexes interact with cAbs on test line and free reporters bound on control line [308]. In other words, the results can be obtained in one step after the sample added without additional operations. Because of their convenience, LFIAs have been commercialized in multiple areas, including COVID-19 antigen test.

AuNPs as labels for LFIAs with naked eye show relatively good performance [309]. Despite that, they suffer from low sensitivity and semi-quantity. To overcome it, a series of improvements, such as new materials, was introduced as mentioned above. AIEs, QDs, and UCNPs were synthesized as luminescent labels, and sensitivity was improved to varying degrees [76,127,130,137,143,153]. Nanohybrids, as labels, catalysts or for signal amplification, have enhanced the practical application of test strips [310,311]. Chemiluminescence was also contained by freeze-drying oxidants to achieve self-contained chemiluminescent LFIAs (Fig. 10C) [312]. In addition, mobile health platforms were established to read and transfer results [73,76,313]. Given throughput, scientists put arrays into use for LFIAs [117,314]. Particularly, Jiang's group embedded skiving stacked sheets of papers into test strips for rapid and multiplexed immunoassays [315]. These platforms showed great potential for practical clinical applications, but the stable materials and the matching equipment need to be developed or improved.

4.4. Microfluidic paper-based analytical devices (μPADs)

Whitesides's group firstly proposed paper-based microfluidic analytical devices (μPADs) for glucose and protein tests [316]. The working principle of μPADs is to build microchannels on paper for fluid control by physical and chemical methods. Typical physical methods are wax jet printing, ink jet printing, and screen printing, while chemical methods are chemical vapor deposition, photolithography, and plasma etching [317]. With the advantages of low cost, simple processing and convenience, μPADs have attracted widespread attention upon discovery and are widely used in medical diagnosis, environmental monitoring, food safety and other fields.

Fu et al. developed a paper-based microfluidic analytical device (μPAD) based on shape memory-polymer-actuated fluid valves for automated multi-step immunoassays (Fig. 10D) [318]. Reagents were preloaded on the storage zone, while a portable colorimetric reader was developed to control the on-chip valve operations, quantify the colorimetric signal output, display the results, and wirelessly transmit the data to a smart phone for the application of telemedicine. In another work, Chen et al. designed a three-dimensional surface-modified origami-paper-based analytical device (3D-soPAD) combined with a sliding strip as a valve to control the serial steps of sample addition, antigen-antibody interaction, incubation, washing, and detection of the ELISA reaction by simply sliding the tabs to a different position [54]. Besides sliding, rotating also has been employed for valve control. For example, Li et al. integrated hand-powered centrifugation with a rotational μPAD with blood-in-answer-out capability [319]. These platforms exhibited high operability, even for untrained users in environments where access to electricity cannot be assumed. Nevertheless, sensitivity and robustness need to be further improved.

The respective features of different microfluidic chip platforms are listed in Table 3. Although these platforms show great potential for POCTs, problems still exist in practical applications. LOCC, with its small size and various actuators, enables multivariate fluid control but suffers from complex peripherals and relatively low integration. LOAD driven by centrifugal actuators is of high throughput but large size. For μPADs, they display excellent performance at low cost, simple assembling and no extra actuators. However, they are limited as fluid control is single and not suitable for multilayer structures. LIFAs have been widely deployed in POCTs for commercial applications due to their low cost, rapidity, and simple and convenient operations, but they have limited capabilities to achieve accurate quantitative and high throughput analysis with relatively low specificity and sensitivity. We ought to admit that all existing platforms are problematic in dealing with the current situation. We need to simplify and optimize the whole process for user-friendly and high performance. Meanwhile, how to reduce cost is still considerable. Therefore, new or modified platforms are claimed to achieve “sample-in/result-out” analysis mode.

Table 3
Comparisons of different integrated microfluidic platforms.

Platforms	Advantages	Disadvantages
LOCC	**Multivariate fluid control, and small size**	**Complex processing, extra actuators with complex peripherals**
LOAD	Simplex actuators, parallelization, integration, and high throughput	Large size, and huge centrifugal actuators
LIFAs	Low cost, good compatibility, convenient operation, and rapidity	Relative low specificity, sensitivity, throughput and lake of fluid control
μPADs	Low cost, good compatibility, simple assembling, and no extra actuators	Simplex fluid control

5. Luminescence immunoassays for COVID-19 POCTs

The continuous widespread of COVID-19 has damaged not only the health of individuals but also the economy of the global society. So it is urgent to develop global wide POCTs targeting the COVID-19. Thankfully, scientists have made great efforts to develop practicable systems to get us through this mess [30,38,320,321]. At this stage, many immunoassays for the rapid detection of SARS-CoV-2 can be broadly divided into two categories. The first is direct detection of SARS-CoV-2 biomarkers, such as spike (S) glycoprotein, envelope (E) protein, nucleocapsid (N), and membrane (M) protein. The second is the detection of antibodies of the immune system responding to SARS-CoV-2, including IgG and IgM. Antibody levels reveal the staging of the body's immune response. Besides, cytokines as evaluation indicators reveal the severity of COVID-19. Next, we introduced some relatively mature microfluidic platforms based on these for the POCTs of COVID-19.

5.1. Luminescence immunoassays for COVID-19 antigen tests

SARS-CoV-2 encodes at least 29 proteins in its RNA genome, including four structural proteins: the S, M, E, and N proteins [322,323]. In particular, S protein plays a pivotal role of virus binding to host cell membrane receptors and membrane fusion and is a key therapeutic target for neutralizing antibodies and vaccine design [324–326]. Therefore, quantifying these antigen proteins is crucial for diagnosing, treating, preventing, and controlling COVID-19.

Up to now, scientists have developed a series of COVID-19 antigen detection platforms [327–330]. Among them, test strips are typical representatives. For example, Guo et al. proposed a UCNP-based ICA platform combining the Internet of Medical Things (IoMT) and 5G for proactive detection of S and N protein, with LOD of 1.6 ng mL^{-1} and 2.2 ng mL^{-1} for S and N protein [331]. Besides, the results were accessible to edge hardware devices through Bluetooth and transmitted to the fog layer of the network and 5G cloud server for both individuals and hospitals. Apart from capillary for self-driven, external force combined with magnetism also works. Lumiradx Co LTD designed a cheap microfluidic chip device for parallel immunoassays by polyethylene terephthalate screen printing technology (Fig. 11A) [332]. The microfluidic chip automatically controlled the movement of liquid in a single capillary by the different extrusions of the gas chamber to achieve accurate control of each reaction process. Take SARS-CoV-2 nucleocapsid immunoassays as an example [333]. The sample was introduced into the first chamber under negative pressure and nucleocapsid protein was captured by cAbs labeled MBs to form complexes. Analogously, the MB-cAb-NP compound bound to Latex labeled detection antibodies (dAbs) in the second chamber. Then the pressure of the gas chamber was fully released, and all reagents entered the detection chamber. The excess liquid was pressurized through the gas chamber and pumped out to the waste liquid chamber, while the Latex-dAb-NP-cAb-MB remained in the detection chamber via an extra magnetic field for fluorescence intensity quantification.

5.2. Luminescence immunoassays for COVID-19 antibody tests

COVID-19 antibody tests can monitor antibody levels produced by the body's humoral immune system, mainly for IgM and IgG antibodies [334–336]. For those vaccinated against COVID-19, antibody tests can reflect the immune state of the population and assess the effectiveness of the vaccine [337,338]. For those not, antibody tests can determine whether previously infected by SARS-CoV-2 and different stages of viral infection [339–341]. However, existing standards and traditional platforms are not enough. There is an urgent need to develop novel and practical POCTs for monitoring antibody levels.

The above-mentioned test strips were also used for antibody quantification [311,342]. Apart from capillary for self-driven, gravity works as well. Innovatively, Chilkoti's group developed DA-D4 POCTs for COVID-19 serology based on gravity and capillary (Fig. 11B) [343]. The sample was first introduced and filled with a reaction chamber. With wash buffer added, it slowly flowed through the time channel, and at the same time, immune complexes formed. The D4 assay was also designed by them before to interrogate multiple analytes from a drop of blood [344]. For antibodies targeting S1 and RBD, the sensitivity of DA-D4 assay reached 100% two weeks after symptom onset, while for antibodies targeting N is 96.3%. But between 6 and 14 days after symptom onset, the sensitivity was 78.9%, 89.5%, 78.9%, respectively. Maybe it's because of the low concentration of antibodies once after symptom onset. Centrifugal microfluidic chips are extensively used because of their high integration density, simple equipment and convenient operations [60,345,346]. For instance, VACURE Co LTD fabricated a LOAD immunoassay platform for detecting biomarkers, including SARS-CoV-2 IgM and IgG [347]. Reagents were freeze-dried and could be stored at room temperature for one year. Moreover, time-resolved fluorescence microspheres with large stokes shift and long decay time improved specificity. The whole test could be done within 18 min for nine parallel and independent tests.

5.3. Luminescence immunoassays for cytokine storm tests

Cytokine storm refers to the phenomenon of rapid and massive production of cytokines such as IL-6 in body fluids caused by microbial infection, which might cause acute respiratory distress syndrome, multiple organ failure, and even death [93]. There is clear evidence that COVID-19 patients, especially those with severe pneumonia, have high levels of inflammatory cytokines [348]. In other words, early detection and close monitoring of cytokine levels enable rapid identification of high-risk COVID-19 patients, which is crucial to assess the severity and improve survival rates [349,350]. Besides, cytokine storm enables predict COVID-19 severity and survival as hyper-inflammatory response induced by SARS-CoV-2 is a major cause of disease severity and death [351]. Hence, it is more than necessary to achieve highly accurate, sensitive, stable and fast immunoassays for cytokine storm tests.

Beckman Coulter, Inc. developed an ACCESS system based on ALP for CLIAs, including IL-6 [352]. Paramagnetic particles with a diameter 2–4 μm and sonic cleaning ensured the adequacy of the whole test. Meanwhile, the tectorial membrane reduces

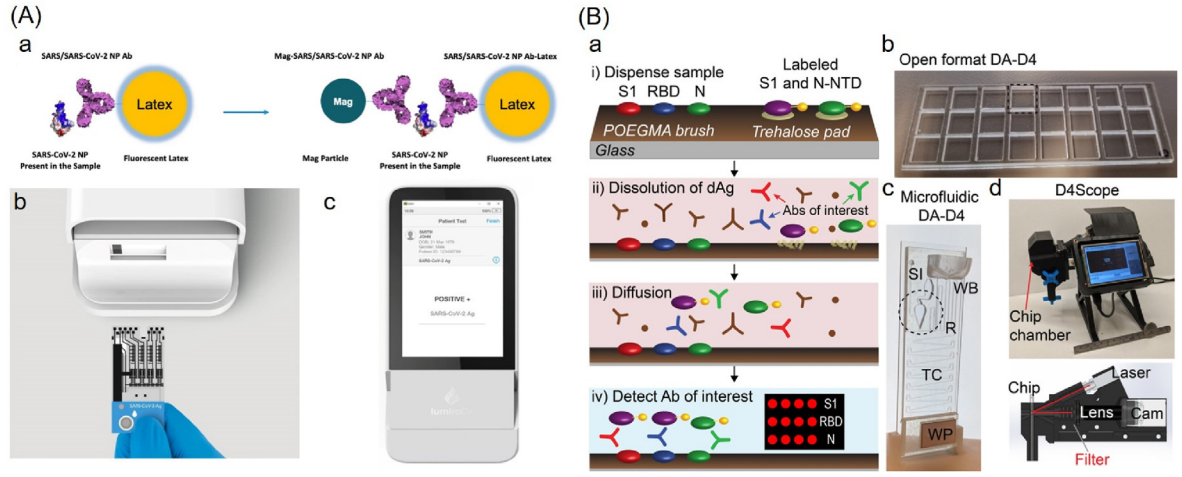

Fig. 11. Luminescence immunoassays for COVID-19 antigen or antibody tests. (A) Schematic illustration of the LumiraDx SARS-CoV-2 antigen assay. (a) Principle of the sandwich immunoassays. (b) Image of the LumiraDx system. (c) Image of instrument result screen. (Reprinted with permission from Ref. [333]). (B) Schematic illustration of DA-D4 POCT and analytical validation. (a) Principle of the sandwich immunoassays on the DA-D4. (b) Images of open format DA-D4. (c) Images of microfluidic DA-D4. (d) D4Scope and cut-away view of the optical path. (e) Analytical validation of the open-format DA-D4. (f) Analytical validation of microfluidic DA-D4. (g) Representative D4 detection spots. (Reprinted with permission from Ref. [343]).

volatilization of the stored liquid and can be directly mechanically punctured to reduce contamination. The shipboard microfluidic chips have low processing requirements but low integration degrees, which do not fully exploit the advantages of microfluidic chips. The above-mentioned pre-equilibrium digital ELISA system proposed by Kurabayashi's group has been applied to monitor COVID-19 cytokine storm clinically [353]. The digital assay worked as a promising candidate for continuous cytokine profiling with a combination of speed and sensitivity. As discussed, cytokines are highly correlated with the degree of COVID-19 inflammation, but still do not meet the diagnostic criteria for COVID-19. Thus, scientists need to grapple with the problem of measuring cytokine levels in COVID-19 patients.

5.4. Luminescence immunoassays for COVID-19 combination tests

As immunoassay platforms for protein quantification are of general applicability, numerous devices are suitable for antigen and antibody tests. One example is the programmable bio-nanochip (p-BNC) platform for biomarkers testing designed by McDevitt's group [354–358]. Inspired by the taste buds of the tongue, they developed an “electronic tongue” [359,360]. Agarose gel microspheres modified with antibodies are able to capture analytes and antibodies for quantification. The platform also used QDs as readout signals [361,362]. Phosphate buffer saline washing buffer is stored in two blisters, which are embedded in the microfluidic chips [356]. The movement of the fluid is controlled and stabilized by the actuator's piercing and pressing mechanism. Fluorescence signals obtained by CCD are then quantified by an algorithm and displayed through an interactive interface. The platform was also used for determining disease severity in patients with COVID-19 (Fig. 12A) [363]. The COVID-19 Severity Score was established to predict mortality and risk factor via combining multiplex biomarker measurements and a statistical learning algorithm. As a representative of LOAD system, Superchip Technology Co LTD developed a POC microfluidic platform integrated a homemade fluorescence analyzer for the detection of IgG/IgM/Antigen of SARS-CoV-2 within 15 min (Fig. 12B) [364]. The microfluidic chip consisted of a top layer with a sample loading chamber, a middle layer with a fluid channel, and a bottom layer with a waster reservoir [365]. Under the capillary effect, sample flow first flowed toward the

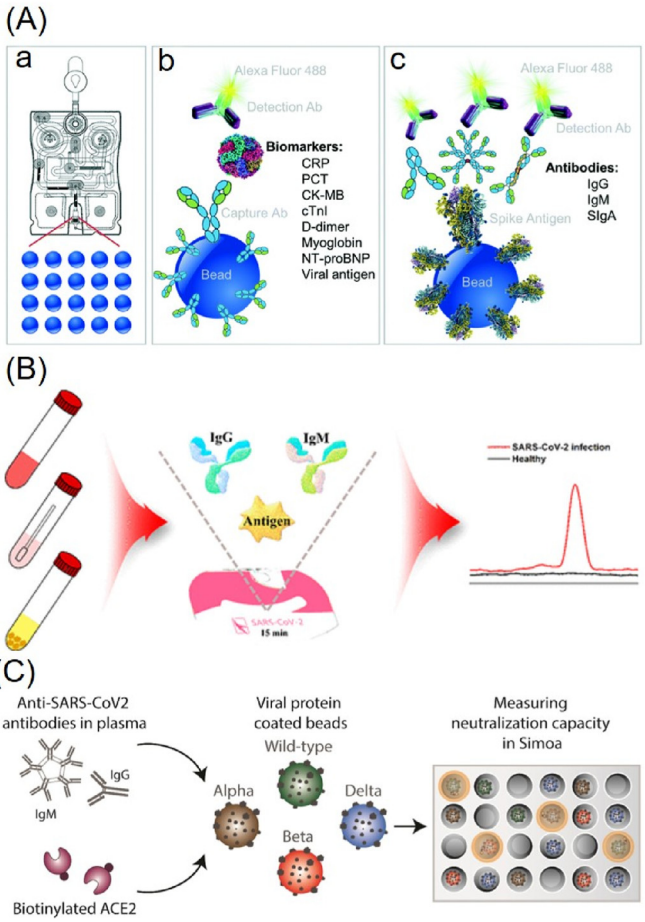

Fig. 12. Luminescence immunoassays for COVID-19 antigen and antibody tests. (A) Schematic illustration of the p-BNC platform for COVID-19 diagnostics. (a) The p-BNC platform with 20 spatially programmable bead sensors for (b) biomarkers and (c) antibodies detection. (Reprinted with permission from Ref. [363]). (B) Schematic illustration of the centrifugal microfluidic immunoassays for IgG, IgM, and antigen detection of SARS-CoV-2. (Reprinted with permission from Ref. [364]). (C) Schematic illustration of Simoa for neutralization assays against SARS-CoV-2. (Reprinted with permission from Ref. [372]).

Table 4
Comparisons of different luminescence immunoassays on microfluidic chips.

Detection Methods	Analytes	LOD	Time	Driving force	Fabrication	Immobilizing matrix	Year	Refs.
Heterogeneous fluorescence immunoassays	CAP	0.05 μg L^{-1}	20min	Pump	Soft lithography	Microspheres	2021	[116]
	cTnI	4 ng mL^{-1}	25min	Capillary force	Soft lithography	PMMA beads	2020	[121]
	EV71 virions	1.4 copiesμL^{-1}	–	Magnetism	–	MBs	2018	[136]
	COVID-19 IgM & IgG	0.236 μg mL^{-1} 0.125 μg mL^{-1}	10min	Capillary force	Paper	Nitrocellulose membrane	2021	[137]
	PCT	0.031 ng mL^{-1}	18min	Magnetism Capillary force	Paper	Nitrocellulose membrane	2021	[143]
	COVID-19 total antibodies	–	15 min	Capillary force	Paper	Nitrocellulose membrane	2021	[144]
	Escherichia coli	240 CFU mL^{-1}	25min	Syringe	Melt extrusion	Fluoropolymer	2019	[151]
	Yersinia pestis EV76	1.2 × 10^4CFU mL^{-1}	5min	Electro osmosis Capillary force	Paper	Nitrocellulose membrane	2020	[153]
	COVID-19S proteinN protein	1.6 ng mL^{-1} 2.2 ng mL^{-1}	10 min	Capillary force	Paper	Nitrocellulose membrane	2021	[331]
	COVID-19N protein	32$TCID_{50}$ mL^{-1}	12min	Magnetism Air pressure	Screen printing	MBs	2021	[333]
	COVID-19S1 proteinN proteinRBD	–	60min	Gravity Capillary force	Laser cutting	POEGMA brush	2021	[343]
	CRP NT-proBNP MYO D-dimer PCT CK-MB cTnI	–	16 min	Pressure	Injection molding	Agarose beads	2020	[363]
	COVID-19IgGIgMAntigen	–	15min	Centrifugal force Capillary force	Injection molding	PET membrane	2020	[364]
Heterogeneous Chemi-luminescence immunoassays	Hb	8.8 g dL^{-1}	25min	Pump	Soft lithography	MBs	2015	[174]
	HbA1c	0.65 g dL^{-1}						
	Ferritin	2.55 ng mL^{-1}	45min	Pump	Laser cutting	MBs	2018	[176]
	copeptin	0.40 pg mL^{-1}	–	Capillary force	Wax screen printing	Magnetic carbon composites	2019	[177]
	h-FABP	0.32 pg mL^{-1}						
	cTnI	0.50 pg mL^{-1}						
	PCT	0.044 ng mL^{-1}	12min	Magnetism	Injection molding 3D printing	MBs	2022	[194]
	IgE	2.4 ng mL^{-1}	27min	Pump	Injection molding	Nitrocellulose layer	2009	[184]
	CRP	1.87 μg mL^{-1}	70min	Pump	Injection molding	Tinfoil layer	2019	[188]
	PCT	0.17 ng mL^{-1}				Electrospun microfibers		
	IL-6	49.75 pg mL^{-1}						
	CEA	0.89 ng mL^{-1}	20min	Gravity, capillary force1.72 ng mL^{-1}	Soft lithography	Substrates	2021	[189]
	AFP	1.72 ng mL^{-1}						
	CA125	3.62 U mL^{-1}		3.62 U mL^{-1}1.05 U mL^{-1}				
	CA19-9	1.05 U mL^{-1}						
	DSG3	0.10 fg mL^{-1}	–	Pump	3D printing	Chitosan	2021	[190]
	VEGF-A	0.20 fg mL^{-1}						
	VEGF-C	0.20 fg mL^{-1}						
	β-Tub	0.20 fg mL^{-1}						
	CEA	0.07 ng mL^{-1}	–	Rotary force	Paper	Chitosan	2018	[201]
	PSA	0.03 ng mL^{-1}		Capillary force				
	anti-HIV1	2.8 nmol L^{-1}	20 min	Capillary force	Spraywax printing	–	2018	[200]
	anti-HA	7.1 nmol L^{-1}						
	anti-DEN1	19.3 nmol L^{-1}						
Homogeneous LRET immunoassays	anti-HIV	4.0 nmol L^{-1}	5min	Capillary force	Spraywax printing	–	2020	[228]
	anti-HA	2.1 nmol L^{-1}						
	anti-DEN	14.9 nmol L^{-1}						
	IL-2	75.4 pg mL^{-1}	–	Pump	Silicon micromachining	–	2019	[234]
Digital immunoassays	GM-CSF	320 amol mL^{-1}	–	Pump	Soft lithography	Fluorescent beads	2019	[240]
	IL-6	350 amol mL^{-1}						
	12 circulating cytokines	0.1–5 pg mL^{-1}	40min	Pump	Soft lithography	MBs	2021	[248]
	IL-6	1.2 fmol L^{-1}	–	Pump	Soft lithography	Polydopamine	2021	[249]
	IL-2	pg ml^{-1} level	2.5min	DEP	–	Fluorescently encoded beads	2021	[261]
	IL-6							
	IL-10							
	TNF-α							
	IFN-γ	30 amol mL^{-1}	–	Pump	Soft lithography	MBs	2020	[272]
	IL-2	20 amol mL^{-1}						
	SARS-CoV-2IgGN protein	0.015 ng mL^{-1} 0.099 pg mL^{-1}	More than 1h	Gravity Vacuum suction	Blu-ray	MBs	2021	[371]

capture region, forming fluorescent microsphere immunocomplexes. Then the complexes were immobilized by dAbs on the test region and control region. Next residual liquid in the channel was thrown into the waste chambers by centrifugation for 10 s without washing. Finally, the fluorescence detection results were read and obtained from the analyzer. With matrix nanospotting, parallel repeats were performed for stable and reliable results. As for CLIAs, Shenzhen Watmind Medical Co Ltd has designed a series of products, including M2/M5 microfluidic chemiluminescence immunoassay analyzer and microfluidic chips for COVID-19 antigen and antibody tests [366,367]. The microfluidic chip channel was a two-layer structure with reagents pre-stored. The upper channel was mainly for sample introduction, filtration, and reaction with dAbs. The lower channel was for washing twice and forming MB-cAb-analyte-dAb immunocomplex, including a reading chamber for the test. With analyzers involved, results were obtained in 13–15 min after the sample was added. Moreover, analyzers were built-in communication modules: GPS, 4G, Wireless Fidelity, Bluetooth, iCloud enable connecting with each other for long-distance monitoring [368]. As for digital immunoassays, Walt's group designed a digital ELISA platform, namely a single-molecule array (Simoa), for detecting serum proteins at subfemtomolar concentrations [369]. And then matched Simoa HD-1 analyzer was developed for automatical analysis [370]. The immunocomplexes linked to the magnetic beads were captured and sealed separately in the spiral-sized micropores on the Simoa disc composed of 24 arrays consisting of 216,000 40 fL-sized wells to achieve digital ELISA with much lower detection and higher sensitivity (Fig. 12C). This device was also adapted for COVID-19 detection with LOD of 0.015 ng mL^{-1} for IgG and 0.099 pg mL^{-1} for N protein [371–374].

6. Conclusion and future outlook

In this review, we have summarized luminescence immunoassays based on microfluidic chips for urgent POCTs of COVID-19. The typical examples are listed in Table 4 to provide a comparative discussion. Although many significant applications have been reported in the fields of luminescence immunoassays on microfluidic systems, they still need to be improved in specificity, dynamic range, sensitivity, throughput, portability, cost, and reproducibility in the future. Besides, false negative rates of immunoassays must not be ignored, particularly in the window period and early stage. Available immunoassay platforms for COVID diagnosis cannot meet the clinical needs with relatively high rates of missed and misdiagnoses. Excitingly, the emerging novel enzyme and nucleic acid-based signal enhancement strategies have significantly improved analytical performance of luminescence immunoassays, such as polymerized catecholamines depositing around HRP for cascade amplification [375,376], nucleic acid chains as labels for amplification [377–381], fluorescent-labeled aptamers based thermophoretic enrichment assays [192,382–386] and clustered regularly interspaced short palindromic repeat (CRISPR) based amplification [387,388]. In addition to methodology, the other perspective is miniaturization of equipment and intellectualization of performance, benefiting from the rapid development of the Internet, such as smartphones and 5G technology [313,331,389–393]. Finally, other than endpoint testing, real-time detecting systems, such as wearable devices, with continuous monitoring of processes can better meet the needs for POCTs on the progress of the immune response [394–398].

Declaration of competing interest

The authors declare that they have no known competing financial interests or personal relationships that could have appeared to influence the work reported in this paper.

Data availability

No data was used for the research described in the article.

Acknowledgments

This work was supported by the National Key Research and Development Program of China (2021YFA1101500), the National Natural Science Foundation of China (22074047, 21775049), and the Fundamental Research Funds for Central Universities, HUST (2020kfyXJJS034, 2021GCRC056).

References

[1] WHO Coronavirus (COVID-19) Dashboard. https://covid19.who.int/(accessed 17 January, 2022).
[2] D. Zhou, W. Dejnirattisai, P. Supasa, C. Liu, A.J. Mentzer, H.M. Ginn, Y. Zhao, H.M.E. Duyvesteyn, A. Tuekprakhon, R. Nutalai, B. Wang, G.C. Paesen, C. Lopez-Camacho, J. Slon-Campos, B. Hallis, N. Coombes, K. Bewley, S. Charlton, T.S. Walter, D. Skelly, S.F. Lumley, C. Dold, R. Levin, T. Dong, A.J. Pollard, J.C. Knight, D. Crook, T. Lambe, E. Clutterbuck, S. Bibi, A. Flaxman, M. Bittaye, S. Belij-Rammerstorfer, S. Gilbert, W. James, M.W. Carroll, P. Klenerman, E. Barnes, S.J. Dunachie, E.E. Fry, J. Mongkolsapaya, J. Ren, D.I. Stuart, G.R. Screaton, Evidence of escape of SARS-CoV-2 variant B.1.351 from natural and vaccine-induced sera, Cell 184 (9) (2021) 2348–2361. e2346.
[3] P. Han, L. Li, S. Liu, Q. Wang, D. Zhang, Z. Xu, P. Han, X. Li, Q. Peng, C. Su, B. Huang, D. Li, R. Zhang, M. Tian, L. Fu, Y. Gao, X. Zhao, K. Liu, J. Qi, G.F. Gao, P. Wang, Receptor binding and complex structures of human ACE2 to spike RBD from omicron and delta SARS-CoV-2, Cell 185 (4) (2022) 630–640. e610.
[4] Y. Cao, J. Wang, F. Jian, T. Xiao, W. Song, A. Yisimayi, W. Huang, Q. Li, P. Wang, R. An, J. Wang, Y. Wang, X. Niu, S. Yang, H. Liang, H. Sun, T. Li, Y. Yu, Q. Cui, S. Liu, X. Yang, S. Du, Z. Zhang, X. Hao, F. Shao, R. Jin, X. Wang, J. Xiao, Y. Wang, X.S. Xie, Omicron escapes the majority of existing SARS-CoV-2 neutralizing antibodies, Nature 602 (7898) (2022) 657–663.
[5] S. Lai, N.W. Ruktanonchai, L. Zhou, O. Prosper, W. Luo, J.R. Floyd, A. Wesolowski, M. Santillana, C. Zhang, X. Du, H. Yu, A.J. Tatem, Effect of non-pharmaceutical interventions to contain COVID-19 in China, Nature 585 (7825) (2020) 410–413.
[6] N.A. Alwan, R.A. Burgess, S. Ashworth, R. Beale, N. Bhadelia, D. Bogaert, J. Dowd, I. Eckerle, L.R. Goldman, T. Greenhalgh, D. Gurdasani, A. Hamdy, W.P. Hanage, E.B. Hodcroft, Z. Hyde, P. Kellam, M. Kelly-Irving, F. Krammer, M. Lipsitch, A. McNally, M. McKee, A. Nouri, D. Pimenta, V. Priesemann, H. Rutter, J. Silver, D. Sridhar, C. Swanton, R.P. Walensky, G. Yamey, H. Ziauddeen, Scientific consensus on the COVID-19 pandemic: we need to act now, Lancet 396 (10260) (2020) e71–e72.
[7] K. Sun, W. Wang, L. Gao, Y. Wang, K. Luo, L. Ren, Z. Zhan, X. Chen, S. Zhao, Y. Huang, Q. Sun, Z. Liu, M. Litvinova, A. Vespignani, M. Ajelli, C. Viboud, H. Yu, Transmission heterogeneities, kinetics, and controllability of SARS-CoV-2, Science 371 (6526) (2021), eabe2424.
[8] M. Lisboa Bastos, G. Tavaziva, S.K. Abidi, J.R. Campbell, L.P. Haraoui, J.C. Johnston, Z. Lan, S. Law, E. MacLean, A. Trajman, D. Menzies, A. Benedetti, F. Ahmad Khan, Diagnostic accuracy of serological tests for covid-19: systematic review and meta-analysis, BMJ 370 (2020) m2516.
[9] W.J. Wiersinga, A. Rhodes, A.C. Cheng, S.J. Peacock, H.C. Prescott, Pathophysiology, transmission, diagnosis, and treatment of coronavirus disease 2019 (COVID-19): a review, JAMA 324 (8) (2020) 782–793.
[10] B. Udugama, P. Kadhiresan, H.N. Kozlowski, A. Malekjahani, M. Osborne, V.Y.C. Li, H. Chen, S. Mubareka, J.B. Gubbay, W.C.W. Chan, Diagnosing COVID-19: the disease and tools for detection, ACS Nano 14 (4) (2020) 3822–3835.
[11] F. Cui, H.S. Zhou, Diagnostic methods and potential portable biosensors for coronavirus disease 2019, Biosens. Bioelectron. 165 (2020), 112349.
[12] K. Li, J. Wu, F. Wu, D. Guo, L. Chen, Z. Fang, C. Li, The clinical and chest CT features associated with severe and critical COVID-19 pneumonia, Invest. Radiol. 55 (6) (2020) 327–331.
[13] Z.Y. Zu, M.D. Jiang, P.P. Xu, W. Chen, Q.Q. Ni, G.M. Lu, L.J. Zhang, Coronavirus disease 2019 (COVID-19): a perspective from China, Radiology 296 (2) (2020) E15–E25.
[14] T. Ai, Z. Yang, H. Hou, C. Zhan, C. Chen, W. Lv, Q. Tao, Z. Sun, L. Xia, Correlation of chest CT and RT-PCR testing for coronavirus disease 2019 (COVID-19) in China: a report of 1014 cases, Radiology 296 (2) (2020) E32–E40.
[15] N. Stogiannos, D. Fotopoulos, N. Woznitza, C. Malamateniou, COVID-19 in the radiology department: what radiographers need to know, Radiography 26 (3) (2020) 254–263.
[16] V.M. Corman, O. Landt, M. Kaiser, R. Molenkamp, A. Meijer, D.K. Chu, T. Bleicker, S. Brünink, J. Schneider, M.L. Schmidt, D.G. Mulders, B.L. Haagmans, B. van der Veer, S. van den Brink, L. Wijsman, G. Goderski, J.-L. Romette, J. Ellis, M. Zambon, M. Peiris, H. Goossens, C. Reusken,

M.P. Koopmans, C. Drosten, Detection of 2019 novel coronavirus (2019-nCoV) by real-time RT-PCR, Euro Surveill. 25 (3) (2020), 2000045.
[17] X. Wang, X.Z. Hong, Y.W. Li, Y. Li, J. Wang, P. Chen, B.F. Liu, Microfluidics-based strategies for molecular diagnostics of infectious diseases, Military Med. Res. 9 (1) (2022) 11.
[18] J.A. Berkenbrock, R. Grecco-Machado, S. Achenbach, Arsenal of microfluidic testing devices may combat COVID-19 pandemic, MRS Bull. 45 (7) (2020) 511–514.
[19] J.J. Deeks, J. Dinnes, Y. Takwoingi, C. Davenport, R. Spijker, S. Taylor-Phillips, A. Adriano, S. Beese, J. Dretzke, L. Ferrante di Ruffano, I.M. Harris, M.J. Price, S. Dittrich, D. Emperador, L. Hooft, M.M. Leeflang, A. Van den Bruel, C.-D.T.A.G. Cochrane, Antibody tests for identification of current and past infection with SARS-CoV-2, Cochrane Database Syst. Rev. 6 (2020) CD013652.
[20] A. Bryan, G. Pepper, M.H. Wener, S.L. Fink, C. Morishima, A. Chaudhary, K.R. Jerome, P.C. Mathias, A.L. Greninger, A.J. McAdam, Performance characteristics of the abbott architect SARS-CoV-2 IgG assay and seroprevalence in boise, Idaho, J. Clin. Microbiol. 58 (8) (2020). e00941-00920.
[21] Y. Pan, X. Li, G. Yang, J. Fan, Y. Tang, J. Zhao, X. Long, S. Guo, Z. Zhao, Y. Liu, H. Hu, H. Xue, Y. Li, Serological immunochromatographic approach in diagnosis with SARS-CoV-2 infected COVID-19 patients, J. Infect. 81 (1) (2020) e28–e32.
[22] R. Rodriguez-Moncayo, D.F. Cedillo-Alcantar, P.E. Guevara-Pantoja, O.G. Chavez-Pineda, J.A. Hernandez-Ortiz, J.U. Amador-Hernandez, G. Rojas-Velasco, F. Sanchez-Munoz, D. Manzur-Sandoval, L.D. Patino-Lopez, D.A. May-Arrioja, R. Posadas-Sanchez, G. Vargas-Alarcon, J.L. Garcia-Cordero, A high-throughput multiplexed microfluidic device for COVID-19 serology assays, Lab Chip 21 (1) (2021) 93–104.
[23] D. Liu, F. Wu, Y. Cen, L. Ye, X. Shi, Y. Huang, S. Fang, L. Ma, Comparative research on nucleocapsid and spike glycoprotein as the rapid immunodetection targets of COVID-19 and establishment of immunoassay strips, Mol. Immunol. 131 (2021) 6–12.
[24] Y. Hirotsu, M. Maejima, M. Shibusawa, Y. Nagakubo, K. Hosaka, K. Amemiya, H. Sueki, M. Hayakawa, H. Mochizuki, T. Tsutsui, Y. Kakizaki, Y. Miyashita, S. Yagi, S. Kojima, M. Omata, Comparison of automated SARS-CoV-2 antigen test for COVID-19 infection with quantitative RT-PCR using 313 nasopharyngeal swabs, including from seven serially followed patients, Int. J. Infect. Dis. 99 (2020) 397–402.
[25] L.J. Carter, L.V. Garner, J.W. Smoot, Y. Li, Q. Zhou, C.J. Saveson, J.M. Sasso, A.C. Gregg, D.J. Soares, T.R. Beskid, S.R. Jervey, C. Liu, Assay techniques and test development for COVID-19 diagnosis, ACS Cent. Sci. 6 (5) (2020) 591–605.
[26] T. Kilic, R. Weissleder, H. Lee, Molecular and immunological diagnostic tests of COVID-19: current status and challenges, iScience 23 (8) (2020), 101406.
[27] C. Sheridan, Fast, portable tests come online to curb coronavirus pandemic, Nat. Biotechnol. 38 (5) (2020) 515–518.
[28] R. Karki, T.D. Kanneganti, The 'cytokine storm': molecular mechanisms and therapeutic prospects, Trends Immunol. 42 (8) (2021) 681–705.
[29] L. Yang, X. Xie, Z. Tu, J. Fu, D. Xu, Y. Zhou, The signal pathways and treatment of cytokine storm in COVID-19, Signal Transduct. Targeted Ther. 6 (1) (2021) 255.
[30] Q. Song, X. Sun, Z. Dai, Y. Gao, X. Gong, B. Zhou, J. Wu, W. Wen, Point-of-care testing detection methods for COVID-19, Lab Chip 21 (9) (2021) 1634–1660.
[31] M.M. Wei, H.H. Rao, Z.R. Niu, X. Xue, M.Y. Luo, X.Y. Zhang, H.Y. Huang, Z.H. Xue, X.Q. Lu, Breaking the time and space limitation of point-of-care testing strategies: photothermometric sensors based on different photothermal agents and materials, Coord. Chem. Rev. 447 (2021), 214149.
[32] A. Sharma, A.I.Y. Tok, P. Alagappan, B. Liedberg, Point of care testing of sports biomarkers: potential applications, recent advances and future outlook, TrAC, Trends Anal. Chem. 142 (2021), 116327.
[33] J.Q. Deng, X.Y. Jiang, Advances in reagents storage and release in self-contained point-of-care devices, Adv. Mater. Technol. 4 (6) (2019), 1800625.
[34] S. Sachdeva, R.W. Davis, A.K. Saha, Microfluidic point-of-care testing: commercial landscape and future directions, Front. Bioeng. Biotechnol. 8 (2020), 602659.
[35] P. Chen, C. Chen, H. Su, M. Zhou, S. Li, W. Du, X. Feng, B.-F. Liu, Integrated and finger-actuated microfluidic chip for point-of-care testing of multiple pathogens, Talanta 224 (2021), 121844.
[36] A.H. Ng, U. Uddayasankar, A.R. Wheeler, Immunoassays in microfluidic systems, Anal. Bioanal. Chem. 397 (3) (2010) 991–1007.
[37] M. Tayyab, M.A. Sami, H. Raji, S. Mushnoori, M. Javanmard, Potential microfluidic devices for COVID-19 antibody detection at point-of-care (POC): a review, IEEE Sensor. J. 21 (4) (2021) 4007–4017.
[38] M. Yafia, O. Ymbern, A.O. Olanrewaju, A. Parandakh, A. Sohrabi Kashani, J. Renault, Z. Jin, G. Kim, A. Ng, D. Juncker, Microfluidic chain reaction of structurally programmed capillary flow events, Nature 605 (7910) (2022) 464–469.
[39] A. Manz, N. Graber, H.M. Widmer, Miniaturized total chemical analysis systems: a novel concept for chemical sensing, Sensor. Actuator. B Chem. 1 (1) (1990) 244–248.
[40] Y. Yang, Y. Chen, H. Tang, N. Zong, X. Jiang, Microfluidics for biomedical analysis, Small Methods 4 (4) (2020), 1900451.
[41] Y. Xiao, S. Li, Z. Pang, C. Wan, L. Li, H. Yuan, X. Hong, W. Du, X. Feng, Y. Li, P. Chen, B.-F. Liu, Multi-reagents dispensing centrifugal microfluidics for point-of-care testing, Biosens. Bioelectron. 206 (2022), 114130.
[42] B. Li, L. Yu, J. Qi, L. Fu, P. Zhang, L. Chen, Controlling capillary-driven fluid transport in paper-based microfluidic devices using a movable valve, Anal. Chem. 89 (11) (2017) 5707–5712.
[43] H. Xiong, X. Ye, Y. Li, J. Qi, X. Fang, J. Kong, Efficient microfluidic-based air sampling/monitoring platform for detection of aerosol SARS-CoV-2 on-site, Anal. Chem. 93 (9) (2021) 4270–4276.
[44] B. Dai, S.J. Chen, W. Li, L.L. Zheng, X.D. Han, Y.F. Fu, J.D. Wu, F. Lin, D.W. Zhang, S.L. Zhuang, Fully-functional semi-automated microfluidic immunoassay platform for quantitation of multiple samples, Sensor. Actuator. B Chem. 300 (2019), 127017.
[45] G. Zou, X. Tan, X. Long, Y. He, W. Miao, Spectrum-resolved dual-color electrochemiluminescence immunoassay for simultaneous detection of two targets with nanocrystals as tags, Anal. Chem. 89 (23) (2017) 13024–13029.
[46] M. Franke, S. Leubner, A. Dubavik, A. George, T. Savchenko, C. Pini, P. Frank, D. Melnikau, Y. Rakovich, N. Gaponik, A. Eychmuller, A. Richter, Immobilization of pH-sensitive CdTe quantum dots in a poly(acrylate) hydrogel for microfluidic applications, Nanoscale Res. Lett. 12 (1) (2017) 314.
[47] A. Khodayari Bavil, J. Kim, A capillary flow-driven microfluidic system for microparticle-labeled immunoassays, Analyst 143 (14) (2018) 3335–3342.
[48] S.A. Jadhav, P. Biji, M.K. Panthalingal, C. Murali Krishna, S. Rajkumar, D.S. Joshi, N. Sundaram, Development of integrated microfluidic platform coupled with Surface-enhanced Raman Spectroscopy for diagnosis of COVID-19, Med, Hypotheses 146 (2021), 110356.
[49] Q. Xiong, C.Y. Lim, J. Ren, J. Zhou, K. Pu, M.B. Chan-Park, H. Mao, Y.C. Lam, H. Duan, Magnetic nanochain integrated microfluidic biochips, Nat. Commun. 9 (1) (2018) 1743.
[50] X. Wang, L. Zhou, G. Wei, T. Jiang, J. Zhou, SERS-based immunoassay using a core–shell SiO2@Ag immune probe and Ag-decorated NiCo2O4 nanorods immune substrate, RSC Adv. 6 (1) (2016) 708–715.
[51] L. Huang, L. Ding, J. Zhou, S. Chen, F. Chen, C. Zhao, J. Xu, W. Hu, J. Ji, H. Xu, G.L. Liu, One-step rapid quantification of SARS-CoV-2 virus particles via low-cost nanoplasmonic sensors in generic microplate reader and point-of-care device, Biosens. Bioelectron. 171 (2021), 112685.
[52] H. Bhardwaj, G. Sumana, C.A. Marquette, A label-free ultrasensitive microfluidic surface Plasmon resonance biosensor for Aflatoxin B1 detection using nanoparticles integrated gold chip, Food Chem. 307 (2020), 125530.
[53] R. Funari, K.Y. Chu, A.Q. Shen, Detection of antibodies against SARS-CoV-2 spike protein by gold nanospikes in an opto-microfluidic chip, Biosens. Bioelectron. 169 (2020), 112578.
[54] C.A. Chen, W.S. Yeh, T.T. Tsai, Y.D. Li, C.F. Chen, Three-dimensional origami paper-based device for portable immunoassay applications, Lab Chip 19 (4) (2019) 598–607.
[55] Y. Liu, Y. Tan, Q. Fu, M. Lin, J. He, S. He, M. Yang, S. Chen, J. Zhou, Reciprocating-flowing on-a-chip enables ultra-fast immunobinding for multiplexed rapid ELISA detection of SARS-CoV-2 antibody, Biosens. Bioelectron. 176 (2021), 112920.
[56] J. Reboud, G. Xu, A. Garrett, M. Adriko, Z. Yang, E.M. Tukahebwa, C. Rowell, J.M. Cooper, Paper-based microfluidics for DNA diagnostics of malaria in low resource underserved rural communities, Proc. Natl. Acad. Sci. U.S.A. 116 (11) (2019) 4834–4842.
[57] D. Liu, Y. Zhang, M. Zhu, Z. Yu, X. Ma, Y. Song, S. Zhou, C. Yang, Microfluidic-integrated multicolor immunosensor for visual detection of HIV-1 p24 antigen with the naked eye, Anal. Chem. 92 (17) (2020) 11826–11833.
[58] L. Zheng, G. Cai, S. Wang, M. Liao, Y. Li, J. Lin, A microfluidic colorimetric biosensor for rapid detection of Escherichia coli O157:H7 using gold nanoparticle aggregation and smart phone imaging, Biosens. Bioelectron. 124–125 (2019) 143–149.
[59] I. Michael, D. Kim, O. Gulenko, S. Kumar, S. Kumar, J. Clara, D.Y. Ki, J. Park, H.Y. Jeong, T.S. Kim, S. Kwon, Y.K. Cho, A fidget spinner for the point-of-care diagnosis of urinary tract infection, Nat. Biomed. Eng 4 (6) (2020) 591–600.
[60] C.T. Lin, S.H. Kuo, P.H. Lin, P.H. Chiang, W.H. Lin, C.H. Chang, P.H. Tsou, B.R. Li, Hand-powered centrifugal microfluidic disc with magnetic chitosan bead-based ELISA for antibody quantitation, Sensor. Actuator. B Chem. 316 (2020), 128003.
[61] D. Liu, X. Li, J. Zhou, S. Liu, T. Tian, Y. Song, Z. Zhu, L. Zhou, T. Ji, C. Yang, A fully integrated distance readout ELISA-Chip for point-of-care testing with sample-in-answer-out capability, Biosens. Bioelectron. 96 (2017) 332–338.
[62] M.S. Draz, N.K. Lakshminaraasimulu, S. Krishnakumar, D. Battalapalli, A. Vasan, M.K. Kanakasabapathy, A. Sreeram, S. Kallakuri, P. Thirumalaraju, Y. Li, S. Hua, X.G. Yu, D.R. Kuritzkes, H. Shafiee, Motion-based immunological detection of zika virus using Pt-nanomotors and a cellphone, ACS Nano 12 (6) (2018) 5709–5718.
[63] C. Ren, Q. Bayin, S. Feng, Y. Fu, X. Ma, J. Guo, Biomarkers detection with magnetoresistance-based sensors, Biosens. Bioelectron. 165 (2020), 112340.
[64] Y. Gao, W. Huo, L. Zhang, J. Lian, W. Tao, C. Song, J. Tang, S. Shi, Y. Gao, Multiplex measurement of twelve tumor markers using a GMR multi-biomarker immunoassay biosensor, Biosens. Bioelectron. 123 (2019) 204–210.
[65] Y. Shen, S. Modha, H. Tsutsui, A. Mulchandani, An origami electrical biosensor for multiplexed analyte detection in body fluids, Biosens. Bioelectron. 171 (2021), 112721.
[66] A. Jones, P. Czarnecki, L. Dhanapala, J.F. Rusling, Multiplexed protein biomarker detection with microfluidic electrochemical immunoarrays, Methods Mol. Biol. 2237 (2021) 69–82.
[67] E. Cesewski, B.N. Johnson, Electrochemical biosensors for pathogen

detection, Biosens. Bioelectron. 159 (2020), 112214.
[68] T. Kalyani, A. Sangili, A. Nanda, S. Prakash, A. Kaushik, S. Kumar Jana, Bio-nanocomposite based highly sensitive and label-free electrochemical immunosensor for endometriosis diagnostics application, Bio-electrochemistry 139 (2021), 107740.
[69] J. Yang, K. Wang, H. Xu, W. Yan, Q. Jin, D. Cui, Detection platforms for point-of-care testing based on colorimetric, luminescent and magnetic assays: a review, Talanta 202 (2019) 96–110.
[70] Q. Lin, Z. Li, Q. Yuan, Recent advances in autofluorescence-free biosensing and bioimaging based on persistent luminescence nanoparticles, Chin. Chem. Lett. 30 (9) (2019) 1547–1556.
[71] J. Wang, Q. Ma, Y. Wang, H. Shen, Q. Yuan, Recent progress in biomedical applications of persistent luminescence nanoparticles, Nanoscale 9 (19) (2017) 6204–6218.
[72] Q.Y. Xie, Y.H. Wu, Q.R. Xiong, H.Y. Xu, Y.H. Xiong, K. Liu, Y. Jin, W.H. Lai, Advantages of fluorescent microspheres compared with colloidal gold as a label in immunochromatographic lateral flow assays, Biosens. Bioelectron. 54 (2014) 262–265.
[73] Z. Liu, Q. Hua, J. Wang, Z. Liang, J. Li, J. Wu, X. Shen, H. Lei, X. Li, A smartphone-based dual detection mode device integrated with two lateral flow immunoassays for multiplex mycotoxins in cereals, Biosens. Bio-electron. 158 (2020), 112178.
[74] X. Tang, P. Li, Q. Zhang, Z. Zhang, W. Zhang, J. Jiang, Time-resolved fluorescence immunochromatographic assay developed using two idiotypic nanobodies for rapid, quantitative, and simultaneous detection of aflatoxin and zearalenone in maize and its products, Anal. Chem. 89 (21) (2017) 11520–11528.
[75] M.A. Antoniak, D. Wawrzyńczyk, J.K. Zaręba, M. Samoć, M. Nyk, Spectrally resolved two-photon absorption properties and switching of the multi-modal luminescence of NaYF4:Yb,Er/CdSe hybrid nanostructures, J. Mater. Chem. C 6 (22) (2018) 5949–5956.
[76] F. Mousseau, C. Feraudet Tarisse, S. Simon, T. Gacoin, A. Alexandrou, C.I. Bouzigues, Luminescent lanthanide nanoparticle-based imaging enables ultra-sensitive, quantitative and multiplexed in vitro lateral flow immuno-assays, Nanoscale 13 (35) (2021) 14814–14824.
[77] Y.Z. Tao, H.C. Shen, K.Y. Deng, H.M. Zhang, C.Y. Yang, Microfluidic devices with simplified signal readout, Sensor. Actuator. B Chem. 339 (2021), 129730.
[78] A. Parihar, P. Ranjan, S.K. Sanghi, A.K. Srivastava, R. Khan, Point-of-Care biosensor-based diagnosis of COVID-19 holds promise to combat current and future pandemics, ACS Appl. Bio Mater. 3 (11) (2020) 7326–7343.
[79] C. Wang, M. Liu, Z. Wang, S. Li, Y. Deng, N. He, Point-of-care diagnostics for infectious diseases: from methods to devices, Nano Today 37 (2021), 101092.
[80] J. Liu, Z. Geng, Z. Fan, J. Liu, H. Chen, Point-of-care testing based on smart-phone: the current state-of-the-art (2017-2018), Biosens. Bioelectron. 132 (2019) 17–37.
[81] X. Qin, J. Liu, Z. Zhang, J. Li, L. Yuan, Z. Zhang, L. Chen, Microfluidic paper-based chips in rapid detection: current status, challenges, and perspec-tives, TrAC, Trends Anal. Chem. 143 (2021), 116371.
[82] W. Chen, F. Shao, Y. Xianyu, Microfluidics-implemented biochemical assays: from the perspective of readout, Small 16 (9) (2020), e1903388.
[83] Y. Fang, Y. Nie, M. Penny, Transmission dynamics of the COVID-19 outbreak and effectiveness of government interventions: a data-driven analysis, J. Med. Virol. 92 (6) (2020) 645–659.
[84] F.-S. Wang, C. Zhang, What to do next to control the 2019-nCoV epidemic? Lancet 395 (10222) (2020) 391–393.
[85] H. Brussow, COVID-19: omicron - the latest, the least virulent, but probably not the last variant of concern of SARS-CoV-2, Microb. Biotechnol. 15 (7) (2022) 1927–1939.
[86] G.R. Whittaker, S. Daniel, J.K. Millet, Coronavirus entry: how we arrived at SARS-CoV-2, Curr. Opin. Virol. 47 (2021) 113–120.
[87] A. Bayati, R. Kumar, V. Francis, P.S. McPherson, SARS-CoV-2 infects cells after viral entry via clathrin-mediated endocytosis, J. Biol. Chem. 296 (2021), 100306.
[88] S. Ornes, Science and Culture: the evolving portrait of a virus, Proc. Natl. Acad. Sci. U.S.A. 118 (29) (2021), e2111544118.
[89] J. Wu, B. Liang, C. Chen, H. Wang, Y. Fang, S. Shen, X. Yang, B. Wang, L. Chen, Q. Chen, Y. Wu, J. Liu, X. Yang, W. Li, B. Zhu, W. Zhou, H. Wang, S. Li, S. Lu, D. Liu, H. Li, A. Krawczyk, M. Lu, D. Yang, F. Deng, U. Dittmer, M. Trilling, X. Zheng, SARS-CoV-2 infection induces sustained humoral immune re-sponses in convalescent patients following symptomatic COVID-19, Nat. Commun. 12 (1) (2021) 1813.
[90] Y. Fu, Y. Li, E. Guo, L. He, J. Liu, B. Yang, F. Li, Z. Wang, Y. Li, R. Xiao, C. Liu, Y. Huang, X. Wu, F. Lu, L. You, T. Qin, C. Wang, K. Li, P. Wu, D. Ma, C. Sun, G. Chen, Dynamics and correlation among viral positivity, seroconversion, and disease severity in COVID-19 : a retrospective study, Ann. Intern. Med. 174 (4) (2021) 453–461.
[91] M. Tre-Hardy, A. Wilmet, I. Beukinga, J. Favresse, J.M. Dogne, J. Douxfils, L. Blairon, Analytical and clinical validation of an ELISA for specific SARS-CoV-2 IgG, IgA, and IgM antibodies, J. Med. Virol. 93 (2) (2021) 803–811.
[92] G.A. Roth, V. Picece, B.S. Ou, W. Luo, B. Pulendran, E.A. Appel, Designing spatial and temporal control of vaccine responses, Nat. Rev. Mater. 7 (3) (2022) 174–195.
[93] D.C. Fajgenbaum, C.H. June, Cytokine storm, N. Engl. J. Med. 383 (23) (2020) 2255–2273.
[94] R. Mulchandani, T. Lyngdoh, A.K. Kakkar, Deciphering the COVID-19 cytokine storm: systematic review and meta-analysis, Eur. J. Clin. Invest. 51 (1) (2021), e13429.
[95] C. Huang, Y. Wang, X. Li, L. Ren, J. Zhao, Y. Hu, L. Zhang, G. Fan, J. Xu, X. Gu, Z. Cheng, T. Yu, J. Xia, Y. Wei, W. Wu, X. Xie, W. Yin, H. Li, M. Liu, Y. Xiao, H. Gao, L. Guo, J. Xie, G. Wang, R. Jiang, Z. Gao, Q. Jin, J. Wang, B. Cao, Clinical features of patients infected with 2019 novel coronavirus in Wuhan, China, Lancet 395 (10223) (2020) 497–506.
[96] S. Hojyo, M. Uchida, K. Tanaka, R. Hasebe, Y. Tanaka, M. Murakami, T. Hirano, How COVID-19 induces cytokine storm with high mortality, Inflamm. Regen. 40 (1) (2020) 37.
[97] D. Ragab, H. Salah Eldin, M. Taeimah, R. Khattab, R. Salem, The COVID-19 cytokine storm; what we know so far, Front. Immunol. 11 (2020) 1446.
[98] Y. Que, C. Hu, K. Wan, P. Hu, R. Wang, J. Luo, T. Li, R. Ping, Q. Hu, Y. Sun, X. Wu, L. Tu, Y. Du, C. Chang, G. Xu, Cytokine release syndrome in COVID-19: a major mechanism of morbidity and mortality, Int. Rev. Immunol. 41 (2) (2022) 217–230.
[99] Y. Xie, Z. Al-Aly, Risks and burdens of incident diabetes in long COVID: a cohort study, Lancet Diabetes Endocrinol. 10 (5) (2022) 311–321.
[100] G. Douaud, S. Lee, F. Alfaro-Almagro, C. Arthofer, C. Wang, P. McCarthy, F. Lange, J.L.R. Andersson, L. Griffanti, E. Duff, S. Jbabdi, B. Taschler, P. Keating, A.M. Winkler, R. Collins, P.M. Matthews, N. Allen, K.L. Miller, T.E. Nichols, S.M. Smith, SARS-CoV-2 is associated with changes in brain structure in UK Biobank, Nature 604 (7907) (2022) 697–707.
[101] E. Kresch, J. Achua, R. Saltzman, K. Khodamoradi, H. Arora, E. Ibrahim, O.N. Kryvenko, V.W. Almeida, F. Firdaus, J.M. Hare, R. Ramasamy, COVID-19 endothelial dysfunction can cause erectile dysfunction: histopathological, immunohistochemical, and ultrastructural study of the human penis, World J. Mens Health 39 (3) (2021) 466–469.
[102] K.H. Wan, G.C.Y. Lui, K.C.F. Poon, S.S.S. Ng, A.L. Young, D.S.C. Hui, C.C.Y. Tham, P.K.S. Chan, C.P. Pang, K.K.L. Chong, Ocular surface disturbance in patients after acute COVID-19, Clin. Exp. Ophthalmol. 50 (4) (2022) 398–406.
[103] Y. Xie, E. Xu, B. Bowe, Z. Al-Aly, Long-term cardiovascular outcomes of COVID-19, Nat. Med. 28 (3) (2022) 583–590.
[104] G.D. de Melo, F. Lazarini, S. Levallois, C. Hautefort, V. Michel, F. Larrous, B. Verillaud, C. Aparicio, S. Wagner, G. Gheusi, L. Kergoat, E. Kornobis, F. Donati, T. Cokelaer, R. Hervochon, Y. Madec, E. Roze, D. Salmon, H. Bourhy, M. Lecuit, P.M. Lledo, COVID-19-related anosmia is associated with viral persistence and inflammation in human olfactory epithelium and brain infection in hamsters, Sci. Transl. Med. 13 (596) (2021), eabf8396.
[105] J.F. Shelton, A.J. Shastri, K. Fletez-Brant, A. Auton, A. Chubb, A. Fitch, A. Kung, A. Altman, A. Kill, A.J. Shastri, A. Symons, C. Weldon, D. Coker, J.F. Shelton, J. Tan, J. Pollard, J. McCreight, J. Bielenberg, J. Matthews, J. Lee, L. Tran, M. Lowe, M. Royce, N. Tang, P. Gandhi, R. d'Amore, R. Tennen, S. Dvorak, S. Hadly, S. Aslibekyan, S. Park, T. Morrow, T.F. Sonmez, T. Le, Y. Zheng, S. Aslibekyan, A. Auton, C.-T. The 23andMe, the UGT2A1/UGT2A2 locus is associated with COVID-19-related loss of smell or taste, Nat. Genet. 54 (2) (2022) 121–124.
[106] N. Sethuraman, S.S. Jeremiah, A. Ryo, Interpreting diagnostic tests for SARS-CoV-2, JAMA 323 (22) (2020) 2249–2251.
[107] N. Ravi, D.L. Cortade, E. Ng, S.X. Wang, Diagnostics for SARS-CoV-2 detection: a comprehensive review of the FDA-EUA COVID-19 testing landscape, Bio-sens. Bioelectron. 165 (2020), 112454.
[108] X. Liu, X. Lin, X. Pan, H. Gai, Multiplexed homogeneous immunoassay based on counting single immunocomplexes together with dark-field and fluo-rescence microscopy, Anal. Chem. 94 (15) (2022) 5830–5837.
[109] Y. Liu, H. Ye, H. Huynh, C. Xie, P. Kang, J.S. Kahn, Z. Qin, Digital plasmonic nanobubble detection for rapid and ultrasensitive virus diagnostics, Nat. Commun. 13 (1) (2022) 1687.
[110] Z. Ashraf, F. Nadeem, A. Mehboob, M. Alam, R. Safdar, Synthesis and appli-cations of advanced luminescent molecules: a review, IJCBS 18 (2020) 1–13.
[111] G.L. Coté, L.V. Wang, S. Rastegar, in: J.D. Enderle, J.D. Bronzino (Editors), Biomedical Optics and Lasers, Academic Press, Boston, 2012, pp. 1111–1173.
[112] C.-C. Lin, J.-H. Wang, H.-W. Wu, G.-B. Lee, Microfluidic immunoassays, JALA 15 (3) (2010) 253–274.
[113] V.T. Upaassana, S. Ghosh, A. Chakraborty, M.E. Birch, P. Joseph, J. Han, B.K. Ku, C.H. Ahn, Highly sensitive lab on a chip (LOC) immunoassay for early diag-nosis of respiratory disease caused by respirable crystalline silica (RCS), Anal. Chem. 91 (10) (2019) 6652–6660.
[114] S. Ghosh, K. Aggarwal, T.U. Vinitha, T. Nguyen, J. Han, C.H. Ahn, A new microchannel capillary flow assay (MCFA) platform with lyophilized chem-iluminescence reagents for a smartphone-based POCT detecting malaria, Microsyst. Nanoeng. 6 (1) (2020) 1–18.
[115] J. Wang, W. Li, L. Ban, W. Du, X. Feng, B.-F. Liu, A paper-based device with an adjustable time controller for the rapid determination of tumor biomarkers, Sensor. Actuator. B Chem. 254 (2018) 855–862.
[116] M. Zhao, X. Li, Y. Zhang, Y. Wang, B. Wang, L. Zheng, D. Zhang, S. Zhuang, Rapid quantitative detection of chloramphenicol in milk by microfluidic immunoassay, Food Chem. 339 (2021), 127857.
[117] R. Charlermroj, S. Phuengwas, M. Makornwattana, T. Sooksimuang, S. Sahasithiwat, W. Panchan, W. Sukbangnop, C.T. Elliott, N. Karoonuthaisiri, Development of a microarray lateral flow strip test using a luminescent organic compound for multiplex detection of five mycotoxins, Talanta 233 (2021), 122540.
[118] X. Huang, Z.P. Aguilar, H. Xu, W. Lai, Y. Xiong, Membrane-based lateral flow

immunochromatographic strip with nanoparticles as reporters for detection: a review, Biosens. Bioelectron. 75 (2016) 166–180.
[119] D. Kong, L. Liu, S. Song, S. Suryoprabowo, A. Li, H. Kuang, L. Wang, C. Xu, A gold nanoparticle-based semi-quantitative and quantitative ultrasensitive paper sensor for the detection of twenty mycotoxins, Nanoscale 8 (9) (2016) 5245–5253.
[120] A. Jo, T.H. Kim, D.-M. Kim, H.-M. Kim, B. Seong, J. Kim, X.-H. Pham, H.S. Jung, S.H. Lee, D.W. Hwang, D.H. Jeong, Y.-S. Lee, D.-E. Kim, B.-H. Jun, Sensitive detection of virus with broad dynamic range based on highly bright quantum dot-embedded nanoprobe and magnetic beads, J. Ind. Eng. Chem. 90 (2020) 319–326.
[121] E. Hemmig, Y. Temiz, O. Gokce, R.D. Lovchik, E. Delamarche, Transposing lateral flow immunoassays to capillary-driven microfluidics using self-coalescence modules and capillary-assembled receptor carriers, Anal. Chem. 92 (1) (2020) 940–946.
[122] Z. Liu, T. Meng, X. Tang, R. Tian, W. Guan, The promise of aggregation-induced emission luminogens for detecting COVID-19, Front. Immunol. 12 (2021), 635558.
[123] J.F. Engels, J. Roose, D.S. Zhai, K.M. Yip, M.S. Lee, B.Z. Tang, R. Renneberg, Aggregation-induced emissive nanoparticles for fluorescence signaling in a low cost paper-based immunoassay, Colloids Surf. B Biointerfaces 143 (2016) 440–446.
[124] Y. Tu, Y. Yu, Z. Zhou, S. Xie, B. Yao, S. Guan, B. Situ, Y. Liu, R.T.K. Kwok, J.W.Y. Lam, S. Chen, X. Huang, Z. Zeng, B.Z. Tang, Specific and quantitative detection of albumin in biological fluids by tetrazolate-functionalized water-soluble AIEgens, ACS Appl. Mater. Interfaces 11 (33) (2019) 29619–29629.
[125] X. Liu, Y. Sun, X. Lin, X. Pan, Z. Wu, H. Gai, Digital duplex homogeneous immunoassay by counting immunocomplex labeled with quantum dots, Anal. Chem. 93 (6) (2021) 3089–3095.
[126] A. Qureshi, A. Tufani, G. Corapcioglu, J.H. Niazi, CdSe/CdS/ZnS nanocrystals decorated with Fe3O4 nanoparticles for point-of-care optomagnetic detection of cancer biomarker in serum, Sensor. Actuator. B Chem. 321 (2020), 128431.
[127] M. Ren, H. Xu, X. Huang, M. Kuang, Y. Xiong, H. Xu, Y. Xu, H. Chen, A. Wang, Immunochromatographic assay for ultrasensitive detection of aflatoxin B(1) in maize by highly luminescent quantum dot beads, ACS Appl. Mater. Interfaces 6 (16) (2014) 14215–14222.
[128] Y. Gong, Y. Zheng, B. Jin, M. You, J. Wang, X. Li, M. Lin, F. Xu, F. Li, A portable and universal upconversion nanoparticle-based lateral flow assay platform for point-of-care testing, Talanta 201 (2019) 126–133.
[129] Z. Tao, J. Deng, Y. Wang, H. Chen, Y. Ding, X. Hua, M. Wang, Competitive immunoassay for simultaneous detection of imidacloprid and thiacloprid by upconversion nanoparticles and magnetic nanoparticles, Environ. Sci. Pollut. Res. 26 (23) (2019) 23471–23479.
[130] W. He, M. You, Z. Li, L. Cao, F. Xu, F. Li, A. Li, Upconversion nanoparticles-based lateral flow immunoassay for point-of-care diagnosis of periodontitis, Sensor. Actuator. B Chem. 334 (2021), 129673.
[131] C. Zhang, L. Zhou, H. Liu, S. Zhang, Y. Tian, J. Huo, F. Li, Y. Zhang, B. Wei, D. Xu, J. Hu, J. Wang, Y. Cheng, W. Shi, X. Xu, J. Zhou, P. Sang, X. Tan, W. Wang, M. Zhang, B. Wang, Y. Zhou, K. Zhang, K. He, Establishing a high sensitivity detection method for SARS-CoV-2 IgM/IgG and developing a clinical application of this method, Emerg, Microb. Infect. 9 (1) (2020) 2020–2029.
[132] W. Xiao, J. Liang, Y. Zhang, Y. Zhang, P. Teng, D. Cao, S. Zou, T. Xu, J. Zhao, Y. Tang, CD8 cell counting in whole blood by a paper-based time-resolved fluorescence lateral flow immunoassay, Anal. Chim. Acta 1179 (2021), 338820.
[133] W. Liu, W. Yu, X. Li, X. Zhao, Y. Zhang, P. Song, Y. Yin, R. Xi, M. Meng, Pyrophosphate-triggered intermolecular cross-linking of tetraphenylethylene molecules for multianalyte detection, Sensor. Actuator. B Chem. 266 (2018) 170–177.
[134] R. Chen, X. Zhou, Y. Wu, Q. Liu, Q. Liu, J. Huang, F. Li, NIR-II emissive lateral flow immunoassay for accurate determination of tumor marker in hemolysis, Sensor. Actuator. B Chem. 328 (2021), 129050.
[135] W. Wu, M. Shen, X. Liu, L. Shen, X. Ke, W. Li, Highly sensitive fluorescence-linked immunosorbent assay based on aggregation-induced emission luminogens incorporated nanobeads, Biosens. Bioelectron. 150 (2020), 111912.
[136] L.H. Xiong, X. He, Z. Zhao, R.T.K. Kwok, Y. Xiong, P.F. Gao, F. Yang, Y. Huang, H.H. Sung, I.D. Williams, J.W.Y. Lam, J. Cheng, R. Zhang, B.Z. Tang, Ultrasensitive virion immunoassay platform with dual-modality based on a multifunctional aggregation-induced emission luminogen, ACS Nano 12 (9) (2018) 9549–9557.
[137] R. Chen, C. Ren, M. Liu, X. Ge, M. Qu, X. Zhou, M. Liang, Y. Liu, F. Li, Early detection of SARS-CoV-2 seroconversion in humans with aggregation-induced near-infrared emission nanoparticle-labeled lateral flow immunoassay, ACS Nano 15 (5) (2021) 8996–9004.
[138] W.T. Sow, F. Ye, C. Zhang, H. Li, Smart materials for point-of-care testing: from sample extraction to analyte sensing and readout signal generator, Biosens. Bioelectron. 170 (2020), 112682.
[139] S.-Y. Jin, L.-P. Lin, X.-H. Chen, F. Liu, X.-B. Zhu, G.-P. Yan, Preparation and properties of fluorescent quantum dots microbeads encapsulated in-situ by polyisobornyl methacrylate for immunochromatography, J. Nanophotonics 15 (1) (2021), 16008.
[140] T. Liu, B. Liu, H. Zhang, Y. Wang, The fluorescence bioassay platforms on quantum dots nanoparticles, J. Fluoresc. 15 (5) (2005) 729–733.
[141] S.R. Ankireddy, J. Kim, Dopamine-functionalized InP/ZnS quantum dots as fluorescence probes for the detection of adenosine in microfluidic chip, Spec Iss, Int. J. Nanomed. 10 (2015) 121–128.
[142] T.H. Nguyen, A. Sedighi, U.J. Krull, C.L. Ren, Multifunctional droplet microfluidic platform for rapid immobilization of oligonucleotides on semiconductor quantum dots, ACS Sens. 5 (3) (2020) 746–753.
[143] L. Huang, Y. Zhang, T. Liao, K. Xu, C. Jiang, D. Zhuo, Y. Wang, H.M. Wen, J. Wang, L. Ao, J. Hu, Compact magneto-fluorescent colloids by hierarchical assembly of dual-components in radial channels for sensitive point-of-care immunoassay, Small 17 (25) (2021), e2100862.
[144] Y. Zhou, Y. Chen, W. Liu, H. Fang, X. Li, L. Hou, Y. Liu, W. Lai, X. Huang, Y. Xiong, Development of a rapid and sensitive quantum dot nanobead-based double-antigen sandwich lateral flow immunoassay and its clinical performance for the detection of SARS-CoV-2 total antibodies, Sensor. Actuator. B Chem. 343 (2021), 130139.
[145] S. Tian, Z. Zhang, J. Chen, M. Du, Z. Li, H. Yang, X. Ji, Z. He, Digital analysis with droplet-based microfluidic for the ultrasensitive detection of β-gal and AFP, Talanta 186 (2018) 24–28.
[146] K. Nishiyama, T. Kasama, S. Nakamata, K. Ishikawa, D. Onoshima, H. Yukawa, M. Maeki, A. Ishida, H. Tani, Y. Baba, M. Tokeshi, Ultrasensitive detection of disease biomarkers using an immuno-wall device with enzymatic amplification, Analyst 144 (15) (2019) 4589–4595.
[147] A.I. Barbosa, A.P. Castanheira, A.D. Edwards, N.M. Reis, A lab-in-a-briefcase for rapid prostate specific antigen (PSA) screening from whole blood, Lab Chip 14 (16) (2014) 2918–2928.
[148] A.I. Barbosa, P. Gehlot, K. Sidapra, A.D. Edwards, N.M. Reis, Portable smartphone quantitation of prostate specific antigen (PSA) in a fluoropolymer microfluidic device, Biosens. Bioelectron. 70 (2015) 5–14.
[149] N.M. Reis, J. Pivetal, A.L. Loo-Zazueta, J.M. Barros, A.D. Edwards, Lab on a stick: multi-analyte cellular assays in a microfluidic dipstick, Lab Chip 16 (15) (2016) 2891–2899.
[150] A.I. Barbosa, A.S. Barreto, N.M. Reis, Transparent, hydrophobic fluorinated ethylene propylene offers rapid, robust, and irreversible passive adsorption of diagnostic antibodies for sensitive optical biosensing, ACS Appl. Bio Mater. 2 (7) (2019) 2780–2790.
[151] I.P. Alves, N.M. Reis, Microfluidic smartphone quantitation of Escherichia coli in synthetic urine, Biosens. Bioelectron. 145 (2019), 111624.
[152] N.M. Reis, S.H. Needs, S.M. Jegouic, K.K. Gill, S. Sirivisoot, S. Howard, J. Kempe, S. Bola, K. Al-Hakeem, I.M. Jones, T. Prommool, P. Luangaram, P. Avirutnan, C. Puttikhunt, A.D. Edwards, Gravity-driven microfluidic siphons: fluidic characterization and application to quantitative immunoassays, ACS Sens. 6 (12) (2021) 4338–4348.
[153] Y. Zhao, P. Zhang, J. Wang, L. Zhou, R. Yang, A novel electro-driven immunochromatography assay based on upconversion nanoparticles for rapid pathogen detection, Biosens. Bioelectron. 152 (2020), 112037.
[154] H.H. Gorris, O.S. Wolfbeis, Photon-upconverting nanoparticles for optical encoding and multiplexing of cells, biomolecules, and microspheres, Angew. Chem. Int. Ed. 52 (13) (2013) 3584–3600.
[155] Z. Qiu, J. Shu, J. Liu, D. Tang, Dual-channel photoelectrochemical ratiometric aptasensor with up-converting nanocrystals using spatial-resolved technique on homemade 3D printed device, Anal. Chem. 91 (2) (2019) 1260–1268.
[156] D. Abdul Hakeem, S. Su, Z. Mo, H. Wen, Upconversion luminescent nanomaterials: a promising new platform for food safety analysis, Crit. Rev. Food Sci. Nutr. (2021) 1–42.
[157] M. You, M. Lin, Y. Gong, S. Wang, A. Li, L. Ji, H. Zhao, K. Ling, T. Wen, Y. Huang, D. Gao, Q. Ma, T. Wang, A. Ma, X. Li, F. Xu, Household fluorescent lateral flow strip platform for sensitive and quantitative prognosis of heart failure using dual-color upconversion nanoparticles, ACS Nano 11 (6) (2017) 6261–6270.
[158] Q. Hu, Q. Wu, F. Huang, Z. Xu, L. Zhou, S. Zhao, Multicolor coding upconversion nanoplatform for rapid screening of multiple foodborne pathogens, ACS Appl. Mater. Interfaces 13 (23) (2021) 26782–26789.
[159] Z. Zhang, Y. Zhang, Orthogonal emissive upconversion nanoparticles: material design and applications, Small 17 (11) (2021), e2004552.
[160] Z. Zhang, M.K.G. Jayakumar, S. Shikha, Y. Zhang, X. Zheng, Y. Zhang, Modularly assembled upconversion nanoparticles for orthogonally controlled cell imaging and drug delivery, ACS Appl. Mater. Interfaces 12 (11) (2020) 12549–12556.
[161] J. Chen, H. Qiu, S. Zhao, Fabrication of chemiluminescence resonance energy transfer platform based on nanomaterial and its application in optical sensing, biological imaging and photodynamic therapy, TrAC, Trends Anal. Chem. 122 (2020), 115747.
[162] L.J. Kricka, Clinical applications of chemiluminescence, Anal. Chim. Acta 500 (1–2) (2003) 279–286.
[163] M. Zangheri, L. Cevenini, L. Anfossi, C. Baggiani, P. Simoni, F. Di Nardo, A. Roda, A simple and compact smartphone accessory for quantitative chemiluminescence-based lateral flow immunoassay for salivary cortisol detection, Biosens. Bioelectron. 64 (2015) 63–68.
[164] V.T. Nguyen, S. Song, S. Park, C. Joo, Recent advances in high-sensitivity detection methods for paper-based lateral-flow assay, Biosens. Bioelectron. 152 (2020), 112015.
[165] K. Zeng, X. Zhang, E. Gyimah, Y. Bu, H. Meng, Z. Zhang, Chemiluminescence imaging immunoassay for simultaneous determination of TBBPA-DHEE and TBBPA-MHEE in aquatic environments, Anal. Bioanal. Chem. 412 (15) (2020) 3673–3681.
[166] B. Al Mughairy, H.A.J. Al-Lawati, Recent analytical advancements in

microfluidics using chemiluminescence detection systems for food analysis, TrAC, Trends Anal. Chem. 124 (2020), 115802.
[167] Y. Zhang, R. Zhang, X. Yang, H. Qi, C. Zhang, Recent advances in electrogenerated chemiluminescence biosensing methods for pharmaceuticals, J. Pharm. Anal. 9 (1) (2019) 9–19.
[168] V. Allwardt, A.J. Ainscough, P. Viswanathan, S.D. Sherrod, J.A. McLean, M. Haddrick, V. Pensabene, Translational roadmap for the organs-on-a-chip industry toward broad adoption, Bioengineering 7 (3) (2020) 112.
[169] Q. Xiao, C. Xu, Research progress on chemiluminescence immunoassay combined with novel technologies, TrAC, Trends Anal. Chem. 124 (2020), 115780.
[170] M. Gu, J. Duan, Q. Mao, S. Zhang, J. Lv, Direct chemiluminescent sensing of para-Phenylenediamine over its isomers and analogues via luminol diazotization, Sensor. Actuator. B Chem. 287 (2019) 173–179.
[171] K. Ling, H. Jiang, X. Huang, Y. Li, J. Lin, F.R. Li, Direct chemiluminescence detection of circulating microRNAs in serum samples using a single-strand specific nuclease-distinguishing nucleic acid hybrid system, Chem. Commun. 54 (15) (2018) 1909–1912.
[172] L. Yue, Y.-T. Liu, Mechanistic insight into pH-dependent luminol chemiluminescence in aqueous solution, J. Phys. Chem. B 124 (35) (2020) 7682–7693.
[173] W.B. Lee, Y.H. Chen, H.I. Lin, S.C. Shiesh, G.B. Lee, An integrated microfluidic system for fast, automatic detection of C-reactive protein, Sensor. Actuator. B Chem. 157 (2) (2011) 710–721.
[174] K.W. Chang, J. Li, C.H. Yang, S.C. Shiesh, G.B. Lee, An integrated microfluidic system for measurement of glycated hemoglobin levels by using an aptamer-antibody assay on magnetic beads, Biosens. Bioelectron. 68 (2015) 397–403.
[175] C.-C. Wu, H.-I. Lin, K.-W. Chang, J.D. Mai, S.-C. Shiesh, G.-B. Lee, Measurement of glycated hemoglobin levels using an integrated microfluidic system, Microfluid. Nanofluidics 18 (4) (2014) 613–621.
[176] X. Min, D. Fu, J. Zhang, J. Zeng, Z. Weng, W. Chen, S. Zhang, D. Zhang, S. Ge, J. Zhang, N. Xia, An automated microfluidic chemiluminescence immunoassay platform for quantitative detection of biomarkers, Biomed, Microdevices 20 (4) (2018) 91.
[177] R. Yang, F. Li, W. Zhang, W. Shen, D. Yang, Z. Bian, H. Cui, Chemiluminescence immunoassays for simultaneous detection of three heart disease biomarkers using magnetic carbon composites and three-dimensional microfluidic paper-based device, Anal. Chem. 91 (20) (2019) 13006–13013.
[178] H. Wu, M. Zhao, J. Li, X. Zhou, T. Yang, D. Zhao, P. Liu, H. Ju, W. Cheng, S. Ding, Novel protease-free long-lasting chemiluminescence system based on the dox-ABEI chimeric magnetic DNA hydrogel for ultrasensitive immunoassay, ACS Appl. Mater. Interfaces 12 (42) (2020) 47270–47277.
[179] J. Dong, Z. Li, Y. Wang, M. Jin, Y. Shen, Z. Xu, A.M. Abd El-Aty, S.J. Gee, B.D. Hammock, Y. Sun, H. Wang, Generation of functional single-chain fragment variable from hybridoma and development of chemiluminescence enzyme immunoassay for determination of total malachite green in tilapia fish, Food Chem. 337 (2021), 127780.
[180] B. Shu, Z. Li, X. Yang, F. Xiao, D. Lin, X. Lei, B. Xu, D. Liu, Active droplet-array (ADA) microfluidics enables multiplexed complex bioassays for point of care testing, Chem. Commun. 54 (18) (2018) 2232–2235.
[181] D. Li, Q. Xiong, D. Lu, Y. Chen, L. Liang, H. Duan, Magnetic nanochains-based dynamic ELISA for rapid and ultrasensitive detection of acute myocardial infarction biomarkers, Anal. Chim. Acta 1166 (2021), 338567.
[182] X. Tan, A. David, J. Day, H. Tang, E.R. Dixon, H. Zhu, Y.C. Chen, M.K. Khaing Oo, A. Shikanov, X. Fan, Rapid mouse follicle stimulating hormone quantification and estrus cycle analysis using an automated microfluidic chemiluminescent ELISA system, ACS Sens. 3 (11) (2018) 2327–2334.
[183] X. Tan, M. Krel, E. Dolgov, S. Park, X. Li, W. Wu, Y.L. Sun, J. Zhang, M.K. Khaing Oo, D.S. Perlin, X. Fan, Rapid and quantitative detection of SARS-CoV-2 specific IgG for convalescent serum evaluation, Biosens. Bioelectron. 169 (2020), 112572.
[184] L.W. Tai, K.Y. Tseng, S.T. Wang, C.C. Chiu, C.H. Kow, P. Chang, C. Chen, J.Y. Wang, J.R. Webster, An automated microfluidic-based immunoassay cartridge for allergen screening and other multiplexed assays, Anal. Biochem. 391 (2) (2009) 98–105.
[185] S.D. Shyur, R.L. Jan, J.R. Webster, P. Chang, Y.J. Lu, J.Y. Wang, Determination of multiple allergen-specific IgE by microfluidic immunoassay cartridge in clinical settings, Pediatr. Allergy Immunol. 21 (4 Pt 1) (2010) 623–633.
[186] B. Hu, J. Li, L. Mou, Y. Liu, J. Deng, W. Qian, J. Sun, R. Cha, X. Jiang, An automated and portable microfluidic chemiluminescence immunoassay for quantitative detection of biomarkers, Lab Chip 17 (13) (2017) 2225–2234.
[187] B.F. Hu, Y. Liu, J.Q. Deng, L. Mou, X.Y. Jiang, An on-chip valve-assisted microfluidic chip for quantitative and multiplexed detection of biomarkers, Anal. Methods 10 (21) (2018) 2470–2480.
[188] L. Mou, R. Dong, B. Hu, Z. Li, J. Zhang, X. Jiang, Hierarchically structured microchip for point-of-care immunoassays with dynamic detection ranges, Lab Chip 19 (16) (2019) 2750–2757.
[189] B. Dai, C. Yin, J. Wu, W. Li, L. Zheng, F. Lin, X. Han, Y. Fu, D. Zhang, S. Zhuang, A flux-adaptable pump-free microfluidics-based self-contained platform for multiplex cancer biomarker detection, Lab Chip 21 (1) (2021) 143–153.
[190] M. Sharafeldin, T. Chen, G.U. Ozkaya, D. Choudhary, A.A. Molinolo, J.S. Gutkind, J.F. Rusling, Detecting cancer metastasis and accompanying protein biomarkers at single cell levels using a 3D-printed microfluidic immunoarray, Biosens. Bioelectron. 171 (2021), 112681.
[191] J. Qi, B. Li, X. Wang, Z. Zhang, Z. Wang, J. Han, L. Chen, Three-dimensional paper-based microfluidic chip device for multiplexed fluorescence detection of Cu2+ and Hg2+ ions based on ion imprinting technology, Sensor. Actuator. B Chem. 251 (2017) 224–233.
[192] J. Zhao, C. Liu, Y. Li, Y. Ma, J. Deng, L. Li, J. Sun, Thermophoretic detection of exosomal microRNAs by nanoflares, J. Am. Chem. Soc. 142 (11) (2020) 4996–5001.
[193] X. Li, J. Huffman, N. Ranganathan, Z. He, P. Li, Acoustofluidic enzyme-linked immunosorbent assay (ELISA) platform enabled by coupled acoustic streaming, Anal. Chim. Acta 1079 (2019) 129–138.
[194] E. Huang, D. Huang, Y. Wang, D. Cai, Y. Luo, Z. Zhong, D. Liu, Active droplet-array microfluidics-based chemiluminescence immunoassay for point-of-care detection of procalcitonin, Biosens. Bioelectron. 195 (2022), 113684.
[195] F. Du, Y. Chen, C. Meng, B. Lou, W. Zhang, G. Xu, Recent advances in electrochemiluminescence immunoassay based on multiple-signal strategy, Curr. Opin. Electrochem. 28 (2021), 100725.
[196] B. Babamiri, D. Bahari, A. Salimi, Highly sensitive bioaffinity electrochemiluminescence sensors: recent advances and future directions, Biosens. Bioelectron. 142 (2019), 111530.
[197] A. Zanut, A. Fiorani, S. Rebeccani, S. Kesarkar, G. Valenti, Electrochemiluminescence as emerging microscopy techniques, Anal. Bioanal. Chem. 411 (19) (2019) 4375–4382.
[198] Y. Liu, W. Guo, B. Su, Recent advances in electrochemiluminescence imaging analysis based on nanomaterials and micro-/nanostructures, Chin. Chem. Lett. 30 (9) (2019) 1593–1599.
[199] J. Jiang, X. Lin, D. Ding, G. Diao, Graphitic-phase carbon nitride-based electrochemiluminescence sensing analyses: recent advances and perspectives, RSC Adv. 8 (35) (2018) 19369–19380.
[200] Y. Chen, J. Wang, Z. Liu, X. Wang, X. Li, G. Shan, A simple and versatile paper-based electrochemiluminescence biosensing platform for hepatitis B virus surface antigen detection, Biochem. Eng. J. 129 (2018) 1–6.
[201] X. Sun, B. Li, C. Tian, F. Yu, N. Zhou, Y. Zhan, L. Chen, Rotational paper-based electrochemiluminescence immunodevices for sensitive and multiplexed detection of cancer biomarkers, Anal. Chim. Acta 1007 (2018) 33–39.
[202] J. Van Houten, R.J. Watts, Temperature dependence of the photophysical and photochemical properties of the tris(2,2'-bipyridyl)ruthenium(II) ion in aqueous solution, J. Am. Chem. Soc. 98 (16) (1976) 4853–4858.
[203] Z. Ding, B.M. Quinn, S.K. Haram, L.E. Pell, B.A. Korgel, A.J. Bard, Electrochemistry and electrogenerated chemiluminescence from silicon nanocrystal quantum dots, Science 296 (5571) (2002) 1293–1297.
[204] P. Li, J. Yu, K. Zhao, A. Deng, J. Li, Efficient enhancement of electrochemiluminescence from tin disulfide quantum dots by hollow titanium dioxide spherical shell for highly sensitive detection of chloramphenicol, Biosens. Bioelectron. 147 (2020), 111790.
[205] W. Guo, H. Ding, C. Gu, Y. Liu, X. Jiang, B. Su, Y. Shao, Potential-resolved multicolor electrochemiluminescence for multiplex immunoassay in a single sample, J. Am. Chem. Soc. 140 (46) (2018) 15904–15915.
[206] A. Ranzoni, G. Sabatte, L.J. van Ijzendoorn, M.W.J. Prins, One-step homogeneous magnetic nanoparticle immunoassay for biomarker detection directly in blood plasma, ACS Nano 6 (4) (2012) 3134–3141.
[207] Z. Huang, Z. Li, M. Jiang, R. Liu, Y. Lv, Homogeneous multiplex immunoassay for one-step pancreatic cancer biomarker evaluation, Anal. Chem. 92 (24) (2020) 16105–16112.
[208] K. Takkinen, A. Zvirbliene, Recent advances in homogenous immunoassays based on resonance energy transfer, Curr. Opin. Biotechnol. 55 (2019) 16–22.
[209] P.G. Wu, L. Brand, Resonance energy transfer: methods and applications, Anal. Biochem. 218 (1) (1994) 1–13.
[210] T. Sun, Y.Y. Su, M.X. Sun, Y. Lv, Homologous chemiluminescence resonance energy transfer on the interface of WS2 quantum dots for monitoring photocatalytic H2O2 evaluation, Microchem. J. 168 (2021), 106344.
[211] D. Kang, H.J. Ahn, J. Lee, S.K. Kim, J. Pyun, C.S. Song, S.J. Kim, J. Lee, An NIR dual-emitting/absorbing inorganic compact pair: a self-calibrating LRET system for homogeneous virus detection, Biosens. Bioelectron. 190 (2021), 113369.
[212] M. Imani, N. Mohajeri, M. Rastegar, N. Zarghami, Recent advances in FRET-Based biosensors for biomedical applications, Anal. Biochem. 630 (2021), 114323.
[213] K.E. Sapsford, L. Berti, I.L. Medintz, Materials for fluorescence resonance energy transfer analysis: beyond traditional donor-acceptor combinations, Angew. Chem., Int. Ed. Engl. 45 (28) (2006) 4562–4589.
[214] S. Wu, N. Duan, X. Ma, Y. Xia, H. Wang, Z. Wang, Q. Zhang, Multiplexed fluorescence resonance energy transfer aptasensor between upconversion nanoparticles and graphene oxide for the simultaneous determination of mycotoxins, Anal. Chem. 84 (14) (2012) 6263–6270.
[215] A.A.S. Samson, J. Lee, J.M. Song, Paper-based inkjet bioprinting to detect fluorescence resonance energy transfer for the assessment of anti-inflammatory activity, Sci. Rep. 8 (1) (2018) 591.
[216] X. Wang, X. Wu, Z. Lu, X. Tao, Comparative study of time-resolved fluorescent nanobeads, quantum dot nanobeads and quantum dots as labels in fluorescence immunochromatography for detection of aflatoxin B1 in grains, Biomolecules 10 (4) (2020) 575.
[217] I. Hemmilä, S. Dakubu, V.-M. Mukkala, H. Siitari, T. Lövgren, Europium as a label in time-resolved immunofluorometric assays, Anal. Biochem. 137 (2) (1984) 335–343.

[218] D. Tu, W. Zheng, Y. Liu, H. Zhu, X. Chen, Luminescent biodetection based on lanthanide-doped inorganic nanoprobes, Coord. Chem. Rev. 273–274 (2014) 13–29.
[219] L.M. Hu, K. Luo, J. Xia, G.M. Xu, C.H. Wu, J.J. Han, G.G. Zhang, M. Liu, W.H. Lai, Advantages of time-resolved fluorescent nanobeads compared with fluorescent submicrospheres, quantum dots, and colloidal gold as label in lateral flow assays for detection of ractopamine, Biosens. Bioelectron. 91 (2017) 95–103.
[220] M. Latva, H. Takalo, V.-M. Mukkala, C. Matachescu, J.C. Rodríguez-Ubis, J. Kankare, Correlation between the lowest triplet state energy level of the ligand and lanthanide(III) luminescence quantum yield, J. Lumin. 75 (2) (1997) 149–169.
[221] X. Yang, Y. Ye, T. Wang, M. Li, L. Yu, M. Xia, J. Qian, Z. Hu, Eu(3+)/Sm(3+) dual-label time-resolved fluoroimmunoassay for measurement of hepatitis C virus antibodies, J. Clin. Lab. Anal. 33 (2) (2019), e22659.
[222] J. Yuan, G. Wang, K. Majima, K. Matsumoto, Synthesis of a terbium fluorescent chelate and its application to time-resolved fluoroimmunoassay, Anal. Chem. 73 (8) (2001) 1869–1876.
[223] E. Soini, I. Hemmilä, Fluoroimmunoassay: present status and key problems, Clin. Chem. 25 (3) (1979) 353–361.
[224] J. Rusanen, L. Kareinen, L. Szirovicza, H. Ugurlu, L. Levanov, A. Jaaskelainen, M. Ahava, S. Kurkela, K. Saksela, K. Hedman, O. Vapalahti, J. Hepojoki, A generic, scalable, and rapid time-resolved forster resonance energy transfer-based assay for antigen detection-SARS-CoV-2 as a proof of concept, mBio 12 (3) (2021). e00902-00921.
[225] Y. Xu, D.W. Piston, C.H. Johnson, A bioluminescence resonance energy transfer (BRET) system: application to interacting circadian clock proteins, Proc. Natl. Acad. Sci. U.S.A. 96 (1) (1999) 151.
[226] R. Arts, I. den Hartog, S.E. Zijlema, V. Thijssen, S.H. van der Beelen, M. Merkx, Detection of antibodies in blood plasma using bioluminescent sensor proteins and a smartphone, Anal. Chem. 88 (8) (2016) 4525–4532.
[227] K. Tenda, B. van Gerven, R. Arts, Y. Hiruta, M. Merkx, D. Citterio, Paper-based antibody detection devices using bioluminescent BRET-switching sensor proteins, Angew. Chem., Int. Ed. Engl. 57 (47) (2018) 15369–15373.
[228] K. Tomimuro, K. Tenda, Y. Ni, Y. Hiruta, M. Merkx, D. Citterio, Thread-based bioluminescent sensor for detecting multiple antibodies in a single drop of whole blood, ACS Sens. 5 (6) (2020) 1786–1794.
[229] E.F. Ullman, H. Kirakossian, S. Singh, Z.P. Wu, B.R. Irvin, J.S. Pease, A.C. Switchenko, J.D. Irvine, A. Dafforn, C.N. Skold, Luminescent oxygen channeling immunoassay: measurement of particle binding kinetics by chemiluminescence, Proc. Natl. Acad. Sci. U.S.A. 91 (12) (1994) 5426.
[230] L. Su, N. Bryan, S. Battista, J. Freitas, A. Garabedian, F. D'Alessio, M. Romano, F. Falanga, A. Fusco, L. Kos, J. Chambers, F. Fernandez-Lima, P.P. Chapagain, S. Vasile, L. Smith, F. Leng, Identification of HMGA2 inhibitors by AlphaScreen-based ultra-high-throughput screening assays, Sci. Rep. 10 (1) (2020), 18850.
[231] C. Lin, Y. Li, Y. Zhang, Z. Liu, X. Mu, C. Gu, J. Liu, Y. Li, G. Li, J. Chen, Ceftazidime is a potential drug to inhibit SARS-CoV-2 infection in vitro by blocking spike protein–ACE2 interaction, Signal Transduct. Targeted Ther. 6 (1) (2021) 198.
[232] L. Beaudet, R. Rodriguez-Suarez, M.-H. Venne, M. Caron, J. Bédard, V. Brechler, S. Parent, M. Bielefeld-Sévigny, AlphaLISA immunoassays: the no-wash alternative to ELISAs for research and drug discovery, Nat. Methods 5 (12) (2008) an8–an9.
[233] H. Pulido-Olmo, E. Rodriguez-Sanchez, J.A. Navarro-Garcia, M.G. Barderas, G. Alvarez-Llamas, J. Segura, M. Fernandez-Alfonso, L.M. Ruilope, G. Ruiz-Hurtado, Rapid, automated, and specific immunoassay to directly measure matrix metalloproteinase-9-tissue inhibitor of metalloproteinase-1 interactions in human plasma using AlphaLISA technology: a new alternative to classical ELISA, Front. Immunol. 8 (2017) 853.
[234] A. Stephens, R. Nidetz, N. Mesyngier, M.T. Chung, Y. Song, J. Fu, K. Kurabayashi, Mass-producible microporous silicon membranes for specific leukocyte subset isolation, immunophenotyping, and personalized immunomodulatory drug screening in vitro, Lab Chip 19 (18) (2019) 3065–3076.
[235] S.H. Su, Y. Song, M.W. Newstead, T. Cai, M. Wu, A. Stephens, B.H. Singer, K. Kurabayashi, Ultrasensitive multiparameter phenotyping of rare cells using an integrated digital-molecular-counting microfluidic well plate, Small 17 (31) (2021), e2101743.
[236] C. Wu, P.M. Garden, D.R. Walt, Ultrasensitive detection of attomolar protein concentrations by dropcast single molecule assays, J. Am. Chem. Soc. 142 (28) (2020) 12314–12323.
[237] J. Dong, H. Ueda, ELISA-type assays of trace biomarkers using microfluidic methods, Wiley Interdiscip. Rev.-Nanomed. Nanobiotechnol. 9 (5) (2017) e1457.
[238] M.J. Mickert, Z. Farka, U. Kostiv, A. Hlavacek, D. Horak, P. Skladal, H.H. Gorris, Measurement of sub-femtomolar concentrations of prostate-specific antigen through single-molecule counting with an upconversion-linked immunosorbent assay, Anal. Chem. 91 (15) (2019) 9435–9441.
[239] Q. Zhang, J. Li, X. Pan, X. Liu, H. Gai, Low-numerical aperture microscope objective boosted by liquid-immersed dielectric microspheres for quantum dot-based digital immunoassays, Anal. Chem. 93 (38) (2021) 12848–12853.
[240] V. Yelleswarapu, J.R. Buser, M. Haber, J. Baron, E. Inapuri, D. Issadore, Mobile platform for rapid sub-picogram-per-milliliter, multiplexed, digital droplet detection of proteins, Proc. Natl. Acad. Sci. U.S.A. 116 (10) (2019) 4489–4495.
[241] Y. Song, E. Sandford, Y. Tian, Q. Yin, A.G. Kozminski, S.-H. Su, T. Cai, Y. Ye, M.T. Chung, R. Lindstrom, A. Goicochea, J. Barabas, M. Olesnavich, M. Rozwadowski, Y. Li, H.B. Alam, B.H. Singer, M. Ghosh, S.W. Choi, M. Tewari, K. Kurabayashi, Rapid single-molecule digital detection of protein biomarkers for continuous monitoring of systemic immune disorders, Blood 137 (12) (2021) 1591–1602.
[242] C.W. Kan, C.I. Tobos, D.M. Rissin, A.D. Wiener, R.E. Meyer, D.M. Svancara, A. Comperchio, C. Warwick, R. Millington, N. Collier, D.C. Duffy, Digital enzyme-linked immunosorbent assays with sub-attomolar detection limits based on low numbers of capture beads combined with high efficiency bead analysis, Lab Chip 20 (12) (2020) 2122–2135.
[243] S.A. Byrnes, T. Huynh, T.C. Chang, C.E. Anderson, J.J. McDermott, C.I. Oncina, B.H. Weigl, K.P. Nichols, Wash-free, digital immunoassay in polydisperse droplets, Anal. Chem. 92 (5) (2020) 3535–3543.
[244] Z. Gao, J. Yi, J. Zhao, H. Gu, H. Zhou, H. Xu, Droplets isolated array: a universal platform of delaying molecule cross-contamination between microdroplets for digital enzyme-based immunoassay, Sensor. Actuator. B Chem. 324 (2020), 128716.
[245] C. Liu, X. Xu, B. Li, B. Situ, W. Pan, Y. Hu, T. An, S. Yao, L. Zheng, Single-exosome-counting immunoassays for cancer diagnostics, Nano Lett. 18 (7) (2018) 4226–4232.
[246] H. Chen, Z. Li, L. Zhang, P. Sawaya, J. Shi, P. Wang, Angew. Chem., Int. Ed. Engl. 58 (39) (2019) 13922–13928.
[247] J. Sun, J. Hu, T. Gou, X. Ding, Q. Song, W. Wu, G. Wang, J. Yin, Y. Mu, Power-free polydimethylsiloxane femtoliter-sized arrays for bead-based digital immunoassays, Biosens. Bioelectron. 139 (2019), 111339.
[248] Y. Song, J. Zhao, T. Cai, A. Stephens, S.H. Su, E. Sandford, C. Flora, B.H. Singer, M. Ghosh, S.W. Choi, M. Tewari, K. Kurabayashi, Machine learning-based cytokine microarray digital immunoassay analysis, Biosens. Bioelectron. 180 (2021), 113088.
[249] S. Qian, H. Wu, B. Huang, Q. Liu, Y. Chen, B. Zheng, Bead-free digital immunoassays on polydopamine patterned perfluorinated surfaces, Sensor. Actuator. B Chem. 345 (2021), 130341.
[250] P.Y. Chiou, H. Moon, H. Toshiyoshi, C.-J. Kim, M.C. Wu, Light actuation of liquid by optoelectrowetting, Sens. Actuator A Phys. 104 (3) (2003) 222–228.
[251] S.-Y. Park, M.A. Teitell, E.P.Y. Chiou, Single-sided continuous optoelectrowetting (SCOEW) for droplet manipulation with light patterns, Lab Chip 10 (13) (2010) 1655–1661.
[252] S.N. Pei, J.K. Valley, Y. Wang, M.C. Wu, Distributed circuit model for multicolor light-actuated opto-electrowetting microfluidic device, J. Lightwave Technol. 33 (16) (2015) 3486–3493.
[253] M.A. Bijarchi, A. Favakeh, E. Sedighi, M.B. Shafii, Ferrofluid droplet manipulation using an adjustable alternating magnetic field, Sens. Actuator A Phys. 301 (2020), 111753.
[254] Y. Zhang, N.-T. Nguyen, Magnetic digital microfluidics – a review, Lab Chip 17 (6) (2017) 994–1008.
[255] H. Cheng, H. Liu, W. Li, M. Li, Recent advances in magnetic digital microfluidic platforms, Electrophoresis 42 (21–22) (2021) 2329–2346.
[256] B.J. Won, W. Lee, S. Song, Estimation of the thermocapillary force and its applications to precise droplet control on a microfluidic chip, Sci. Rep. 7 (1) (2017) 3062.
[257] A. Gao, X. Liu, T. Li, X. Gao, Y. Wang, Thermocapillary actuation of droplets on a microfluidic chip, J. Adhes. Sci. Technol. 26 (12–17) (2012) 2165–2176.
[258] S.P. Zhang, J. Lata, C. Chen, J. Mai, F. Guo, Z. Tian, L. Ren, Z. Mao, P.-H. Huang, P. Li, S. Yang, T.J. Huang, Digital acoustofluidics enables contactless and programmable liquid handling, Nat. Commun. 9 (1) (2018) 2928.
[259] M. Sesen, T. Alan, A. Neild, Microfluidic on-demand droplet merging using surface acoustic waves, Lab Chip 14 (17) (2014) 3325–3333.
[260] M. Sesen, T. Alan, A. Neild, Microfluidic plug steering using surface acoustic waves, Lab Chip 15 (14) (2015) 3030–3038.
[261] S.-M. Yang, Q. Lin, H. Zhang, R. Yin, W. Zhang, M. Zhang, Y. Cui, Dielectrophoresis assisted high-throughput detection system for multiplexed immunoassays, Biosens. Bioelectron. 180 (2021), 113148.
[262] T. Lienard-Mayor, M. Taverna, S. Descroix, T.D. Mai, Droplet-interfacing strategies in microscale electrophoresis for sample treatment, separation and quantification: a review, Anal. Chim. Acta 1143 (2021) 281–297.
[263] S.I. Han, H.S. Kim, K.H. Han, A. Han, Digital quantification and selection of high-lipid-producing microalgae through a lateral dielectrophoresis-based microfluidic platform, Lab Chip 19 (24) (2019) 4128–4138.
[264] J. Li, N.S. Ha, T. Liu, R.M. van Dam, C.J. cj' Kim, Ionic-surfactant-mediated electro-dewetting for digital microfluidics, Nature 572 (7770) (2019) 507–510.
[265] J. Li, C.C. Kim, Current commercialization status of electrowetting-on-dielectric (EWOD) digital microfluidics, Lab Chip 20 (10) (2020) 1705–1712.
[266] S.R. Barman, I. Khan, S. Chatterjee, S. Saha, D. Choi, S. Lee, Z.-H. Lin, Electrowetting-on-dielectric (EWOD): current perspectives and applications in ensuring food safety, J. Food Drug Anal. 28 (4) (2020) 596–622.
[267] M. Shojaeian, F.-X. Lehr, H.U. Göringer, S. Hardt, On-demand production of femtoliter drops in microchannels and their use as biological reaction compartments, Anal. Chem. 91 (5) (2019) 3484–3491.
[268] N.C. Speller, G.G. Morbioli, M.E. Cato, Z.A. Duca, A.M. Stockton, Green, low-cost, user-friendly, and elastomeric (GLUE) microfluidics, ACS Appl. Polym. Mater. 2 (3) (2020) 1345–1355.
[269] O. Scheler, N. Pacocha, P.R. Debski, A. Ruszczak, T.S. Kaminski, P. Garstecki, Optimized droplet digital CFU assay (ddCFU) provides precise quantification of bacteria over a dynamic range of 6 logs and beyond, Lab Chip 17 (11) (2017) 1980–1987.

[270] Z. Whiteley, H.M.K. Ho, Y.X. Gan, L. Panariello, G. Gkogkos, A. Gavriilidis, D.Q.M. Craig, Microfluidic synthesis of protein-loaded nanogels in a coaxial flow reactor using a design of experiments approach, Nanoscale Adv. 3 (7) (2021) 2039–2055.
[271] A. Dewandre, J. Rivero-Rodriguez, Y. Vitry, B. Sobac, B. Scheid, Microfluidic droplet generation based on non-embedded co-flow-focusing using 3D printed nozzle, Sci. Rep. 10 (1) (2020), 21616.
[272] L. Cohen, N. Cui, Y. Cai, P.M. Garden, X. Li, D.A. Weitz, D.R. Walt, Single molecule protein detection with attomolar sensitivity using droplet digital enzyme-linked immunosorbent assay, ACS Nano 14 (8) (2020) 9491–9501.
[273] http://en.lansionbio.com/article/type/354_1.html. (Accessed 5 May 2022).
[274] https://www.blusense-diagnostics.com/products. (Accessed 5 May 2022).
[275] R. Gao, Z. Lv, Y. Mao, L. Yu, X. Bi, S. Xu, J. Cui, Y. Wu, SERS-based pump-free microfluidic chip for highly sensitive immunoassay of prostate-specific antigen biomarkers, ACS Sens. 4 (4) (2019) 938–943.
[276] Y. Wang, J. Zhao, Y. Zhu, S. Dong, Y. Liu, Y. Sun, L. Qian, W. Yang, Z. Cao, Monolithic integration of nanorod arrays on microfluidic chips for fast and sensitive one-step immunoassays, Microsyst. Nanoeng. 7 (2021) 65.
[277] J.M.D. Machado, R.R.G. Soares, V. Chu, J.P. Conde, Multiplexed capillary microfluidic immunoassay with smartphone data acquisition for parallel mycotoxin detection, Biosens. Bioelectron. 99 (2018) 40–46.
[278] X. Xiang, Q. Ye, Y. Shang, F. Li, B. Zhou, Y. Shao, C. Wang, J. Zhang, L. Xue, M. Chen, Y. Ding, Q. Wu, Quantitative detection of aflatoxin B1 using quantum dots-based immunoassay in a recyclable gravity-driven microfluidic chip, Biosens. Bioelectron. 190 (2021), 113394.
[279] H. Li, J.V. Sorensen, K.V. Gothelf, Quantitative detection of digoxin in plasma using small-molecule immunoassay in a recyclable gravity-driven microfluidic chip, Adv. Sci. 6 (6) (2019), 1802051.
[280] C.H. Lu, T.S. Shih, P.C. Shih, G.P. Pendharkar, C.E. Liu, C.K. Chen, L. Hsu, H.Y. Chang, C.L. Yang, C.H. Liu, Finger-powered agglutination lab chip with CMOS image sensing for rapid point-of-care diagnosis applications, Lab Chip 20 (2) (2020) 424–433.
[281] W. Qi, L. Zheng, Y. Hou, H. Duan, L. Wang, S. Wang, Y. Liu, Y. Li, M. Liao, J. Lin, A finger-actuated microfluidic biosensor for colorimetric detection of foodborne pathogens, Food Chem. 381 (2022), 131801.
[282] Z. Wang, Y. Wang, L. Lin, T. Wu, Z. Zhao, B. Ying, L. Chang, A finger-driven disposable micro-platform based on isothermal amplification for the application of multiplexed and point-of-care diagnosis of tuberculosis, Biosens. Bioelectron. 195 (2022), 113663.
[283] T. Kokalj, Y. Park, M. Vencelj, M. Jenko, L.P. Lee, Self-powered imbibing microfluidic pump by liquid encapsulation: simple, Lab Chip 14 (22) (2014) 4329–4333.
[284] F. Dal Dosso, T. Kokalj, J. Belotserkovsky, D. Spasic, J. Lammertyn, Self-powered infusion microfluidic pump for ex vivo drug delivery, Biomed, Microdevices 20 (2) (2018) 44.
[285] F. Dal Dosso, L. Tripodi, D. Spasic, T. Kokalj, J. Lammertyn, Innovative hydrophobic valve allows complex liquid manipulations in a self-powered channel-based microfluidic device, ACS Sens. 4 (3) (2019) 694–703.
[286] J.H. Qu, H. Ordutowski, C. Van Tricht, R. Verbruggen, A. Barcenas Gallardo, M. Bulcaen, M. Ciwinska, C. Gutierrez Cisneros, C. Devriese, S. Guluzade, X. Janssens, S. Kornblum, Y. Lu, N. Marolt, C. Nanjappan, E. Rutten, E. Vanhauwaert, N. Geukens, D. Thomas, F. Dal Dosso, S. Safdar, D. Spasic, J. Lammertyn, Point-of-care therapeutic drug monitoring of adalimumab by integrating a FO-SPR biosensor in a self-powered microfluidic cartridge, Biosens. Bioelectron. 206 (2022), 114125.
[287] H. Ordutowski, F. Dal Dosso, W. De Wispelaere, C. Van Tricht, S. Vermeire, N. Geukens, A. Gils, D. Spasic, J. Lammertyn, Next generation point-of-care test for therapeutic drug monitoring of adalimumab in patients diagnosed with autoimmune diseases, Biosens. Bioelectron. 208 (2022), 114189.
[288] S.P. Huang, Y.J. Chuang, W.B. Lee, Y.C. Tsai, C.N. Lin, K.F. Hsu, G.B. Lee, An integrated microfluidic system for rapid, automatic and high-throughput staining of clinical tissue samples for diagnosis of ovarian cancer, Lab Chip 20 (6) (2020) 1103–1109.
[289] N.H. Bhuiyan, J.H. Hong, M.J. Uddin, J.S. Shim, Artificial intelligence-controlled microfluidic device for fluid automation and bubble removal of immunoassay operated by a smartphone, Anal. Chem. 94 (9) (2022) 3872–3880.
[290] J.M. Marc, J.K. Gregory, LabCD: a centrifuge-based microfluidic platform for diagnostics, Proc. SPIE 3259 (1998) 80–93.
[291] S. Lai, S. Wang, J. Luo, L.J. Lee, S.-T. Yang, M.J. Madou, Design of a compact disk-like microfluidic platform for enzyme-linked immunosorbent assay, Anal. Chem. 76 (7) (2004) 1832–1837.
[292] H.V. Nguyen, V.D. Nguyen, H.Q. Nguyen, T.H.T. Chau, E.Y. Lee, T.S. Seo, Nucleic acid diagnostics on the total integrated lab-on-a-disc for point-of-care testing, Biosens. Bioelectron. 141 (2019), 111466.
[293] D. Mark, S. Haeberle, G. Roth, F. von Stetten, R. Zengerle, Microfluidic lab-on-a-chip platforms: requirements, characteristics and applications, Chem. Soc. Rev. 39 (3) (2010) 1153–1182.
[294] C. Dincer, R. Bruch, A. Kling, P.S. Dittrich, G.A. Urban, Multiplexed point-of-care testing - xPOCT, Trends Biotechnol. 35 (8) (2017) 728–742.
[295] V. Sunkara, S. Kumar, J. Sabaté del Río, I. Kim, Y.-K. Cho, Lab-on-a-Disc for point-of-care infection diagnostics, Accounts Chem. Res. 54 (19) (2021) 3643–3655.
[296] W.S. Lee, V. Sunkara, J.R. Han, Y.S. Park, Y.K. Cho, Electrospun TiO2 nanofiber integrated lab-on-a-disc for ultrasensitive protein detection from whole blood, Lab Chip 15 (2) (2015) 478–485.
[297] J.-M. Park, Y.-K. Cho, B.-S. Lee, J.-G. Lee, C. Ko, Multifunctional microvalves control by optical illumination on nanoheaters and its application in centrifugal microfluidic devices, Lab Chip 7 (5) (2007) 557–564.
[298] S.M. Torres Delgado, D.J. Kinahan, L.A. Nirupa Julius, A. Mallette, D.S. Ardila, R. Mishra, C.M. Miyazaki, J.G. Korvink, J. Ducree, D. Mager, Wirelessly powered and remotely controlled valve-array for highly multiplexed analytical assay automation on a centrifugal microfluidic platform, Biosens. Bioelectron. 109 (2018) 214–223.
[299] S.M. Torres Delgado, J.G. Korvink, D. Mager, The eLoaD platform endows centrifugal microfluidics with on-disc power and communication, Biosens. Bioelectron. 117 (2018) 464–473.
[300] Y. Chen, M. Shen, Y. Zhu, Y. Xu, A novel electromagnet-triggered pillar valve and its application in immunoassay on a centrifugal platform, Lab Chip 19 (10) (2019) 1728–1735.
[301] K. Wang, R. Liang, H. Chen, S. Lu, S. Jia, W. Wang, A microfluidic immunoassay system on a centrifugal platform, Sensor. Actuator. B Chem. 251 (2017) 242–249.
[302] N. Li, M. Shen, Y. Zhu, Y. Xu, Euler force-assisted sequential liquid release on the centrifugal microfluidic platform, Sensor. Actuator. B Chem. 359 (2022), 131642.
[303] M. Shen, Y. Chen, Y. Zhu, M. Zhao, Y. Xu, Enhancing the sensitivity of lateral flow immunoassay by centrifugation-assisted flow control, Anal. Chem. 91 (7) (2019) 4814–4820.
[304] B.D. Henderson, D.J. Kinahan, J. Rio, R. Mishra, D. King, S.M. Torres-Delgado, D. Mager, J.G. Korvink, J. Ducree, Siphon-controlled automation on a lab-on-a-disc using event-triggered dissolvable film valves, Biosens. Bioelectron. 11 (3) (2021) 73.
[305] M. Shen, N. Li, Y. Lu, J. Cheng, Y. Xu, An enhanced centrifugation-assisted lateral flow immunoassay for the point-of-care detection of protein biomarkers, Lab Chip 20 (15) (2020) 2626–2634.
[306] F.O. Romero-Soto, M.M. Aeinehvand, S.O. Martinez-Chapa, Wirelessly-controlled electrolysis pumps on lab-on-a-disc for automation of bioanalytical assays, Mater. Today Proc. 48 (2022) 50–55.
[307] Q. Wu, L. Yao, P. Qin, J. Xu, X. Sun, B. Yao, F. Ren, W. Chen, Time-resolved fluorescent lateral flow strip for easy and rapid quality control of edible oil, Food Chem. 357 (2021), 129739.
[308] F. Li, M. You, S. Li, J. Hu, C. Liu, Y. Gong, H. Yang, F. Xu, Paper-based point-of-care immunoassays: recent advances and emerging trends, Biotechnol. Adv. 39 (2020), 107442.
[309] B.B. Dzantiev, N.A. Byzova, A.E. Urusov, A.V. Zherdev, Immunochromatographic methods in food analysis, TrAC, Trends Anal. Chem. 55 (2014) 81–93.
[310] R. Chen, X. Chen, Y. Zhou, T. Lin, Y. Leng, X. Huang, Y. Xiong, Three-in-One" multifunctional nanohybrids with colorimetric magnetic catalytic activities to enhance immunochromatographic diagnosis, ACS Nano 16 (2) (2022) 3351–3361.
[311] F. Ghorbanizamani, K. Tok, H. Moulahoum, D. Harmanci, S.B. Hanoglu, C. Durmus, F. Zihnioglu, S. Evran, C. Cicek, R. Sertoz, B. Arda, T. Goksel, K. Turhan, S. Timur, Dye-loaded polymersome-based lateral flow assay: rational design of a COVID-19 testing platform by repurposing SARS-CoV-2 antibody cocktail and antigens obtained from positive human samples, ACS Sens. 6 (8) (2021) 2988–2997.
[312] J. Deng, M. Yang, J. Wu, W. Zhang, X. Jiang, A self-contained chemiluminescent lateral flow assay for point-of-care testing, Anal. Chem. 90 (15) (2018) 9132–9137.
[313] S. Jain, M. Nehra, R. Kumar, N. Dilbaghi, T. Hu, S. Kumar, A. Kaushik, C.Z. Li, Internet of medical things (IoMT)-integrated biosensors for point-of-care testing of infectious diseases, Biosens. Bioelectron. 179 (2021), 113074.
[314] H. Zhang, R. Liu, Q. Li, X. Hu, L. Wu, Y. Zhou, G. Qing, R. Yuan, J. Huang, W. Gu, Y. Ye, C. Qi, M. Han, X. Chen, X. Zhu, Y. Deng, L. Zhang, H. Chen, H. Zhang, W. Gao, Y. Liu, Y. Luo, Flipped quick-response code enables reliable blood grouping, ACS Nano 15 (4) (2021) 7649–7658.
[315] M. Yang, W. Zhang, J. Yang, B. Hu, F. Cao, W. Zheng, Y. Chen, X. Jiang, Skiving stacked sheets of paper into test paper for rapid and multiplexed assay, Sci. Adv. 3 (12) (2017), eaao4862.
[316] A.W. Martinez, S.T. Phillips, M.J. Butte, G.M. Whitesides, Patterned paper as a platform for inexpensive, low-volume, portable bioassays, Angew. Chem. 119 (8) (2007) 1340–1342.
[317] L.-M. Fu, Y.-N. Wang, Detection methods and applications of microfluidic paper-based analytical devices, TrAC, Trends Anal. Chem. 107 (2018) 196–211.
[318] H. Fu, P. Song, Q. Wu, C. Zhao, P. Pan, X. Li, N.Y.K. Li-Jessen, X. Liu, A paper-based microfluidic platform with shape-memory-polymer-actuated fluid valves for automated multi-step immunoassays, Microsyst. Nanoeng. 5 (2019) 50.
[319] B. Li, J. Qi, L. Fu, J. Han, J. Choo, A.J. deMello, B. Lin, L. Chen, Integrated hand-powered centrifugation and paper-based diagnosis with blood-in/answer-out capabilities, Biosens. Bioelectron. 165 (2020), 112282.
[320] Y. Rasmi, X. Li, J. Khan, T. Ozer, J.R. Choi, Emerging point-of-care biosensors for rapid diagnosis of COVID-19: current progress, challenges, and future prospects, Anal. Bioanal. Chem. 413 (16) (2021) 4137–4159.
[321] A. Gowri, N. Ashwin Kumar, B.S. Suresh Anand, Recent advances in nanomaterials based biosensors for point of care (PoC) diagnosis of Covid-19 - a minireview, TrAC, Trends Anal. Chem. 137 (2021), 116205.

[322] D. Kim, J.Y. Lee, J.S. Yang, J.W. Kim, V.N. Kim, H. Chang, The architecture of SARS-CoV-2 transcriptome, Cell 181 (4) (2020) 914–921 e910.
[323] H. Yao, Y. Song, Y. Chen, N. Wu, J. Xu, C. Sun, J. Zhang, T. Weng, Z. Zhang, Z. Wu, L. Cheng, D. Shi, X. Lu, J. Lei, M. Crispin, Y. Shi, L. Li, S. Li, Molecular architecture of the SARS-CoV-2 virus, Cell 183 (3) (2020) 730–738. e713.
[324] Y. Huang, C. Yang, X.F. Xu, W. Xu, S.W. Liu, Structural and functional properties of SARS-CoV-2 spike protein: potential antivirus drug development for COVID-19, Acta Pharmacol. Sin. 41 (9) (2020) 1141–1149.
[325] S. Jiang, X. Zhang, Y. Yang, P.J. Hotez, L. Du, Neutralizing antibodies for the treatment of COVID-19, Nat. Biomed. Eng 4 (12) (2020) 1134–1139.
[326] L. Du, Y. Yang, X. Zhang, Neutralizing antibodies for the prevention and treatment of COVID-19, Cell, Mol. Immunol. 18 (10) (2021) 2293–2306.
[327] C.H. Chau, J.D. Strope, W.D. Figg, COVID-19 clinical diagnostics and testing technology, Pharmacotherapy 40 (8) (2020) 857–868.
[328] N. Chauhan, S. Soni, A. Gupta, U. Jain, New and developing diagnostic platforms for COVID-19: a systematic review, Expert Rev. Mol. Diagn. 20 (9) (2020) 971–983.
[329] Z. Qin, R. Peng, I.K. Baravik, X. Liu, Fighting COVID-19: integrated micro- and nanosystems for viral infection diagnostics, Matter 3 (3) (2020) 628–651.
[330] A. Asghari, C. Wang, K.M. Yoo, A. Rostamian, X. Xu, J.D. Shin, H. Dalir, R.T. Chen, Fast, accurate, point-of-care COVID-19 pandemic diagnosis enabled through advanced lab-on-chip optical biosensors: opportunities and challenges, Appl. Phys. Rev. 8 (3) (2021), 031313.
[331] J. Guo, S. Chen, S. Tian, K. Liu, J. Ni, M. Zhao, Y. Kang, X. Ma, J. Guo, 5G-enabled ultra-sensitive fluorescence sensor for proactive prognosis of COVID-19, Biosens. Bioelectron. 181 (2021), 113160.
[332] https://www.lumiradx.com/uk-en/. (Accessed 10 September 2021). accessed.
[333] P.K. Drain, M. Ampajwala, C. Chappel, A.B. Gvozden, M. Hoppers, M. Wang, R. Rosen, S. Young, E. Zissman, M. Montano, A rapid, high-sensitivity SARS-CoV-2 nucleocapsid immunoassay to aid diagnosis of acute COVID-19 at the point of care: a clinical performance study, Infect. Dis. Ther. 10 (2) (2021) 753–761.
[334] D. Jacofsky, E.M. Jacofsky, M. Jacofsky, Understanding antibody testing for COVID-19, 7, Supplement, J. Arthroplasty 35 (2020) S74–S81.
[335] R. West, A. Kobokovich, N. Connell, G.K. Gronvall, COVID-19 antibody tests: a valuable public health tool with limited relevance to individuals, Trends Microbiol. 29 (3) (2021) 214–223.
[336] J. Kopel, H. Goyal, A. Perisetti, Antibody tests for COVID-19, Baylor Univ. Med. Center. Proceed. 34 (1) (2021) 63–72.
[337] S.H. Hodgson, K. Mansatta, G. Mallett, V. Harris, K.R.W. Emary, A.J. Pollard, What defines an efficacious COVID-19 vaccine? A review of the challenges assessing the clinical efficacy of vaccines against SARS-CoV-2, Lancet Infect. Dis. 21 (2) (2021) e26–e35.
[338] K. Maneikis, K. Šablauskas, U. Ringelevičiūtė, V. Vaitekėnaitė, R. Čekauskienė, L. Kryžauskaitė, D. Naumovas, V. Banys, V. Pečeliūnas, T. Beinortas, L. Griškevičius, Immunogenicity of the BNT162b2 COVID-19 mRNA vaccine and early clinical outcomes in patients with haematological malignancies in Lithuania: a national prospective cohort study, Lancet Haematol 8 (8) (2021) e583–e592.
[339] B. Lou, T.-D. Li, S.-F. Zheng, Y.-Y. Su, Z.-Y. Li, W. Liu, F. Yu, S.-X. Ge, Q.-D. Zou, Q. Yuan, S. Lin, C.-M. Hong, X.-Y. Yao, X.-J. Zhang, D.-H. Wu, G.-L. Zhou, W.-H. Hou, T.-T. Li, Y.-L. Zhang, S.-Y. Zhang, J. Fan, J. Zhang, N.-S. Xia, Y. Chen, Serology characteristics of SARS-CoV-2 infection after exposure and post-symptom onset, Eur. Respir. J. 56 (2) (2020), 2000763.
[340] P. Kellam, W. Barclay, The dynamics of humoral immune responses following SARS-CoV-2 infection and the potential for reinfection, J. Gen. Virol. 101 (8) (2020) 791–797.
[341] D. Jacofsky, E.M. Jacofsky, M. Jacofsky, Understanding antibody testing for COVID-19, J. Arthroplasty 35 (7S) (2020) S74–S81.
[342] Z. Chen, Z. Zhang, X. Zhai, Y. Li, L. Lin, H. Zhao, L. Bian, P. Li, L. Yu, Y. Wu, G. Lin, Rapid and sensitive detection of anti-SARS-CoV-2 IgG, using lanthanide-doped nanoparticles-based lateral flow immunoassay, Anal. Chem. 92 (10) (2020) 7226–7231.
[343] J.T. Heggestad, D.S. Kinnamon, L.B. Olson, J. Liu, G. Kelly, S.A. Wall, S. Oshabaheebwa, Z. Quinn, C.M. Fontes, D.Y. Joh, A.M. Hucknall, C. Pieper, J.G. Anderson, I.A. Naqvi, L. Chen, L.G. Que, T. Oguin 3rd, S.K. Nair, B.A. Sullenger, C.W. Woods, T.W. Burke, G.D. Sempowski, B.D. Kraft, A. Chilkoti, Multiplexed, quantitative serological profiling of COVID-19 from blood by a point-of-care test, Sci. Adv. 7 (26) (2021), eabg4901.
[344] D.Y. Joh, A.M. Hucknall, Q. Wei, K.A. Mason, M.L. Lund, C.M. Fontes, R.T. Hill, R. Blair, Z. Zimmers, R.K. Achar, D. Tseng, R. Gordan, M. Freemark, A. Ozcan, A. Chilkoti, Inkjet-printed point-of-care immunoassay on a nanoscale polymer brush enables subpicomolar detection of analytes in blood, Proc. Natl. Acad. Sci. U.S.A. 114 (34) (2017) E7054.
[345] R.R.G. Soares, A.S. Akhtar, I.F. Pinto, N. Lapins, D. Barrett, G. Sandh, X. Yin, V. Pelechano, A. Russom, Sample-to-answer COVID-19 nucleic acid testing using a low-cost centrifugal microfluidic platform with bead-based signal enhancement and smartphone read-out, Lab Chip 21 (2021) 2932–2944.
[346] H. Xiong, X. Ye, Y. Li, L. Wang, J. Zhang, X. Fang, J. Kong, Rapid differential diagnosis of seven human respiratory coronaviruses based on centrifugal microfluidic nucleic acid assay, Anal. Chem. 92 (21) (2020) 14297–14302.
[347] http://www.v-acure.com/product/9.html. (Accessed 11 September 2021).
[348] J.S. Kim, J.Y. Lee, J.W. Yang, K.H. Lee, M. Effenberger, W. Szpirt, A. Kronbichler, J.I. Shin, Immunopathogenesis and treatment of cytokine storm in COVID-19, Theranostics 11 (1) (2021) 316–329.
[349] R.Q. Cron, R. Caricchio, W.W. Chatham, Calming the cytokine storm in COVID-19, Nat. Med. 27 (10) (2021) 1674–1675.
[350] P.A. Mudd, J.C. Crawford, J.S. Turner, A. Souquette, D. Reynolds, D. Bender, J.P. Bosanquet, N.J. Anand, D.A. Striker, R.S. Martin, A.C.M. Boon, S.L. House, K.E. Remy, R.S. Hotchkiss, R.M. Presti, J.A. O'Halloran, W.G. Powderly, P.G. Thomas, A.H. Ellebedy, Distinct inflammatory profiles distinguish COVID-19 from influenza with limited contributions from cytokine storm, Sci. Adv. 6 (50) (2020), eabe3024.
[351] D.M. Del Valle, S. Kim-Schulze, H.H. Huang, N.D. Beckmann, S. Nirenberg, B. Wang, Y. Lavin, T.H. Swartz, D. Madduri, A. Stock, T.U. Marron, H. Xie, M. Patel, K. Tuballes, O. Van Oekelen, A. Rahman, P. Kovatch, J.A. Aberg, E. Schadt, S. Jagannath, M. Mazumdar, A.W. Charney, A. Firpo-Betancourt, D.R. Mendu, J. Jhang, D. Reich, K. Sigel, C. Cordon-Cardo, M. Feldmann, S. Parekh, M. Merad, S. Gnjatic, An inflammatory cytokine signature predicts COVID-19 severity and survival, Nat. Med. 26 (10) (2020) 1636–1643.
[352] https://www.beckmancoulter.cn/diagnostics/immunoassay/access-2/details.html. (Accessed 25 April 2022).
[353] Y. Song, Y. Ye, S.H. Su, A. Stephens, T. Cai, M.T. Chung, M.K. Han, M.W. Newstead, L. Yessayan, D. Frame, H.D. Humes, B.H. Singer, K. Kurabayashi, A digital protein microarray for COVID-19 cytokine storm monitoring, Lab Chip 21 (2) (2021) 331–343.
[354] J.V. Jokerst, J. Chou, J.P. Camp, J. Wong, A. Lennart, A.A. Pollard, P.N. Floriano, N. Christodoulides, G.W. Simmons, Y. Zhou, M.F. Ali, J.T. McDevitt, Location of biomarkers and reagents within agarose beads of a programmable bio-nanochip, Small 7 (5) (2011) 613–624.
[355] E. Kulla, J. Chou, G. Simmons, J. Wong, M.P. McRae, R. Patel, P.N. Floriano, N. Christodoulides, R.J. Leach, I.M. Thompson, J.T. McDevitt, Enhancement of performance in porous bead-based microchip sensors: effects of chip geometry on bio-agent capture, RSC Adv. 5 (60) (2015) 48194–48206.
[356] M.P. McRae, G.W. Simmons, J. Wong, B. Shadfan, S. Gopalkrishnan, N. Christodoulides, J.T. McDevitt, Programmable bio-nano-chip system: a flexible point-of-care platform for bioscience and clinical measurements, Lab Chip 15 (20) (2015) 4020–4031.
[357] B.H. Shadfan, A.R. Simmons, G.W. Simmons, A. Ho, J. Wong, K.H. Lu, R.C. Bast Jr., J.T. McDevitt, A multiplexable, microfluidic platform for the rapid quantitation of a biomarker panel for early ovarian cancer detection at the point-of-care, Cancer Prev. Res. 8 (1) (2015) 37–48.
[358] M.P. McRae, G. Simmons, J. Wong, J.T. McDevitt, Programmable bio-nanochip platform: a point-of-care biosensor system with the capacity to learn, Accounts Chem. Res. 49 (7) (2016) 1359–1368.
[359] J.J. Lavigne, S. Savoy, M.B. Clevenger, J.E. Ritchie, B. McDoniel, S.-J. Yoo, E.V. Anslyn, J.T. McDevitt, J.B. Shear, D. Neikirk, Solution-based analysis of multiple analytes by a sensor array: toward the development of an "electronic tongue", J. Am. Chem. Soc. 120 (25) (1998) 6429–6430.
[360] Y.S. Sohn, A. Goodey, E.V. Anslyn, J.T. McDevitt, J.B. Shear, D.P. Neikirk, A microbead array chemical sensor using capillary-based sample introduction: toward the development of an "electronic tongue, Biosens. Bioelectron. 21 (2) (2005) 303–312.
[361] J.V. Jokerst, P.N. Floriano, N. Christodoulides, G.W. Simmons, J.T. McDevitt, Integration of semiconductor quantum dots into nano-bio-chip systems for enumeration of CD4+ T cell counts at the point-of-need, Lab Chip 8 (12) (2008) 2079–2090.
[362] J.V. Jokerst, A. Raamanathan, N. Christodoulides, P.N. Floriano, A.A. Pollard, G.W. Simmons, J. Wong, C. Gage, W.B. Furmaga, S.W. Redding, J.T. McDevitt, Nano-bio-chips for high performance multiplexed protein detection: determinations of cancer biomarkers in serum and saliva using quantum dot bioconjugate labels, Biosens. Bioelectron. 24 (12) (2009) 3622–3629.
[363] M.P. McRae, G.W. Simmons, N.J. Christodoulides, Z. Lu, S.K. Kang, D. Fenyo, T. Alcorn, I.P. Dapkins, I. Sharif, D. Vurmaz, S.S. Modak, K. Srinivasan, S. Warhadpande, R. Shrivastav, J.T. McDevitt, Clinical decision support tool and rapid point-of-care platform for determining disease severity in patients with COVID-19, Lab Chip 20 (12) (2020) 2075–2085.
[364] Q. Lin, D. Wen, J. Wu, L. Liu, W. Wu, X. Fang, J. Kong, Microfluidic immunoassays for sensitive and simultaneous detection of IgG/IgM/antigen of SARS-CoV-2 within 15 min, Anal. Chem. 92 (14) (2020) 9454–9458.
[365] Q. Lin, J. Wu, X. Fang, J. Kong, Washing-free centrifugal microchip fluorescence immunoassay for rapid and point-of-care detection of protein, Anal. Chim. Acta 1118 (2020) 18–25.
[366] https://en.watmind.com/prod_view.aspx?nid=3&typeid=10&id=231. (Accessed 27 September 2021). accessed.
[367] https://en.watmind.com/prod_view.aspx?nid=3&typeid=85&id=235. (Accessed 25 September 2021). accessed.
[368] https://en.watmind.com/prod_view.aspx?nid=3&typeid=13&id=233. (Accessed 26 September 2021). accessed.
[369] D.M. Rissin, C.W. Kan, T.G. Campbell, S.C. Howes, D.R. Fournier, L. Song, T. Piech, P.P. Patel, L. Chang, A.J. Rivnak, E.P. Ferrell, J.D. Randall, G.K. Provuncher, D.R. Walt, D.C. Duffy, Single-molecule enzyme-linked immunosorbent assay detects serum proteins at subfemtomolar concentrations, Nat. Biotechnol. 28 (6) (2010) 595–599.
[370] D.H. Wilson, D.M. Rissin, C.W. Kan, D.R. Fournier, T. Piech, T.G. Campbell, R.E. Meyer, M.W. Fishburn, C. Cabrera, P.P. Patel, E. Frew, Y. Chen, L. Chang, E.P. Ferrell, V. von Einem, W. McGuigan, M. Reinhardt, H. Sayer, C. Vielsack, D.C. Duffy, The Simoa HD-1 analyzer: a novel fully automated digital immunoassay analyzer with single-molecule sensitivity and multiplexing,

J. Lab. Autom. 21 (4) (2016) 533–547.
[371] D. Shan, J.M. Johnson, S.C. Fernandes, H. Suib, S. Hwang, D. Wuelfing, M. Mendes, M. Holdridge, E.M. Burke, K. Beauregard, Y. Zhang, M. Cleary, S. Xu, X. Yao, P.P. Patel, T. Plavina, D.H. Wilson, L. Chang, K.M. Kaiser, J. Nattermann, S.V. Schmidt, E. Latz, K. Hrusovsky, D. Mattoon, A.J. Ball, N-protein presents early in blood, dried blood and saliva during asymptomatic and symptomatic SARS-CoV-2 infection, Nat. Commun. 12 (1) (2021) 1931.
[372] T. Gilboa, L. Cohen, C.A. Cheng, R. Lazarovits, A. Uwamanzu-Nna, I. Han, K. Griswold Jr., N. Barry, D.B. Thompson, R.E. Kohman, A.E. Woolley, E.W. Karlson, D.R. Walt, A SARS-CoV-2 neutralization assay using single molecule arrays, Angew. Chem., Int. Ed. Engl. 60 (2021) 25966–25972.
[373] A.F. Ogata, A.M. Maley, C. Wu, T. Gilboa, M. Norman, R. Lazarovits, C.P. Mao, G. Newton, M. Chang, K. Nguyen, M. Kamkaew, Q. Zhu, T.E. Gibson, E.T. Ryan, R.C. Charles, W.A. Marasco, D.R. Walt, Ultra-sensitive serial profiling of SARS-CoV-2 antigens and antibodies in plasma to understand disease progression in COVID-19 patients with severe disease, Clin. Chem. 66 (12) (2020) 1562–1572.
[374] M. Norman, T. Gilboa, A.F. Ogata, A.M. Maley, L. Cohen, E.L. Busch, R. Lazarovits, C.P. Mao, Y. Cai, J. Zhang, J.E. Feldman, B.M. Hauser, T.M. Caradonna, B. Chen, A.G. Schmidt, G. Alter, R.C. Charles, E.T. Ryan, D.R. Walt, Ultrasensitive high-resolution profiling of early seroconversion in patients with COVID-19, Nat. Biomed. Eng 4 (12) (2020) 1180–1187.
[375] J. Li, M.A. Baird, M.A. Davis, W. Tai, L.S. Zweifel, K.M. Adams Waldorf, M. Gale Jr., L. Rajagopal, R.H. Pierce, X. Gao, Dramatic enhancement of the detection limits of bioassays via ultrafast deposition of polydopamine, Nat. Biomed. Eng 1 (6) (2017), 0082.
[376] S. Kim, S. Hong, Nature-inspired adhesive catecholamines for highly concentrated colorimetric signal in spatial biomarker labeling, Adv. Healthc. Mater. 9 (16) (2020), e2000540.
[377] V. Ruzicka, W. März, A. Russ, W. Gross, Immuno-PCR with a commercially available avidin system, Science 260 (5108) (1993) 698–699.
[378] L. Chang, J. Li, L. Wang, Immuno-PCR: an ultrasensitive immunoassay for biomolecular detection, Anal. Chim. Acta 910 (2016) 12–24.
[379] L. Zhao, H. Zhou, T. Sun, W. Liu, H. He, B. Ning, S. Li, Y. Peng, D. Han, Z. Zhao, J. Cui, Z. Gao, Complete antigen-bridged DNA strand displacement amplification immuno-PCR assay for ultrasensitive detection of salbutamol, Sci. Total Environ. 748 (2020), 142330.
[380] D. Wang, Y. Dai, X. Wang, P. Yu, S. Qu, Z. Liu, Y. Cao, L. Zhang, Y. Ping, W. Liu, Z. Tao, Determination of plasma beta-amyloids by rolling circle amplification chemiluminescent immunoassay for noninvasive diagnosis of Alzheimer's disease, Mikrochim. Acta 188 (1) (2021) 24.
[381] P. Zhang, L. Chen, J. Hu, A.Y. Trick, F.E. Chen, K. Hsieh, Y. Zhao, B. Coleman, K. Kruczynski, T.R. Pisanic 2nd, C.D. Heaney, W.A. Clarke, T.H. Wang, Magnetofluidic immuno-PCR for point-of-care COVID-19 serological testing, Biosens. Bioelectron. 195 (2022), 113656.
[382] C. Liu, J. Zhao, F. Tian, L. Cai, W. Zhang, Q. Feng, J. Chang, F. Wan, Y. Yang, B. Dai, Y. Cong, B. Ding, J. Sun, W. Tan, Low-cost thermophoretic profiling of extracellular-vesicle surface proteins for the early detection and classification of cancers, Nat. Biomed. Eng 3 (3) (2019) 183–193.
[383] J. Deng, F. Tian, C. Liu, Y. Liu, S. Zhao, T. Fu, J. Sun, W. Tan, Rapid one-step detection of viral particles using an aptamer-based thermophoretic assay, J. Am. Chem. Soc. 143 (19) (2021) 7261–7266.
[384] Z. Han, F. Wan, J. Deng, J. Zhao, Y. Li, Y. Yang, Q. Jiang, B. Ding, C. Liu, B. Dai, J. Sun, Ultrasensitive detection of mRNA in extracellular vesicles using DNA tetrahedron-based thermophoretic assay, Nano Today 38 (2021), 101203.
[385] Y. Li, J. Deng, Z. Han, C. Liu, F. Tian, R. Xu, D. Han, S. Zhang, J. Sun, Molecular identification of tumor-derived extracellular vesicles using thermophoresis-mediated DNA computation, J. Am. Chem. Soc. 143 (3) (2021) 1290–1295.
[386] E.M. Hassan, M.C. DeRosa, Recent advances in cancer early detection and diagnosis: role of nucleic acid based aptasensors, TrAC, Trends Anal. Chem. 124 (2020) 115806.
[387] Q. He, D. Yu, M. Bao, G. Korensky, J. Chen, M. Shin, J. Kim, M. Park, P. Qin, K. Du, High-throughput and all-solution phase African Swine Fever Virus (ASFV) detection using CRISPR-Cas12a and fluorescence based point-of-care system, Biosens. Bioelectron. 154 (2020), 112068.
[388] Q. Zhao, Y. Pan, X. Luan, Y. Gao, X. Zhao, Y. Liu, Y. Wang, Y. Song, Nano-immunosorbent assay based on Cas12a/crRNA for ultra-sensitive protein detection, Biosens. Bioelectron. 190 (2021), 113450.
[389] Z. Gao, Y. Song, T.Y. Hsiao, J. He, C. Wang, J. Shen, A. MacLachlan, S. Dai, B.H. Singer, K. Kurabayashi, P. Chen, Machine-learning-assisted microfluidic nanoplasmonic digital immunoassay for cytokine storm profiling in COVID-19 patients, ACS Nano 15 (11) (2021) 18023–18036.
[390] D.Y. Joh, J.T. Heggestad, S. Zhang, G.R. Anderson, J. Bhattacharyya, S.E. Wardell, S.A. Wall, A.B. Cheng, F. Albarghouthi, J. Liu, S. Oshima, A.M. Hucknall, T. Hyslop, A.H.S. Hall, K.C. Wood, E. Shelley Hwang, K.C. Strickland, Q. Wei, A. Chilkoti, Cellphone enabled point-of-care assessment of breast tumor cytology and molecular HER2 expression from fine-needle aspirates, npj Breast Cancer 7 (1) (2021) 85.
[391] A. Shokr, L.G.C. Pacheco, P. Thirumalaraju, M.K. Kanakasabapathy, J. Gandhi, D. Kartik, F.S.R. Silva, E. Erdogmus, H. Kandula, S. Luo, X.G. Yu, R.T. Chung, J.Z. Li, D.R. Kuritzkes, H. Shafiee, Mobile health (mHealth) viral diagnostics enabled with adaptive adversarial learning, ACS Nano 15 (1) (2021) 665–673.
[392] Y. Zhou, A. Yasumoto, C. Lei, C.J. Huang, H. Kobayashi, Y. Wu, S. Yan, C.W. Sun, Y. Yatomi, K. Goda, Intelligent classification of platelet aggregates by agonist type, Elife 9 (2020), e52938.
[393] F. Ellett, J. Jorgensen, A.L. Marand, Y.M. Liu, M.M. Martinez, V. Sein, K.L. Butler, J. Lee, D. Irimia, Diagnosis of sepsis from a drop of blood by measurement of spontaneous neutrophil motility in a microfluidic assay, Nat. Biomed. Eng 2 (4) (2018) 207–214.
[394] M. Poudineh, C.L. Maikawa, E.Y. Ma, J. Pan, D. Mamerow, Y. Hang, S.W. Baker, A. Beirami, A. Yoshikawa, M. Eisenstein, S. Kim, J. Vuckovic, E.A. Appel, H.T. Soh, A fluorescence sandwich immunoassay for the real-time continuous detection of glucose and insulin in live animals, Nat. Biomed. Eng 5 (1) (2021) 53–63.
[395] Q. Xue, X. Kan, Z. Pan, Z. Li, W. Pan, F. Zhou, X. Duan, An intelligent face mask integrated with high density conductive nanowire array for directly exhaled coronavirus aerosols screening, Biosens. Bioelectron. 186 (2021), 113286.
[396] Y. Zhang, H. Guo, S.B. Kim, Y. Wu, D. Ostojich, S.H. Park, X. Wang, Z. Weng, R. Li, A.J. Bandodkar, Y. Sekine, J. Choi, S. Xu, S. Quaggin, R. Ghaffari, J.A. Rogers, Passive sweat collection and colorimetric analysis of biomarkers relevant to kidney disorders using a soft microfluidic system, Lab Chip 19 (9) (2019) 1545–1555.
[397] P.Q. Nguyen, L.R. Soenksen, N.M. Donghia, N.M. Angenent-Mari, H. de Puig, A. Huang, R. Lee, S. Slomovic, T. Galbersanini, G. Lansberry, H.M. Sallum, E.M. Zhao, J.B. Niemi, J.J. Collins, Wearable materials with embedded synthetic biology sensors for biomolecule detection, Nat. Biotechnol. 39 (2021) 1366–1374.
[398] A.J. Bandodkar, P. Gutruf, J. Choi, K. Lee, Y. Sekine, J.T. Reeder, W.J. Jeang, A.J. Aranyosi, S.P. Lee, J.B. Model, R. Ghaffari, C.J. Su, J.P. Leshock, T. Ray, A. Verrillo, K. Thomas, V. Krishnamurthi, S. Han, J. Kim, S. Krishnan, T. Hang, J.A. Rogers, Battery-free, skin-interfaced microfluidic/electronic systems for simultaneous electrochemical, colorimetric, and volumetric analysis of sweat, Sci. Adv. 5 (1) (2019), eaav3294.